INVESTIGATION OF THE MECHANICS OF WINDBORNE MISSILE IMPACT ON WINDOW GLASS

by

SCOTT A. BOLE, B.S.C.E.

A THESIS

IN

CIVIL ENGINEERING

Submitted to the Graduate Faculty
of Texas Tech University in
Partial Fulfillment of
the Requirements for
the Degree of

MASTER OF SCIENCE

IN

CIVIL ENGINEERING

Approved

Chairperson of the Committee

James R. McDonald

Milton L Smith

Accepted

D. J. Schmidly

Dean of the Graduate School

December, 1999

REPORT DOCUMENTATION PAGE			Form Approved OMB No. 0704-0188

1. AGENCY USE ONLY *(Leave blank)*	2. REPORT DATE	3. REPORT TYPE AND DATES COVERED
	24.Jan.00	THESIS

4. TITLE AND SUBTITLE
INVESTIGATION OF THE MECHANICS OF WINDBORNE MISSILE IMPACT ON WINDOW GLASS

5. FUNDING NUMBERS

6. AUTHOR(S)
2D LT BOLE SCOTT A

7. PERFORMING ORGANIZATION NAME(S) AND ADDRESS(ES)
TEXAS TECH UNIVERSITY AT LUBBOCK

8. PERFORMING ORGANIZATION REPORT NUMBER

9. SPONSORING/MONITORING AGENCY NAME(S) AND ADDRESS(ES)
THE DEPARTMENT OF THE AIR FORCE
AFIT/CIA, BLDG 125
2950 P STREET
WPAFB OH 45433

10. SPONSORING/MONITORING AGENCY REPORT NUMBER
FY00-2

11. SUPPLEMENTARY NOTES

12a. DISTRIBUTION AVAILABILITY STATEMENT
Unlimited distribution
In Accordance With AFI 35-205/AFIT Sup 1

12b. DISTRIBUTION CODE

13. ABSTRACT *(Maximum 200 words)*

14. SUBJECT TERMS

15. NUMBER OF PAGES
135

16. PRICE CODE

17. SECURITY CLASSIFICATION OF REPORT	18. SECURITY CLASSIFICATION OF THIS PAGE	19. SECURITY CLASSIFICATION OF ABSTRACT	20. LIMITATION OF ABSTRACT

ACKNOWLEDGEMENTS

I would like to thank Dr. H. Scott Norville for the support and guidance that he provided to me as chairman of my thesis committee. I would also like to thank Dr. James R. McDonald and Dr. Milton L. Smith for serving on my thesis committee. I would also like to thank the National Institute of Standards and Technology for funding this research. In addition, I would like to thank the entire faculty and staff of the Civil Engineering Department for providing me with a first-rate education at both the undergraduate and graduate levels.

To Frank Wyatt, Mario Torres, Paul Estrada, and Doug Haynes, I would like to say thank you for providing assistance while building the apparatus needed to conduct the experimental research for this thesis. To Lani Lynn, Tyson Cox, Scott Hammond, and Nebil Hamza, I would like to extend my gratitude for your help while conducting the experiments throughout this research project.

Finally, I would like to thank my family for their support throughout my tenure as an undergraduate and graduate student at Texas Tech University. Without your support, I probably would not have done as well as I did as a student.

TABLE OF CONTENTS

ABSTRACT

Engineers have recognized that failure of the building envelope is one mechanism that can lead to severe damage of structures during windstorms. The building envelope consists of the roof, doorways, windows, and cladding components that form the exterior wall system of a building. Failure of the building envelope results in internal pressurization of the structure which may lead to structural failure. For this reason, engineers have begun to focus on ways to make the building envelope resistant to the effects of severe windstorms.

Window glass is one type of cladding material. Of the threats posed by a windstorm, the major threat to window glass consists of windborne debris. ASTM E1886, ASTM E1996, and SSTD 12-99 address the issue of resistance to windborne missile impacts.

This thesis concludes that a simple statement of an object's kinetic energy upon impact by itself cannot serve to predict the outcome of the impact. Conservation of angular momentum occurs during a missile impact on window glass. Finally, energy is lost during a missile impact on window glass.

LIST OF TABLES

LIST OF FIGURES

CHAPTER 1

INTRODUCTION

Severe windstorms have plagued the planet as long as man has been recording history. Engineering for extreme windstorms and their effects is a rather new process that has gained the attention of engineers in the last thirty years. Hurricanes and tornadoes constitute the primary severe windstorms that concern United States residents. In 1992, Hurricane Andrew ravaged South Florida after achieving Category IV intensity on the Saffir-Simpson Scale (Simiu and Scanlan, 1996). In the aftermath of this disaster, one response consisted of the creation of standards governing the design of engineered structures to improve resistance to hurricane effects. More recently, a devastating tornado struck the heart of Oklahoma City in May of 1999. During both events, high winds ripped across populated residential and urban areas, picking up large amounts of debris. The windborne debris impacted existing structures resulting in major damage.

Hurricane Andrew and the Oklahoma City Tornado resulted in billions of dollars in losses and caused numerous casualties and deaths. Disasters nowadays can commonly cost large amounts of money because more and more people continue to move to disaster prone areas. If this trend continues without

a solution to the problem of engineering for severe winds, the natural disasters of tomorrow are going to be even more costly.

Damage resulting from a strong hurricane impacting a populated area can be widespread. Hurricanes are tropical events that impact large areas at a time. In the United States, the main regions subjected to hurricanes are the Gulf Coast and Atlantic states.

Hurricanes attack a structure with strong, turbulent winds that continuously vary in direction. In addition, the winds pick up and carry debris that impact structures. The impact breaks windows and penetrates walls and doors. Recently, model building codes began addressing the issue of windborne missile impact resistance. ASTM E1886 (1997) and Southern Standard Technical Document (SSTD) 12-94 (SBCCI, 1999) provide two examples of standards concerned with windborne missile impact resistance.

When dealing with impacts, conservation of momentum leads to the solution of the equations of motion for objects involved in an impact. Conservation of linear momentum, angular momentum, or both occurs during an impact. The research for this thesis concerns itself with the angular momentum of the objects involved in a simulated windborne missile impact. The primary objective of this research consists of determining whether a simple statement of missile energy is sufficient to define the outcome of a missile impact test. Secondary objectives include the determination of whether or not the energy or

momentum associated with the objects involved in an impact defines the outcome of an impact

Chapter 2 of this thesis presents the statement of the research problem and a summary of the previous research pertinent to this research topic. Chapter 3 explains the design of an experiment to support the research objectives as well as the apparatus and procedures used during the experiment. Chapter 4 discusses the results of the experimental research. Chapter 5 outlines the conclusions and recommendations based on the findings in Chapter 4.

CHAPTER 2

RESEARCH PROBLEM AND OBJECTIVES

2.1. Statement of Research Problem

The role of the building envelope in the survival of a structure during severe windstorms, especially hurricanes, has become increasingly important to engineers. Numerous storm damage investigations have indicated that building envelope failure leads to internal pressurization resulting in wind and water damage and, often, structural failure. Window glass is a popular cladding material. Unfortunately, window glass fractures when impacted by windborne debris. Thus, many building codes are beginning to require the use of impact resistant glazing systems or protective shutter systems in hurricane prone regions of the U.S.

Model building codes incorporate missile impact standards in an attempt to reduce the damage to structures resulting from the effects of hurricane force winds. Current impact standards include ASTM E1886-97 (ASTM, 1997) and SSTD 12-99 (SBCCI, 1999). These two standards, which are very similar, use selected missiles to represent classes of windborne debris. These standards deal with impacting doors, windows, and glazing components that form the cladding of a building. Both standards prescribe representative missiles to test for a given wind speed and height above grade. Representative missile sizes

and their impact speeds depend on design wind speed, elevation above grade of a cladding component, and proximity to the coast.

Quantities involved in impact mechanics include kinetic energy, linear momentum, and angular momentum (Hibbeler, 1995). Equation 2.1 defines the kinetic energy of a translating body.

$$T = 1/2mv^2 \tag{2.1}$$

In Equation 2.1, T denotes the kinetic energy of the body, m denotes the mass of the body, and v denotes the velocity of the body. Equation 2.2 defines the kinetic energy of a body rotating about a fixed axis passing through point O.

$$T = 1/2I_o\omega^2 \tag{2.2}$$

In equation 2.2, I_o denotes the mass moment of inertia of the rotating body about point O and ω denotes the angular velocity with which the body rotates. Equation 2.3 defines the linear momentum, L, of a translating body.

$$L = mv \tag{2.3}$$

Equation 2.4 defines the linear momentum of a body rotating about a fixed axis passing through point O.

$$L = mv_g \tag{2.4}$$

In equation 2.4, v_g denotes the velocity of the mass center of the body. Equation 2.5 defines the angular momentum of a translating body with respect to a reference point, point O.

$$H = mvh \tag{2.5}$$

In equation 2.5, H denotes the angular momentum of the body while h denotes the length of the moment arm between the mass center of the body and point O. Equation 2.6 denotes the angular momentum of a body rotating about a fixed axis passing through point O.

$$H = I_o\omega \tag{2.6}$$

While the energy involved in any impact may be important, the governing equations in impact problems rely on conservation of momentum principles. A 9.00-lb., 2x4-in., timber missile traveling at 50.0 feet per second (ft/sec.) has a kinetic energy of 350 foot-pounds (ft-lb.). A 4.50-lb., 2x4-in., missile traveling at 70.8 ft/sec. also has a kinetic energy of 350 ft-lb. In order to keep the energy the same as the missile weight changes in an impact, the velocity change is exponential. However, the momentum change between the two missile weights is linear. Thus, if one increases the mass of a missile impacting a structure, its speed must be reduced to keep the same energy. At the same time, the momentum involved in the collision has increased (Figure 2.1). The author's intent is to determine whether the impact characteristics of missiles having different masses, should they impact similar objects, are different because of the difference in the momentum associated with the two missiles even though they have the same kinetic energy.

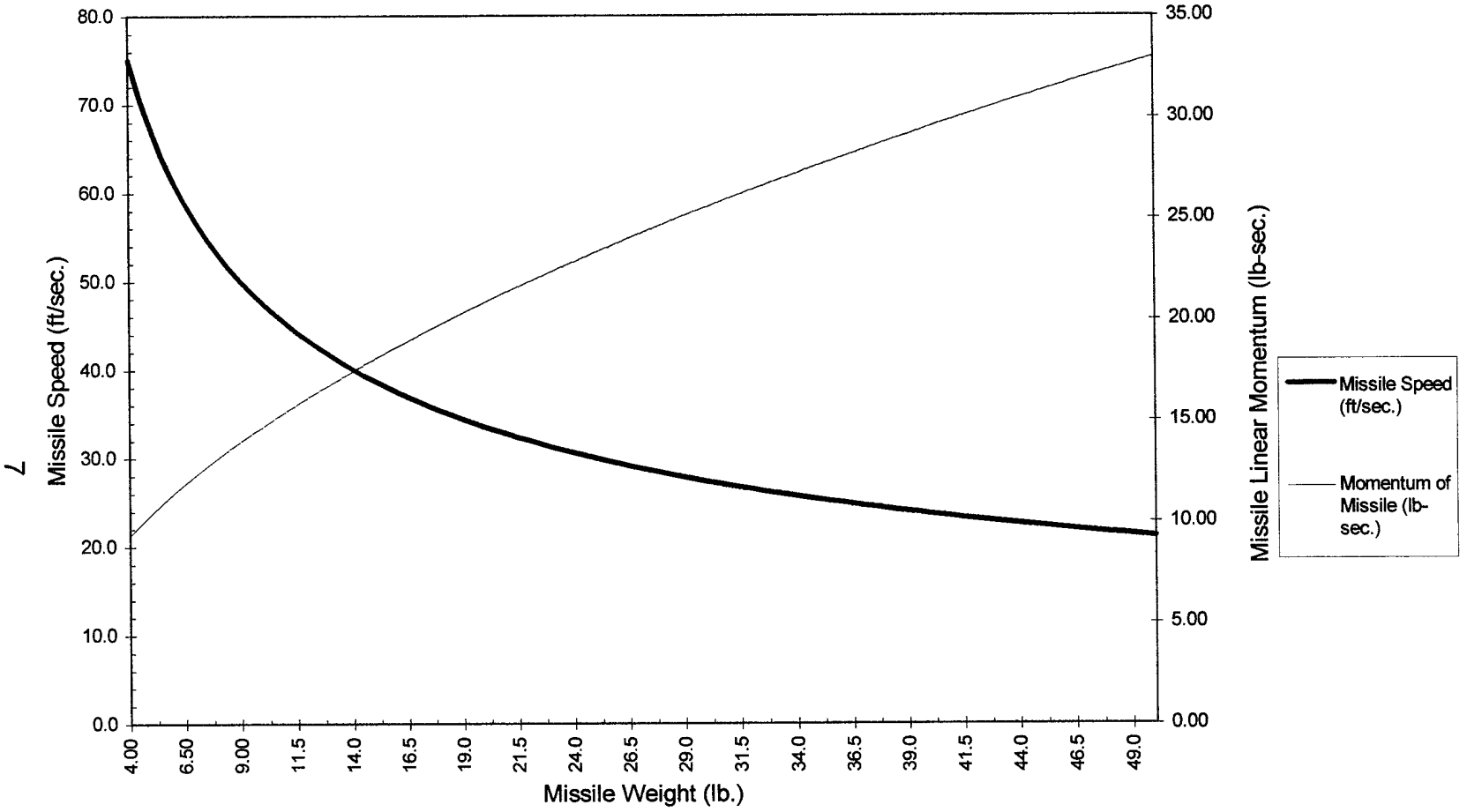

Figure 2.1. Speed and Momentum Versus Weight for a Missile Having a Kinetic Energy of 350 ft-lb.

2.2. Research Objectives

The primary objective of this research consists of determining whether a simple statement of missile energy is sufficient to define the outcome of a missile impact test. This research consists of impacting window glass in a frame that rotates about a fixed axis with different weight 2x4-in. timber missiles having the same kinetic energy. Secondary objectives include the determination of whether or not the energy or momentum associated with the objects involved in an impact defines the outcome of an impact. The impact characteristics of importance when discussing the effects of timber missiles on glazing assemblies are:

1. Whether or not the glass fractures.
2. Whether or not the missile rebounds after impact.
3. The magnitude of momentum transferred to the glass.
4. The magnitude of energy transferred to the glass.

A failure of the glass may not be inherently bad. Small holes (less than 5% of the total window area) in the glass present after an impact while the glass remains within its glazing assembly may not result in internal pressurization. These holes do allow wind and rain damage to occur in a small area of the structure.

2.3. Background Information

This section presents a summary of the literature pertinent to the research problem. The author presents sub-sections to give background information relevant to the research problem. Windborne debris impacts the building envelope; however, it is the hurricane winds that pick up and carry the debris prior to impact. Therefore, basic knowledge of hurricane wind fields, the effects of hurricane winds on buildings, the methods that missiles are injected into the wind field, and how missiles travel while in the wind field is important. Finally, the author presents a brief discussion on impact dynamics to enable the reader to understanding the results of this research.

2.3.1. Hurricane Wind Field

A hurricane, typhoon, or tropical cyclone consists of a circulating area of low pressure that is generally a few hundred kilometers in diameter. The eye of the storm is the central region of relatively calm winds. Maximum wind speeds occur along the eye wall located along the outer circumference of the eye. The eye wall is generally 30-40 km. thick but can be as little as 8 km. thick and as large as 100 km. thick (Batts et al., 1980). The wind speeds observed tend to decrease as the radial distance from the eye wall increases.

Hurricane wind fields depend on many factors. According to Batts et al. (1980), physical models of hurricanes and their associated wind speeds depend

on the atmospheric pressure difference between the central low pressure of the hurricane and surrounding atmosphere, the radius of maximum wind speeds, and the translational speed of the storm. The winds seen at a particular point depend on the distance from the eye wall to the point in question and the surface roughness of the surrounding area of the point in question. As surface friction increases, wind speeds decrease. As hurricanes move inland after landfall, they begin to decay, or undergo filling. Observed wind speeds reduce as the surface friction begins to shear apart the organization of the hurricane along with the loss of water vapor which fuels the hurricane (Willis et al., 1998).

2.3.2. Wind Effects on Buildings

Hurricane winds affect a structure in a unique way. As the eye of the storm passes near a point, the wind direction changes due to the rotation of the storm resulting in wind loading the structure from several directions. Wind interacting with the blunt end of a structure causes the air flow to separate. This interaction causes a positive pressure to act inward on the windward wall while the roof and other walls experience outward acting (or negative) pressure. An opening in a wall causes a change in the internal pressure within a structure. If the opening occurs on the windward side of the structure, the internal pressure increases causing a net increase in the pressure acting on the roof and other walls and a net decrease in the pressure acting on the windward wall. Openings

in the other walls or roof of a structure result in a decrease in internal pressure and a net reduction in pressures acting on all walls except the windward wall and a net increase in the pressure acting on the windward wall (Willis, 1994). According to Minor (1984), internal pressurization can "effectively double the forces acting on the walls and roof of a structure" (p. 61).

A hurricane's sustained, high, turbulent winds attack a structure for hours from several directions seeking out any vulnerable areas. The building envelope must bear the brunt of this attack. The building envelope consists of the roof, doorways, windows, and cladding components that form the exterior wall system of a building. The integrity of the building envelope has become a matter of increasing importance since engineers began to understand the effects of internal pressurization on building performance (Minor, 1997).

The building envelope is susceptible to two damage modes: wind pressure loading and impact from windborne debris. Turbulent winds in a hurricane pick up and carry debris that impacts structures. Window glass is highly susceptible to damage from windborne debris; however, before addressing that subject, the next section gives a brief discussion on the properties of window glass.

2.3.3. General Properties of Glass

Window glass is a brittle material. Table 2.1 lists mean physical properties of window glass. Variations in window glass strength can occur because of its brittle nature.

Designers use three types of monolithic window glass for architectural purposes today. Annealed window glass is the basic glass produced by the manufacturing process. Heat strengthened and fully tempered window glass consist of an annealed window glass lite that has undergone a heat treatment

Table 2.1. Mechanical Properties of Glass

Mechanical Property	Symbol	English Units	SI Units
Modulus of Elasticity	E	10.4×10^6 psi.	72 GPa.
Shear Modulus	G	4.3×10^6 psi.	30 GPa.
Poisson's Ratio	ν	0.22	0.22
Coefficient of Thermal Expansion	α	49×10^{-7}/°F.	88×10^{-7}/°C.
Density	ρ	157 lb/ft^3.	2.5 g/cm^3.
Modulus of Rupture (flexure)	σ_r	----------	----------
- Annealed Glass		6000 psi.	41.3 MPa.
- Heat Strengthened Glass		12000 psi.	82.7 MPa.
- Fully Tempered Glass		24000 psi.	165 MPa.

process. Heat treated window glass has its outer surfaces in compression and its center in tension. Heat strengthened window glass lites have a surface compression between 3500 psi. and 7500 psi., while fully tempered window glass lites have a surface compression above 10000 psi. The physical properties of glass remain unchanged after heat treatment except for an increase in the strength of the glass under a uniform static load or thermal stresses (AAMA, 1984).

Glazers utilize three major window glass constructions in glazing systems. First, when glazers use a single lite of window glass by itself, regardless of the type, everyone calls it a monolithic lite. Laminated glass consists of two or more monolithic glass lites bonded together with an elastomeric interlayer, usually polyvinyl butyral (PVB), to form one lite. The last window glass construction is insulating glass. Insulating glass consists of two window glass lites sealed around an air-space (Minor, 1985). Insulating glass construction may consist of any combination of monolithic or laminated glass. Laminated glass lites may consist of any combination of annealed or heat treated lites.

Window glass design consists of selecting the necessary thickness, type, and construction of window glass to glaze a specific opening. ASTM E1300 (ASTM, 1997) provides guidelines for designing window glass. ASTM E1300 (ASTM, 1997) does not provide design guidelines concerning debris impact, blast loadings, or other extreme events. Abraham (1995) listed several common

failure modes for window glass lite damage that investigators documented in the aftermath of Hurricane Andrew. Table 2.2 lists common failure modes for window glass in windstorms. The contents of Table 2.2 are in no particular order. ASTM E1886 (ASTM, 1997) and SSTD 12-99 (SBCCI, 1999) address the effects of windborne debris.

2.3.4. Hurricane Debris Field

The strong, turbulent winds of a hurricane carry debris, called windborne missiles. For a missile to become airborne, the force of the wind must overcome the gravitational forces acting on the potential missiles. If the potential missile is attached to a structure, the force of the wind will release the missile when the

- Impact by windborne debris
- Excessive wind pressures
- Out-of-plane-deflection of framing assembly
- In-plane deflection of framing assembly
- Improper Installation

Figure 2.2. Common Failure Modes of Glass

strength of the restraining system is overcome (Twisdale et al., 1979). Gwaltney (1968) and McDonald (1970) describe three types of injection mechanisms associated with tornado wind fields. Explosive injections occur because of a sudden, imposed pressure differential. Aerodynamic injection lifts a missile after a vertical restraint, such as gravity is overcome. Finally, ramp injection can lift a sliding missile if it impacts other debris. These injection mechanisms also apply to hurricane wind fields.

Nearly an infinite number of possible missile sources exist. Any object that might become airborne comprises a potential windborne missile. Windborne missiles are divided into two categories: large and small. Small missiles are objects such as roof gravel (McDonald, 1994). Broken glass is also a small missile candidate (Minor, 1984). Beason (1974) and Harris et al. (1978) address the effects of small missile impacts.

Large missile sources are varied, however. Typical sources consist of roofing material, timber framing material, edge flashing, coping tiles, siding (sheet metal), shingles, lawn furniture/ornaments, and tree limbs (Twisdale et al., 1996). Figures 2.3a through 2.3g show examples of windborne debris sources. The author photographed the debris sources in the aftermath of Hurricanes Bonnie and Georges in August and September, 1998. Model code writing bodies have adopted a wood, 2x4-in. as a representative missile. The impact

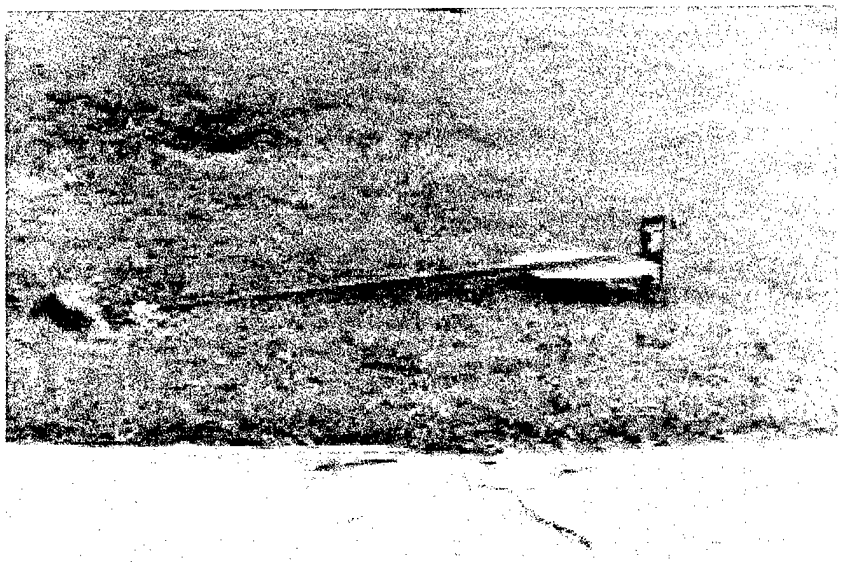

a. Signage

b. Metal Siding

Figure 2.3. Debris Sources

c. Scattered Wood 2x4s

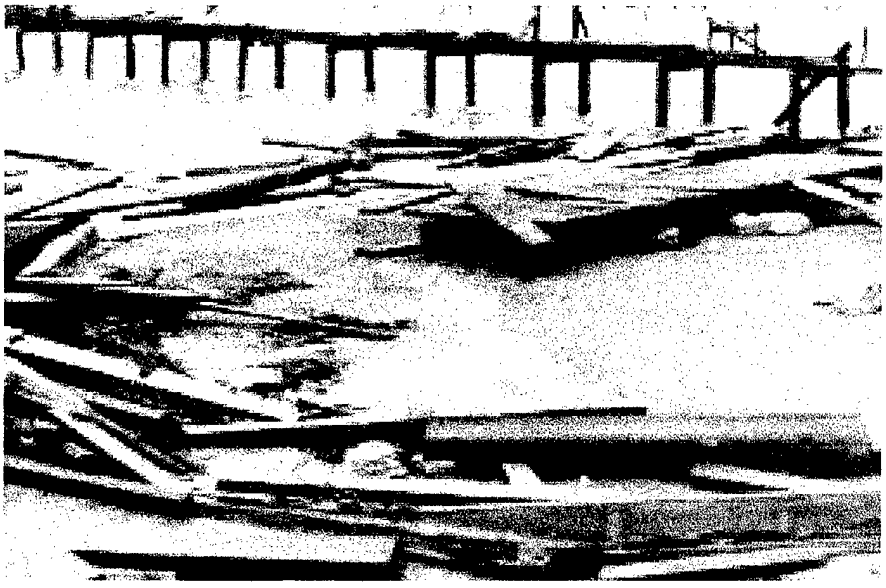

d. Debris From Damaged Dock

Figure 2.3. Continued

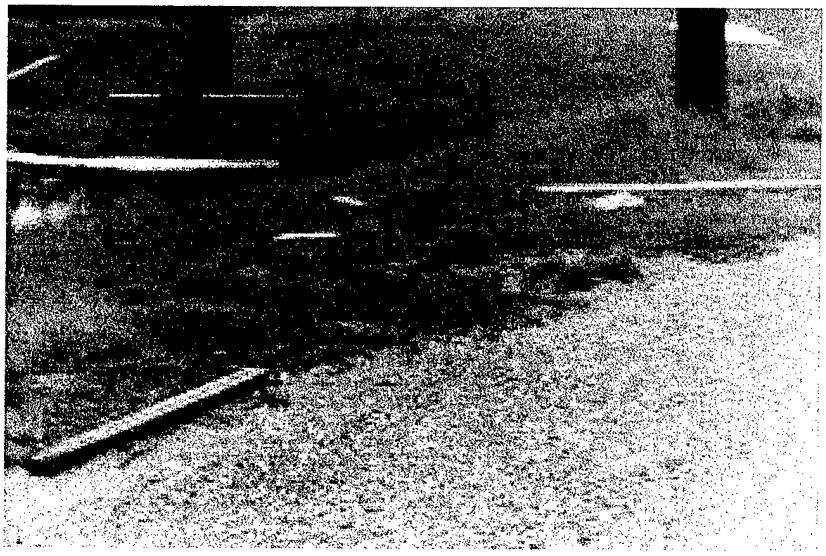

e. Timber 2x4

f. Metal Roof Decking

Figure 2.3. Continued

g. Lawn Statue

Figure 2.3. Continued

standard for hurricane winds above 110 mph is a 9.00-lb., 2X4-in., timber missile traveling at 50.0 ft/sec (SBCCI, 1999).

Windborne debris poses the major threat to the building envelope. This is especially true for window glass. Minor et al. (1978) defined three zones within a building for debris impact. The first three floors of a building comprise Zone 1. Zone 2 consists of the area of the building from the third floor up to the height of the tallest adjacent structure. Any additional portion of the building that extends above the tallest adjacent buildings comprise Zone 3.

Minor et al. (1978) defined typical windborne missiles for each zone. Large missiles can travel great distances, but generally attain limited heights in

their flight. Thus, large missile impacts generally occur in Zone 1. In Zone 2, roof gravel and broken glass constitute typical missiles. Window glass in Zone 3 should be able to resist small missile impacts since winds commonly carry roof gravel above the highest adjacent roof. The required thickness of a window glass lite is the smallest thickness required to satisfy all loading conditions that the lite may see in its lifetime.

Post-breakage performance of glazing systems is as important as the damage mechanism. Post-breakage performance consists of the ability of the glass to protect the interior of a building after failure (Minor, 1997). If the glass fails, two problems can occur. First, if window glass fractures and vacates the glazing assembly, winds can carry the resulting shards as additional small missiles. Second, the glazing material may remain intact but fall out of the glazing assembly. This poses a threat to structural components or people who happen to be below the location of the failed unit (Minor, 1997).

2.3.5. Damage Models

Projectile motion provides a reasonable model for the motion of wind generated missiles. The Institute of Disaster Research at Texas Tech University completed pioneering work for calculating missile trajectories of wind generated missiles (McDonald, 1973).

Twisdale et al. (1996) developed a computer code to model the probabilities of impact and damage from windborne debris in hurricanes. The computer code simulates a hurricane windfield in terms of mean winds and turbulence. The code incorporates both unrestrained and restrained missile sources and has a transport model for the flight of the missiles. The program produces missile trajectories, speeds, impact locations, and probabilities of impact. The final output is the probability of exceeding a threshold value of energy or momentum. The missile model that Twisdale et al. (1996) use and recommend is a six-degree-of-freedom model that takes into account the effects of lift, drag, and side forces. The model accounts for tumbling and reorientation within turbulent winds.

Another model, submitted by Willis et al. (1998), indicates flight speeds for missiles and bases damage potential on a kinetic energy absorption model. Willis et al. (1998) state that below a threshold value, no damage occurs. If the threshold value is exceeded, the damage observed is proportional to the kinetic energy of the missile. Abrate (1998) expresses a similar notion.

2.3.6. Current Impact Test Standards

Current test standards for impact resistance to windborne debris reduce the probability of compromising the integrity of the building envelope. ASTM E1886 (ASTM, 1997) defines procedures and requirements for a glazing system

to withstand missile impacts. The glazing system must resist the missile impact while remaining in its glazing assembly. Following the survival of a missile impact, the specimen must undergo a specified set of pressure cycles. For large missile impacts, the standard weight is between 4.50 lb. and 15.00 lb. The length parameters of the missiles allow for consistency in the stiffness of the missile. The standard requires that the missile impact speed should be between 10 and 55 percent of the basic wind speed. The standard prescribes that timber missiles should be No. 2 or better Southern Yellow pine or Douglas Fir wood specimens. During the course of this research, ASTM E1996 (ASTM, 1999) was adopted. This standard concerns itself with the impact resistance of the building envelope subject to impact from windborne debris during hurricanes.

SSTD 12-99 (SBCCI, 1999) is the missile impact standard used by the Gulf States and Atlantic Coast States northward to North Carolina. It is very similar to ASTM E1886 (ASTM, 1997). Both SSTD 12-99 (SBCCI, 1999) and ASTM E1886 (ASTM, 1997) allow for full scale missile testing using an air-actuated cannon, however, SSTD 12-99 (SBCCI, 1999) also allows for an equivalent pendulum impact test. If the test uses an equivalent pendulum impact apparatus, it must have at least a 12-in. timber 2x4 at its impact end. This test measures three levels of energy for the basic wind speeds over 90 mph. Table 2.2 shows the missiles and their associated impact energies.

Table 2.2. Impact Standards From SSTD 12-99

Wind Speed U (mph.)	Missile Weight (lb.)	Impact Speed (ft/sec.)	Missile Length ± 1 ft. 0 in.	Missile Energy (ft-lb.)
$90 < U \leq 100$	4.50	40.0	3 ft. 9 in.	100
$100 < U < 110$	8.00	40.0	7 ft. 6 in.	200
$U \geq 110$	9.00	50.0	9 ft. 0 in.	350

Two counties in Florida (Dade and Brower County) have adopted codes with provisions similar to ASTM E1886 (ASTM, 1997) and SSTD 12-99 (SBCCI, 1999). Both of these counties use the Southern Florida Building Code as their primary building code with local enforcement of the impact standard.

2.3.7. Review of Impact Dynamics

An impact occurs when one object strikes another. During an impact, momentum in some form is conserved. Energy is not conserved except during a "perfectly elastic" impact. A plastic impact occurs when the impacting object becomes embedded in the impacted object. A central impact occurs when the line of impact coincides with the line connecting the two mass centers of the objects involved in the impact. Otherwise, one refers to the impact as eccentric (Hibbeler, 1995).

Brach (1991) discusses some further classifications of impact. A direct impact occurs when the motion of the objects is parallel to the line of impact. If the motion of the objects is not parallel to the line of impact, the impact is oblique. Thus, according to Brach (1991), four types of impact generally occur.

They are: direct central impact, oblique central impact, direct eccentric impact, and oblique eccentric impact. Twisdale (1977) discusses the same types of impact, but uses different names. Figure 2.4 illustrates the different types of impacts.

Impacts occur over a very short time period. The contact forces involved in a missile impact for this research act for short periods of time. Carter (1998) states that contact between the impacting objects involved in a missile impact lasts for 0.5-1.5 milliseconds. These values are for elastic impacts and the time may increase if penetration or perforation of one of the objects involved in the impact occurs. Perforation occurs when the missile passes through the impacted object. Penetration occurs when the missile proceeds to pass through a target, but stops short of full perforation.

Immediately upon impact, compressive, shear, and surface waves begin to act away from the impact location. These waves travel through the materials involved in an impact. The stress levels remain low as the waves pass through the surfaces. Abrate (1998) discusses several parameters that affect the possibilities of damage. These include the material properties of both objects, the thickness and dimensions of the impacted object, and the support conditions of the impacted object. The missile's properties are also important. Properties such as the size, stiffness, density, mass, and impact velocity all affect the

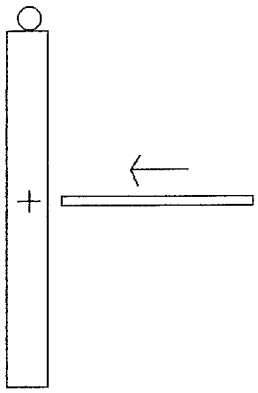

a) Direct Central Impact

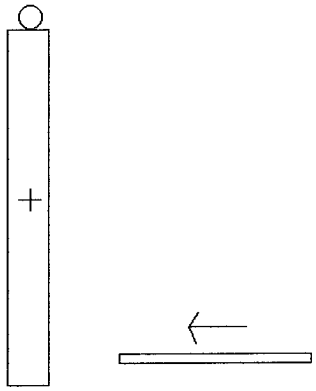

b) Direct Eccentric Impact

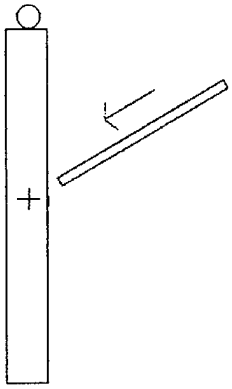

c) Oblique Central Impact

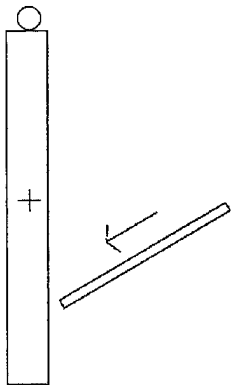

d) Oblique Eccentric Impact

Figure 2.4. Types of Impact

outcome of an impact. Abrate (1998) also states that the initial kinetic energy of the projectile is of importance. Another important issue is whether the projectile impacts the object normal to its surface or not. A normal impact transfers the most momentum to the impacted object. As the angle of incidence of the missile increases, less of the missiles momentum is traveling in the direction of the line of impact, thus less momentum is transferred (Twisdale, 1977).

2.3.8. Concerns With Previous Research

Previous research mostly concerns itself with the energy involved in an impact. Treatise on dynamics indicate that the momentum of a missile is the controlling factor in an impact (Hibbeler, 1995). As such, the next step in the research consists of designing an experiment that attempts to prove that the momentum of a missile, not its energy, governs the outcome of an impact.

CHAPTER 3

EXPERIMENTAL PLAN

In order to determine the parameters that govern a windborne missile impact, the author designed an experiment. This chapter discusses the planning of the experiment, the apparatus involved, and the testing procedures followed throughout the experiment.

3.1. Experimental Design

After reviewing ASTM E1886 (1997) and SSTD 12 (SBCCI, 1999), the author decided to conduct an investigation into the mechanics of windborne missile impact. The focal point of the experiment would be the 9.00-lb., 2x4-in., timber missile. When traveling at 50.0 ft/sec., the 9.00-lb. missile has a kinetic energy of 350 ft-lb. The missile has a linear momentum of 14.0 pound-seconds (lb-sec.). If a 4.50-lb. or 18.0-lb. missile travels through the air, they must move with different speeds to have the same energy as the 9.00-lb. missile traveling at 50.0 ft/sec. Table 3.1 shows that while the energy of each missile is 350 ft-lb., each respective missile has a different linear momentum. The research objective consists of determining whether the difference in momentum results in different outcomes after an impact.

Table 3.1. Missile Energy and Momentum for Various Weights

Missile Weight (lb.)	Missile Speed (ft/sec.)	Missile Energy (ft-lb.)	Missile Linear Momentum (lb-sec.)
4.50	70.8	350	9.89
9.00	50.0	350	14.0
18.0	35.4	350	19.8

In order to achieve the research objectives, the author tested several glass lites and an aluminum plate. Table 3.2 describes the test specimens obtained for this experiment. All test specimens have rectangular dimensions of 48x48 in. Table 3.3 shows the weights and velocities of the impacting missiles on the test specimens.

The same aluminum plate acts as the test specimen for the aluminum series. The series TPM2 consisted of the same tempered lite acting as the test specimen, thus the last letter of the series name designates the different test runs. In series LHS, the heat strengthened side of the laminated lite will face the non-impact side of the window frame. This will put the annealed lite in compression and the heat strengthened side in tension.

Researchers chose the thickness of the aluminum plate so that its weight would be comparable to that of the glass tested. Aluminum has some material properties comparable to that of window glass.

Table 3.2. Test Specimens

Number Ordered	Glass Construction	Nominal Thickness (in.)	Description of Glass*	Test Series
6	Laminated	1/4	1/4 AN - 0.030 - 1/4 AN	LAM
3	Laminated	1/4	1/4 AN - 0.030 - 1/4 HS	LHS
9	Laminated	3/8	3/16 HS - 0.090 - 3/16 HS	HS9
3	Monolithic	1/4	Annealed Monolithic	MON
1	Monolithic	1/2	Tempered Monolithic	TPM2
1	Aluminum Plate	1/4	Not Applicable	ALM

* All Dimensions are inches, AN - Annealed, HS - Heat Strengthened

Table 3.3. Testing Plan

Number To Test	Missile Velocity (ft/sec.)	Missile Weight (lb.)	Series Designations
3	50.0	9.00	LAM01-LAM03
3	50.0	9.00	LHS01-LHS03
3	50.0	9.00	MON01-MON03
3	50.0	9.00	HS9_01, HS9_02, and HS9_07
3	70.8	4.50	HS9_05, HS9_06, and HS9_08
3	35.4	18.0	HS9_03, HS9_04, and HS9_09
3	50.0	9.00	ALM04-ALM06
3	70.8	4.50	ALM01-ALM03
3	35.4	18.0	ALM07-ALM09
3	70.8	4.50	LAM04-LAM06
3^{+}	50.0	9.00	TPM2A-TPM2C

$^{+}$ Test Specimen Destroyed After 1st 9 lb. Lower Corner Impact

3.2. Experimental Apparatus

The experiment uses six major pieces of equipment. They are:

1. An air-actuated cannon;
2. A Reaction frame;
3. A glazing frame that supports the test specimens;
4. Timber missiles;
5. An angle measuring system;
6. A video recorder.

3.2.1. The Air Cannon

An air-actuated cannon (Figure 3.1) served as the launching device for the missiles. An air compressor supplies air to a 60-gallon holding tank (Figure 3.2). The holding tank connects to a 4-in. diameter Pegler ball valve assembly (Figure 3.3) with 2, 4-in. diameter hoses coupled through a T-connector into a single, 4-in. diameter hose. The ball valve assembly has a 1/2-in. relief valve connected to a manometer that displays the pressure in the air tank. The cannon support frame has wheels that enable easy movement and aiming. A pulley and cable system facilitate height adjustment. The cannon support frame prevents excessive deflection of the barrel.

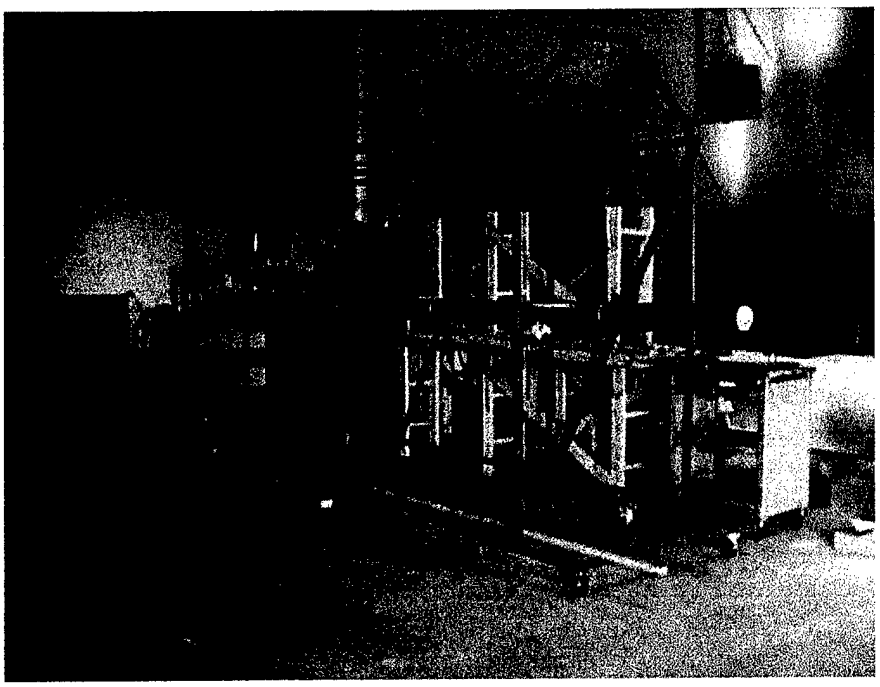

Figure 3.1. Air-Actuated Cannon

Figure 3.2. Holding Tank

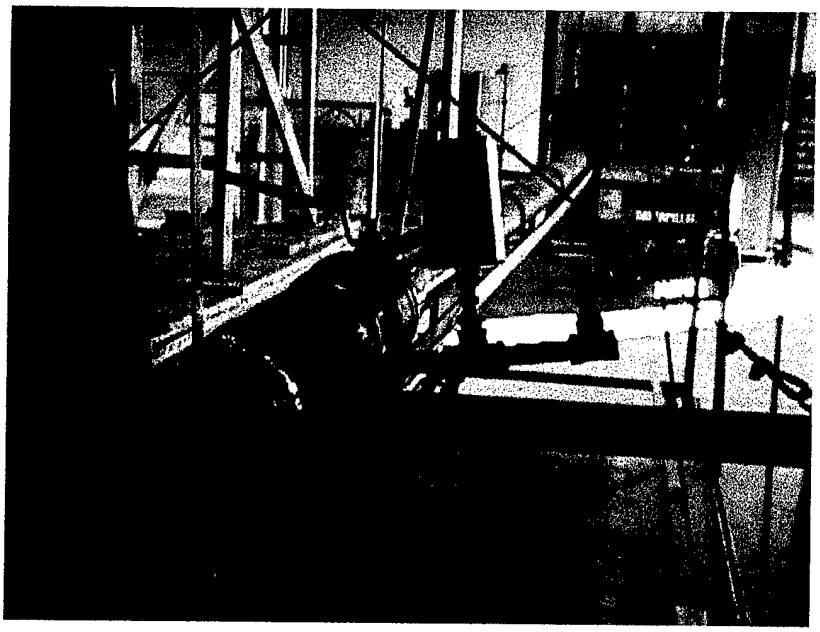

Figure 3.3. Pegler Ball Valve Assembly and Manometer

To fire a missile, the air compressor pressurizes the tank and the researcher releases the ball valve at the pressure required to achieve the desired missile speed. Two timing gates spaced 2 feet apart are located at the free end of the barrel. The timing gates (Figure 3.4) connect electronically to a Projectile Timer Signal Coordinator and a BK Precision Universal Counter (Figure 3.5). The Universal Counter displays the time it takes for the missile to pass through the gates in milliseconds. To determine the velocity of the missile in ft/sec., divide the 2-foot distance by the time displayed by the Universal Counter after converting the time from milliseconds to seconds.

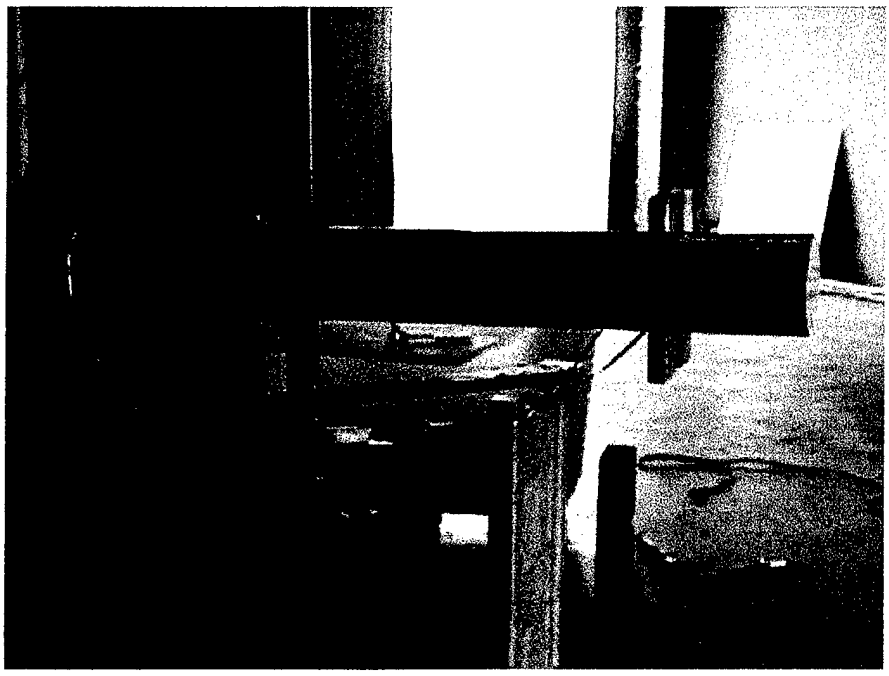

Figure 3.4. Timing Gates

Figure 3.5. Timer Display Equipment

3.2.2. The Reaction Frame

The reaction frame (Figures 3.6 and 3.7) supports the glazing frame assembly. The base of the reaction frame consists of two structural steel channels. Four anchor bolts tie the reaction frame into the concrete floor. These bolts keep the frame from sliding upon impact. The columns of the reaction frame consist of 5-in. structural steel tubes. Structural steel angles support the columns and maintain them in a vertical position. Both columns have 6-in. structural steel tube extensions mounted on top of them. The extensions support a 1-1/4-in. diameter steel bar placed horizontally between them. The glazing support frame hangs from this bar. An intermediate support limits the deflection of the steel bar.

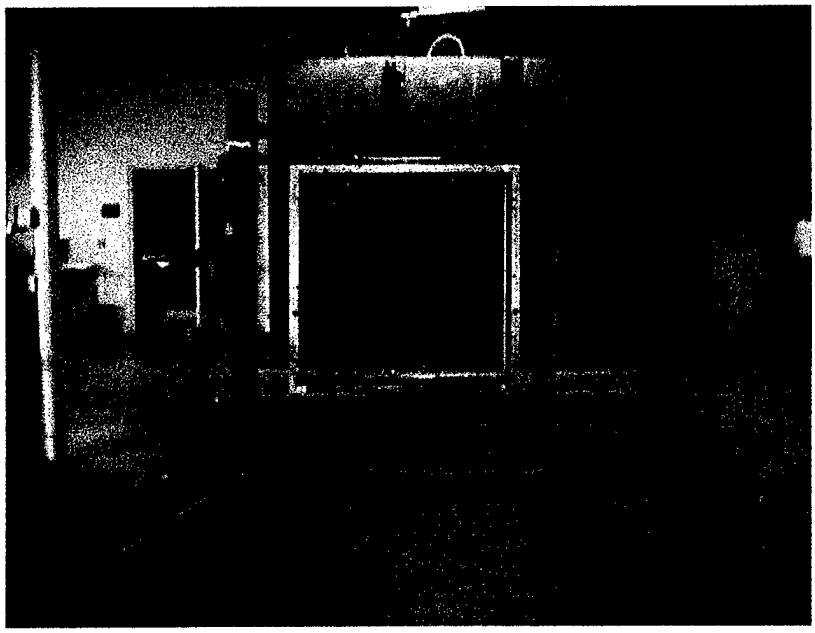

Figure 3.6. Reaction Frame and Glazing Support Frame, Front View

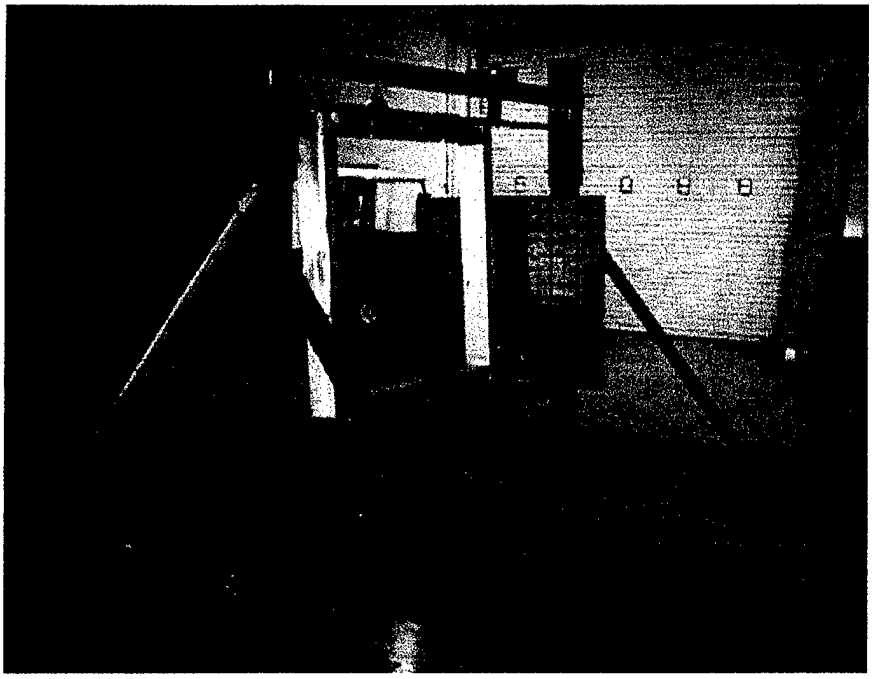

Figure 3.7. Reaction Frame and Glazing Support Frame, Profile View

3.2.3. The Glazing Support Frame

The glazing support frame consists of four identical aluminum channels welded to one another (Figure 3.8). The test specimens rest on the two glazing stops along the bottom channel of the glazing support frame (Figure 3.9). Outer glazing stops secure the test specimens to the glazing support frame with bolts (Figures 3.10, 3.11, and 3.12). The bolts pass through the outer glazing stops and both flanges of the glazing support frame. Neoprene strips line the edges of the glazing stops and the glazing support frame to prevent any glass to metal contact that may cause a premature failure of the lites. The neoprene provides 1 in. of bite to the test specimens. The glazing support frame hangs from two

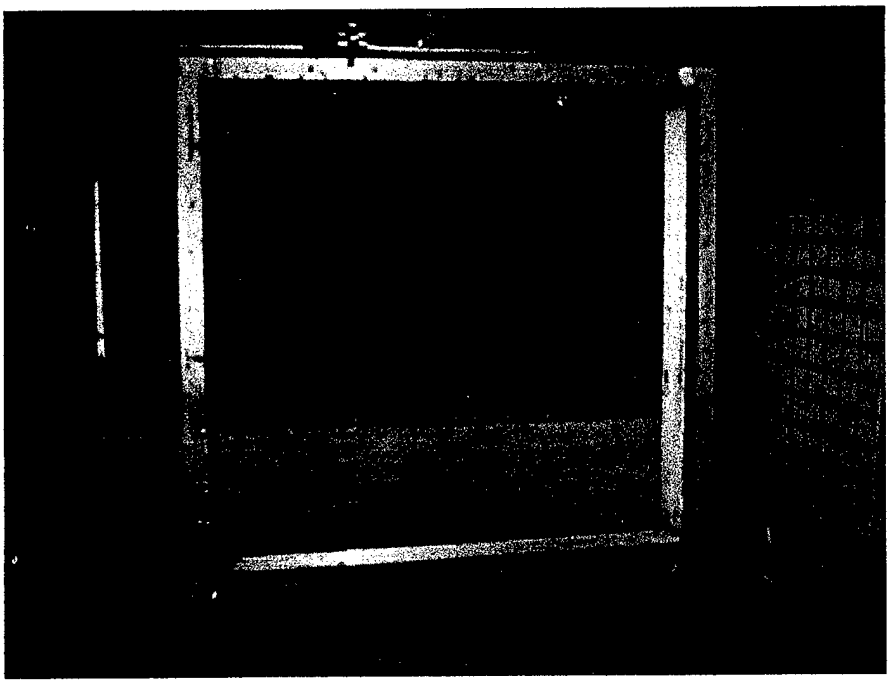

Figure 3.8. Glazing Support Frame

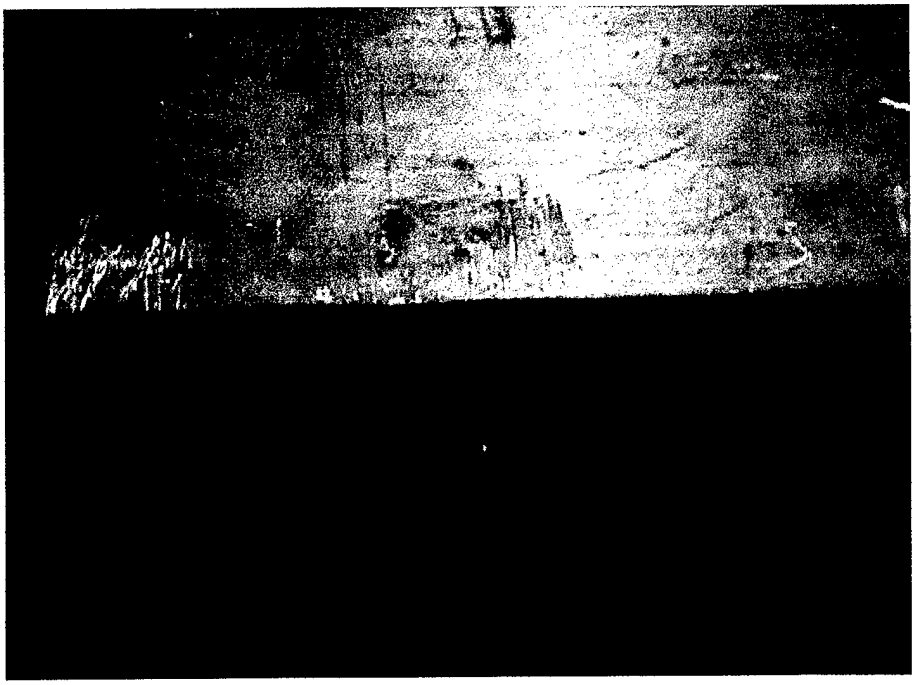

Figure 3.9. Glazing Stop at Bottom of Glazing Support Frame

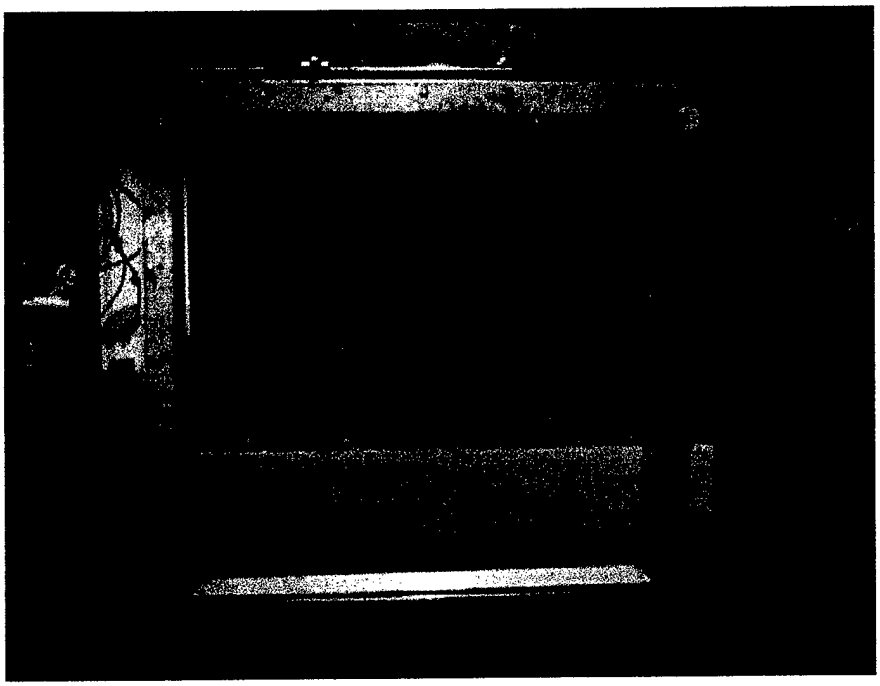

Figure 3.10. Glazing Support Frame with Outer Glazing Stops

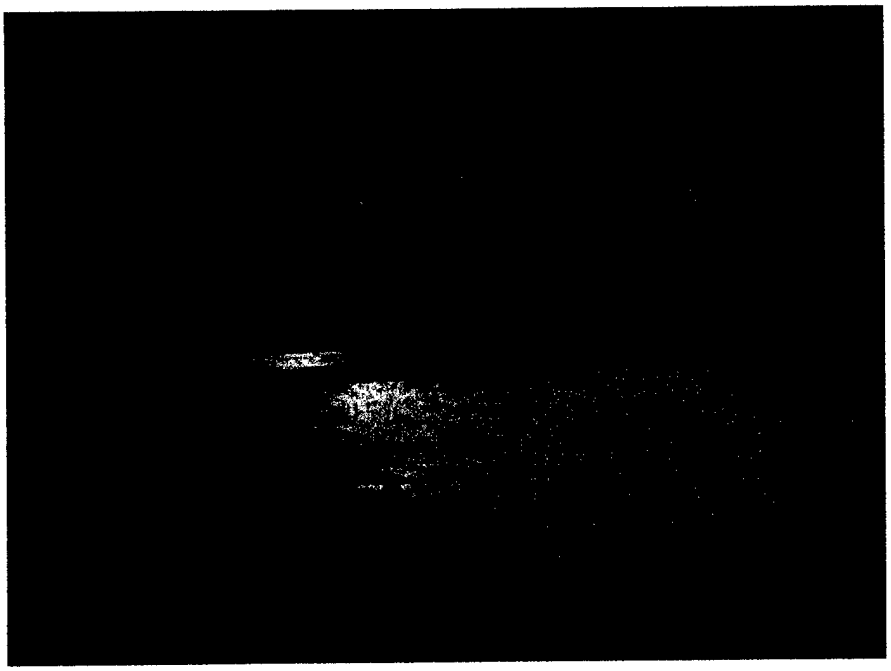

Figure 3.11. Inside of Outer Glazing Stop

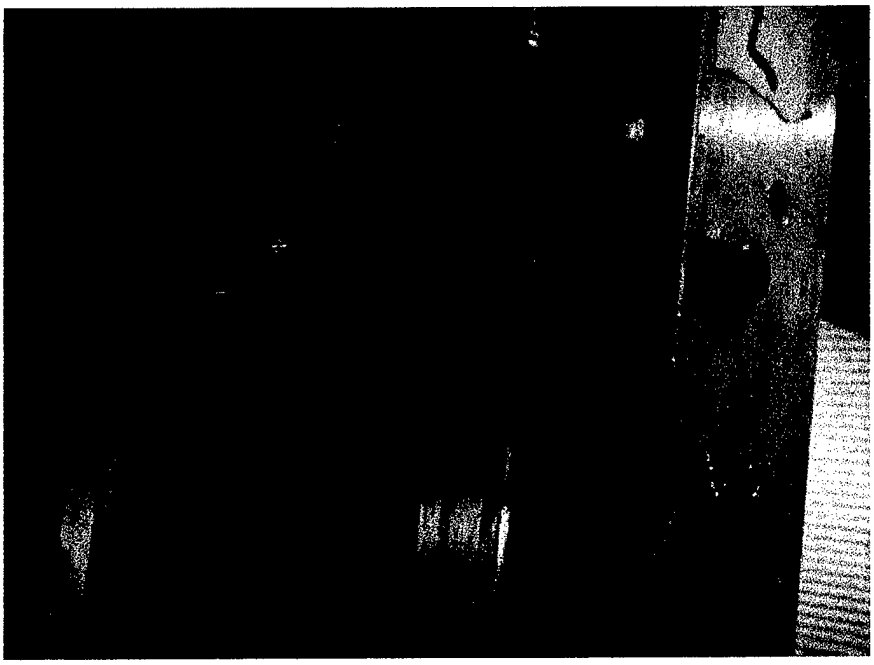

Figure 3.12. Bolted Connection of Outer Glazing Stop

tubular bearings. The bearings rest directly on the steel bar. A negligible amount of friction occurs during the rotation of the frame. WD-40 applied periodically to the bearings ensures that as little friction as possible is present.

3.2.4. Angle Measuring System

The glazing support frame rotates freely about the 1-1/4-in. steel bar after impact. An electronic device measures the angle that the frame swings through after impact. Using this angle and the principle of conservation of energy, the angular velocity of the frame immediately after impact can be calculated. A potentiometer mounted to a wooden block (Figure 3.13) that extends from the

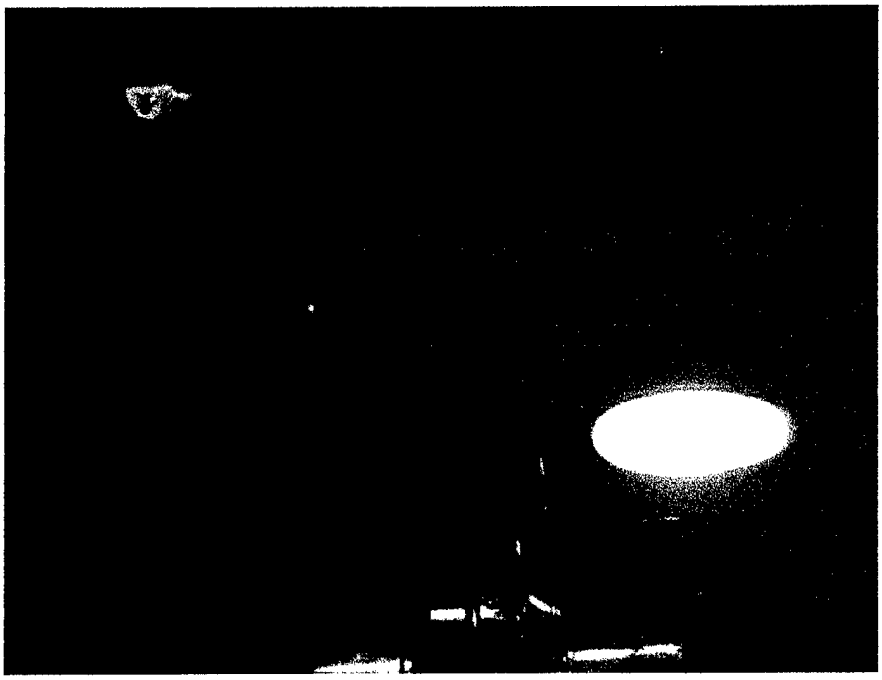

Figure 3.13. Potentiometer

intermediate supporting device varies a voltage as its shaft turns. A steel, semi-circular section is welded to one of the bearings of the glazing support frame. The diameter of the large section of the steel is known. The addition of a pulley to the shaft of the potentiometer creates the gear ratio system seen in Figure 3.14. String tied to a screw that rests on one side of the steel section wraps around the pulley and connects to another screw on the other side of the steel section via a spring. The spring serves to keep tension in the string and prevent slippage along the surface of the pulley. As the glazing support frame rotates after impact, so does the pulley. The angle that the frame moves through relates

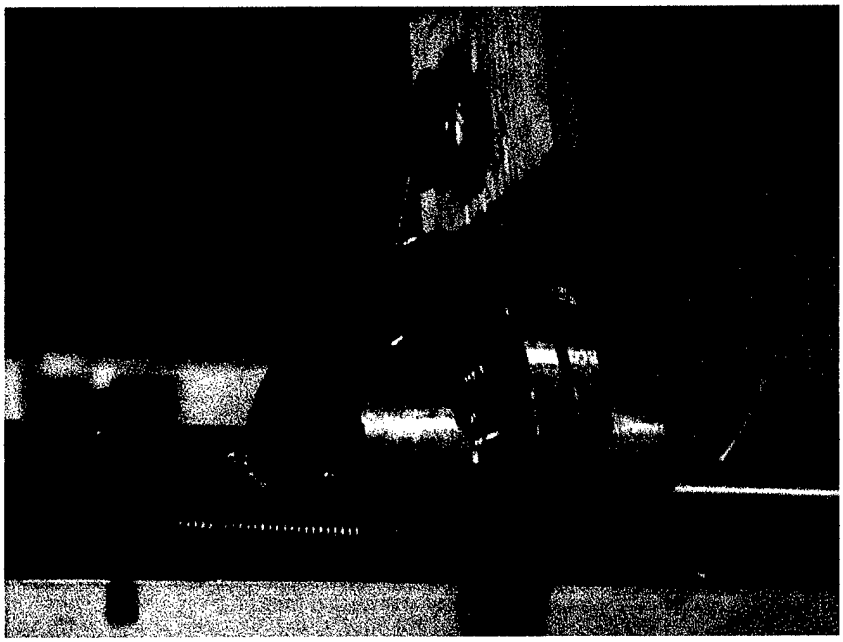

Figure 3.14. Angle Measuring System

to the potentiometer's voltage through a pre-determined calibration factor. The potentiometer connects to a digital oscilloscope (Figure 3.15). The oscilloscope records the voltage of the potentiometer versus time. An angle versus time plot is obtained from the oscilloscope's data.

The oscilloscope has the ability to record data over a wide variety of time intervals, but records the voltage every 0.002 seconds over a 2.5 second period for this experiment. The angular velocity of the glazing support frame results from taking the change in angle over a specified time period.

Since the potentiometer and the digital oscilloscope are electrical components, they might be subject to failure. Thus, a backup device exists for measuring the maximum angle that the frame reaches after impact. Figure 3.10

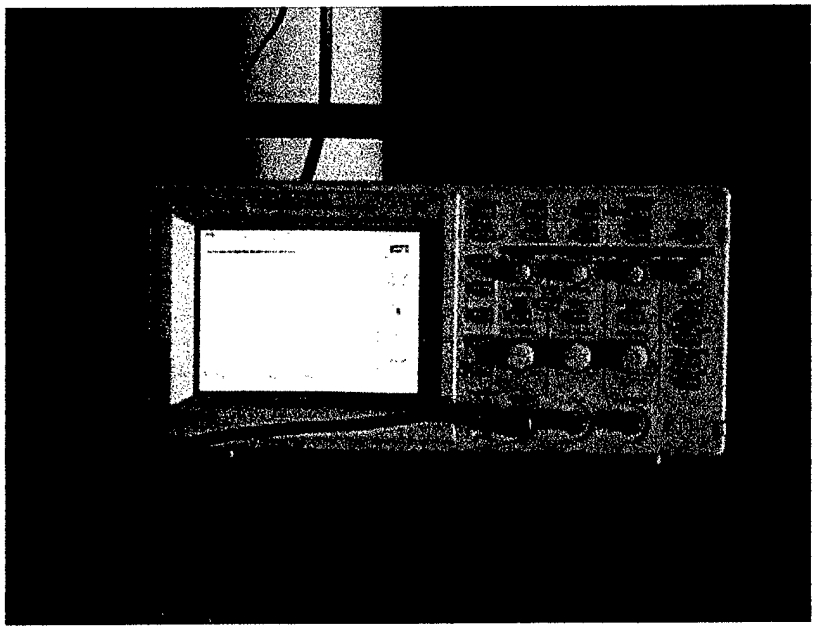

Figure 3.15. Digital Oscilloscope

shows two arms extending from the right side of the glazing support frame. A board sits to the right of these arms. Markers placed in the arms (Figure 3.16), mark the position of the frame as it swings. Springs placed on the back of the markers keep them in contact with the board. A piece of paper placed over the board during each test run records the position of the glazing support frame.

3.2.5. Timber Missiles

As mentioned in the experimental plan, this experiment uses missiles of different masses. A missile consists of a 2x4-in. timber member. The scale has the ability to measure the weight of the missiles to the nearest 0.05 lb. Two steel

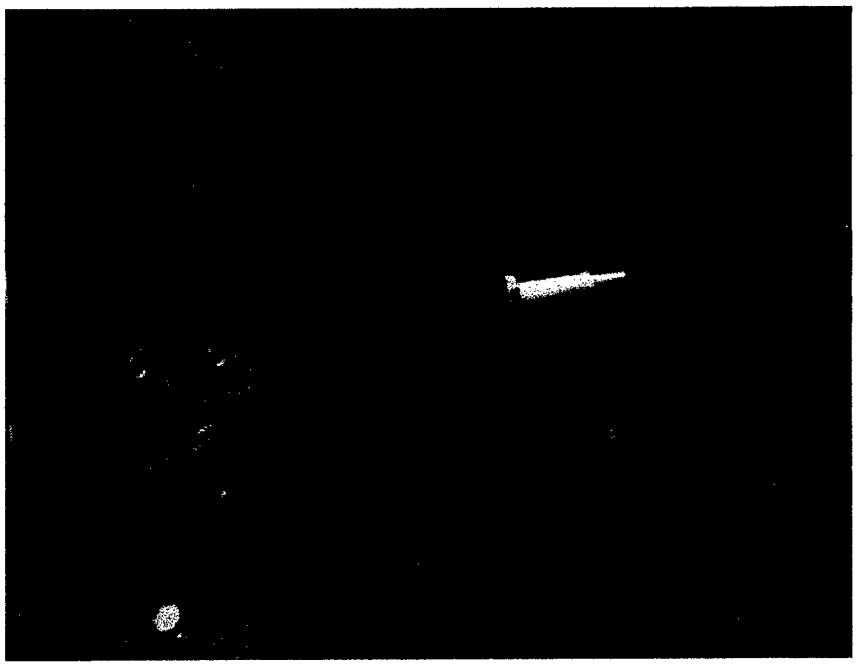

Figure 3.16. Backup Pen Device

plates bolted to the 9.00-lb. missile form an 18.0-lb. missile. A plastic sabot (Figure 3.17) attaches to the non-impact end of the missile in order to facilitate the launch of a missile. The length and weight of the missile includes the length and weight of the sabot.

3.2.6. Video Recording System

The final component is a Sony hi-fi, 8-mm., VHS recorder. The 8-mm. tapes provide the ability to estimate the speed of the missile in the horizontal direction after impact. The missile speed after impact is the final component needed to determine whether conservation of angular momentum occurs within

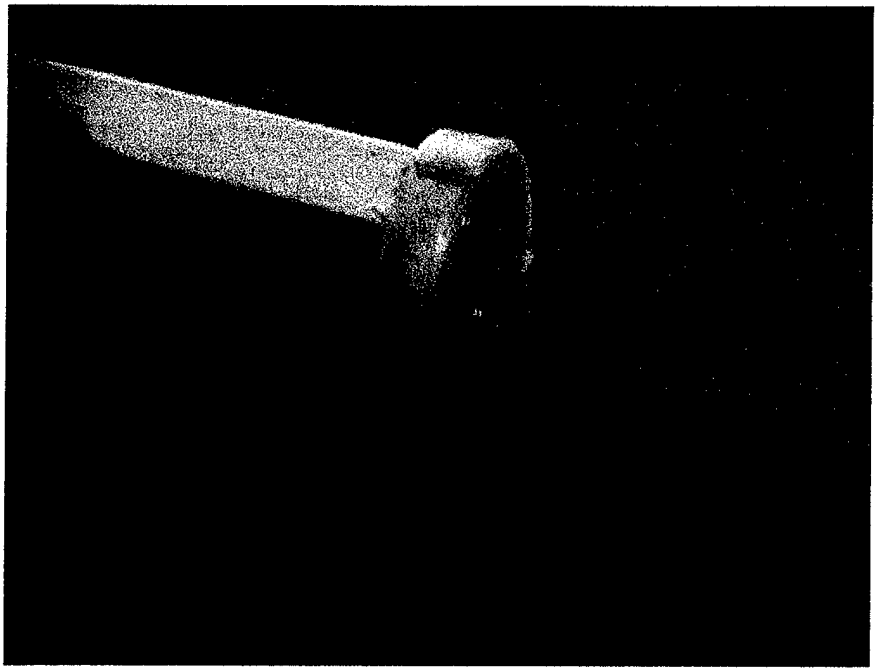

Figure 3.17. Sabot

the system. An 8x4-ft. board is placed as a backdrop behind the traveling missile (Figure 3.18). The board has reference lines painted at 6-in. intervals on it. The missiles have reference lines marked at 3-in. intervals on them. The video camera records at 30 frames per second. The velocity of the missile after impact is obtained from the number of reference lines on the missile that pass a reference line on the board in a set number of frames.

3.3. Experimental Procedure

The same experimental procedure applies for the aluminum plate and each type of glass. A test run on each test specimen consists of four major

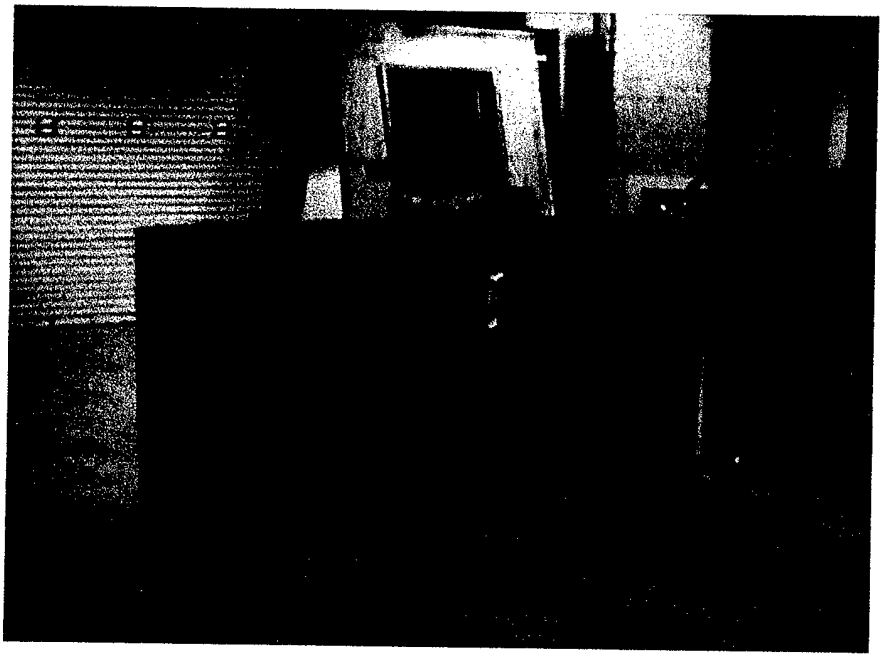

Figure 3.18. Missile Backdrop

steps:

1. Installation of the test specimen.
2. Determination of the center of mass and mass moment of inertia.
3. Missile impact near center of mass.
4. Missile impact near lower left or right corner, if possible.

Researchers follow the same test procedure for each test run. The researchers recorded all pertinent data for each test run on a data sheet.

3.3.1. Installation of Test Specimen

The first step consists of recording the glass type, its heat treatment, and the lites nominal thickness from the label on the glass lite prior to installing a glass lite. For the aluminum plate, the first step consists of recording the nominal thickness of the plate. Researchers then designate a series number for classification purposes. The determination of the weight, thickness, and length of the lite from top to bottom for each test specimen is the last step taken before installing the test specimen in the glazing support frame. Researchers averaged five data measurements in order to obtain a mean value of the measured property.

The outer glazing stops secure the test specimen in place with bolted connections. The space between the neoprene and the surface of the test specimen is 0.01 in. The author used a feeler gage to check this spacing. Small, black, plastic shims placed between the edges of the outer supports and the main portion of the glazing support frame prevent any glass to metal contact during the impact.

3.3.2. Determination of the Center of Mass and the Mass Moment of Inertia

After installing the test specimen, the potentiometer and oscilloscope aid the researchers in determining the vertical location of the center of mass of the glazing support frame. By applying a known force to the lower end of the frame

and measuring the angle through which the frame swings, the vertical location of the glazing support frame's center of mass can be found using statics. Next, the frame is released from rest at a known angle. The angle of the frame versus time as it passes through its natural resting position (zero degrees) is recorded. By calculating the change in angle over a specified time period, the researchers determine the glazing support frame's angular velocity. The change in angle is the change in voltage over a 100 millisecond time frame multiplied by the appropriate calibration factor. The principle of conservation of energy leads to the calculation of the glazing support frame's mass moment of inertia.

3.3.3. Missile Impact Near Center of Mass

The window glass tested must undergo two missile impacts if it is not damaged by the first impact. The first impact occurs within a 6-in. radius circle around the center of mass of the glazing support frame. The second impact, discussed in the next section, is near a lower corner.

The first step consists of cutting a missile to the desired length and weight. Next, researchers aim the cannon to create a missile impact at the desired location. Researchers then set up the pen and paper backup system as well as the oscilloscope. After setting up the angle measuring system, the researcher records the at rest voltage displayed by the oscilloscope and turns on the video camera. Researchers launch the missile by pressurizing the air

tank to the required pressure and releasing the ball valve at the rear of the barrel.

After impact, researchers download the data from the oscilloscope and save it on a computer. Next, the researchers record the maximum voltage difference observed and the missile impact location. The voltage difference determines the angle that the frame swings through after impact. The researchers determine the glazing support frame's center of mass and mass moment of inertia again after impact if appreciable damage occurred. Researchers launch a second missile if the test specimen is still intact within the glazing support frame.

3.3.4. Missile Impact Near Lower Corner

The second missile is aimed to strike the test specimen within an area 6 in. from any supporting member in the lower left or right corner of the lite. The author alternated the location (left versus right) of the impact point in order to minimize the deformation of the glazing support frame. Researchers follow the same procedure for firing the second missile at the lower corner as with the first one on the center of mass.

CHAPTER 4

DISCUSSION OF RESULTS

4.1. Data Analysis

The data analysis consisted of determining the properties of motion of each component of the system before and after the impact. The system consists of the missile and the glass support frame with a test specimen installed. Figure 4.1 shows the state of the system immediately before impact. Figure 4.2 shows the state of the system immediately after impact. The corresponding axis systems on each figure indicate the positive directions of motion.

The first step is to determine the angular velocity of the glazing support frame after impact. Equation 4.1 shows the formula used to determine the angular velocity of the frame after impact.

$$\omega_{frame}\ (\text{rad/s}) = \sqrt{(2 * W * y_c * (1 - \cos\theta) / I_o} \qquad (4.1)$$

W denotes the total weight of the glazing support frame and test specimen, ω denotes the angular velocity of the frame after impact, y_c denotes the vertical distance from the center of rotation to the mass center of the glazing support frame, θ denotes the maximum angle that the frame passes through after impact, and I_o denotes the mass moment of inertia of the glass support frame about point O, the center of rotation for the glazing frame.

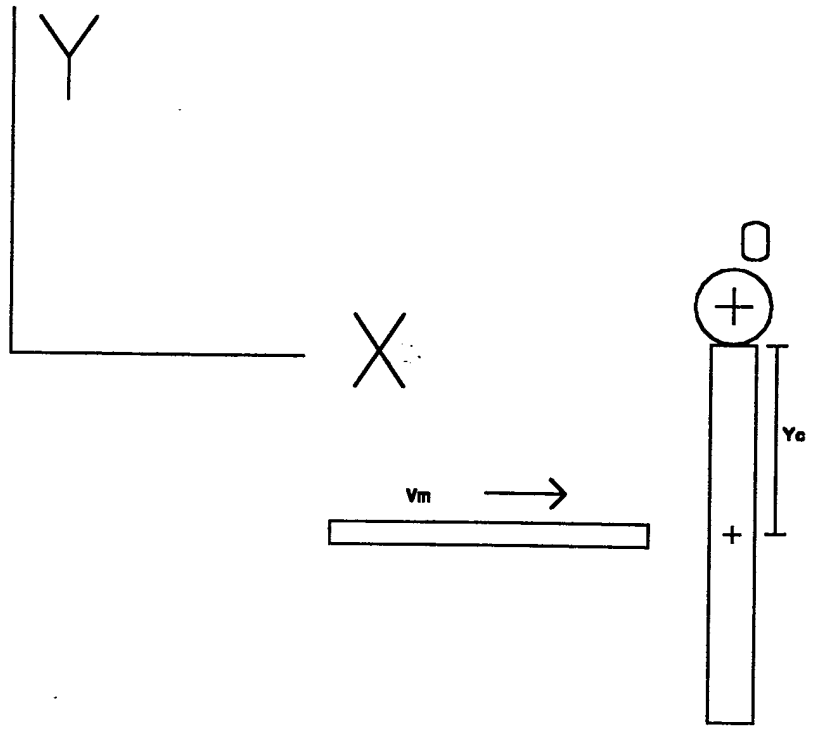

Figure 4.1. Status of System Components Immediately Before Impact

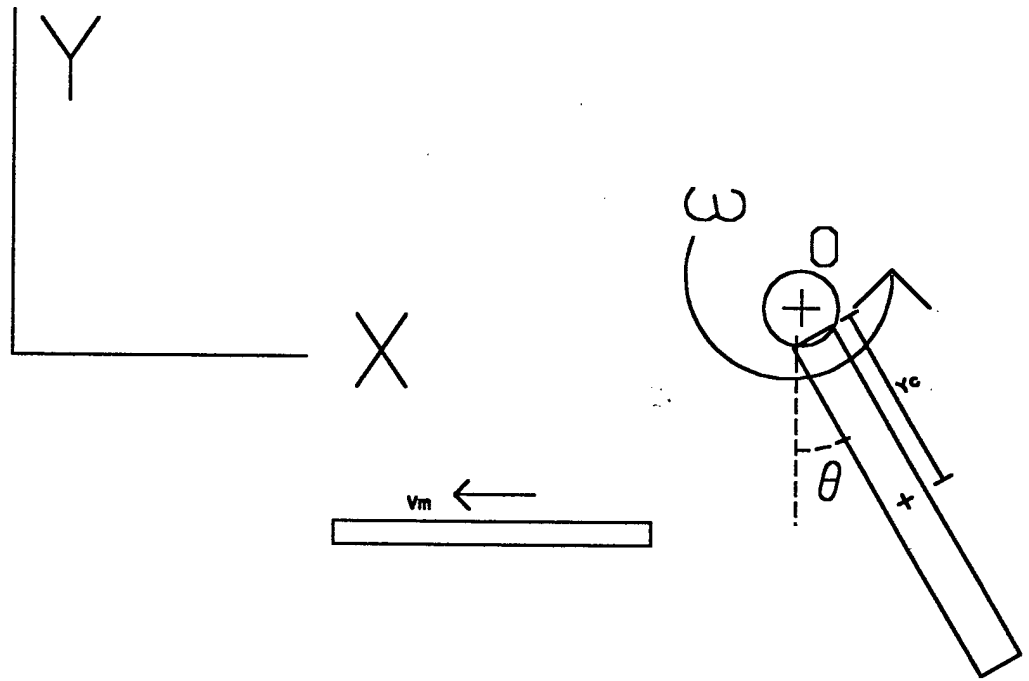

Figure 4.2. Status of System Components Immediately After Impact (Missile Rebound)

After determining the angular velocity of the glazing support frame after impact, researchers determined the kinetic energy of each component of the system before and after the impact. Equation 2.1 gives the formula that defines the energy of the missile.

$$T = 1/2\ mv^2 \tag{2.1}$$

Equation 2.1 is valid for calculating the kinetic energy of the missile before and after impact. Equation 2.2 displays the equation for determining the kinetic energy of the frame after impact.

$$T = 1/2\ I_o\omega^2 \tag{2.2}$$

The next step in the analysis of the data consists of calculating the angular momentum of each component of the system with respect to the axis of rotation. Equation 2.6 illustrates the angular momentum calculation of the frame after impact.

$$H = I_o\omega \tag{2.6}$$

Equation 2.5 illustrates how to calculate the angular momentum of the missile before and after impact about point O.

$$H = mvh \tag{2.5}$$

Equation 2.5 is valid for calculating the angular momentum of the missile about point O before and after impact. In equation 2.5, h is the vertical distance from the impact location to the point O.

The angular momentum of the system is the sum of the angular momentum of its corresponding parts, the missile and the frame. Equation 4.2 defines the angular momentum of the system.

$$H_{sys} = H_{missile} + H_{frame} \tag{4.2}$$

Equation 4.2 is valid for calculating the system angular momentum both before and after impact. For conservation of angular momentum, the values for the angular momentum of the system before and after impact should be equal.

A problem exists when analyzing the system momentum after impact when a missile passes through a test specimen. When a missile perforates a laminated glass lite specimen, the missile remains in contact with the specimen until it has passed completely through the lite. The prolonged contact results in the missile exerting frictional forces on the laminated glass while the missile passes through it. The friction forces cause the frame to swing further than it would if the impulse from the impact was the only force acting on the test specimen. The use of an incorrect maximum angle results in the incorrect calculation of the glazing support frame's angular velocity. This leads to the calculation of an incorrect angular momentum for the glass support frame after impact. Also, the corresponding energy transferred to the glazing support frame is incorrect. The addition of friction forces is not a problem when a missile perforates an annealed or tempered monolithic lite specimen because the fractured glass does not remain in the glazing support frame upon failure.

To correct this problem, researches used the oscilloscope to determine the angular velocity of the frame immediately after impact. Figure 4.3 shows typical data recorded by the oscilloscope during a missile impact. The horizontal line shows that the frame is at rest before impact. As the slope of the line begins to fall, this represents the motion of the glazing support frame immediately after impact. The change in the angle of the glazing support frame over a time period comprises the angular velocity of a frame. Using the Wavestar software acquired with the oscilloscope, one can see the cursors used to determine the coordinates of the data points (Figure 4.3). The difference in the voltages divided by the time between the two points lends itself to the calculation of the angular velocity of the frame immediately after impact. The researchers used this process for the test specimens which cause the missile to rebound after impact. Little difference exists between the angular velocities of the two procedures and the resulting angular momentum of the glazing support frame. Table 4.1 lists the angular momentum of the frame after impact calculated using both methods for the test specimens that resisted the missile impact. Both methods appear to be acceptable for this research.

The author decided to use the method based on the maximum angle achieved as the basis of calculating the angular momentum of the frame after impact for all series except for those having a missile perforating a laminated glass lite. The reason behind this choice is that the method appears to give

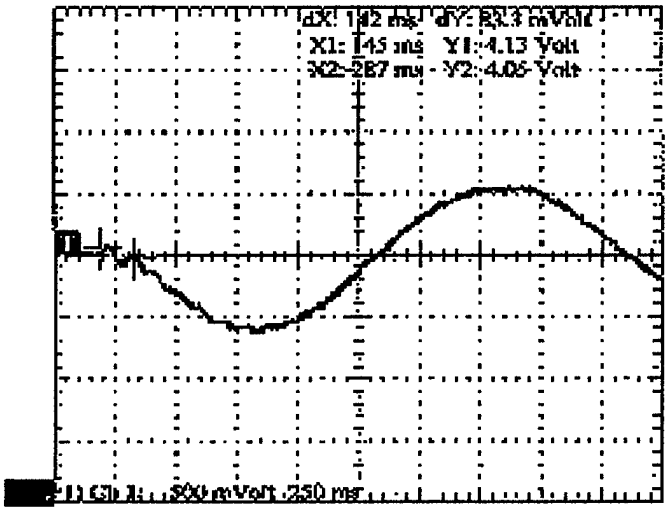

(a) Center Of Mass Impact

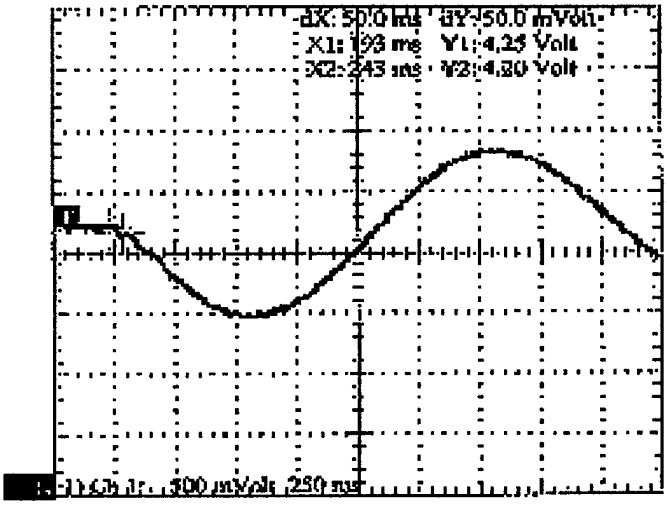

(b) Lower Corner Impact

Figure 4.3. Oscilloscope Data for Test Run LAM02

Table 4.1. Comparison of Methods of Obtaining Frame's Angular Velocity after Impact

	Center of Mass Impact		Lower Corner Impact	
Series	Angular Momentum Of Frame from Maximum Angle Method (ft-lb-sec.)	Angular Momentum Of Frame Obtained Directly From Oscilloscope (ft-lb-sec.)	Angular Momentum Of Frame from Maximum Angle Method (ft-lb-sec.)	Angular Momentum Of Frame Obtained Directly From Oscilloscope (ft-lb-sec.)
HS901	35.2	34.3	54.0	51.4
HS902	33.8	33.2	54.3	51.4
HS903	31.2	----------[c]	79.2	79.0
HS904	39.4	38.9	66.1	63.4
HS905	22.9	21.5	42.2	41.5
HS906	23.3	23.0	38.2	38.8
HS907	29.8	----------[c]	52.9	53.0
HS908	22.2	23.3	39.0	35.5
HS909	49.1	50.9	72.2	69.3
ALM01	21.8	20.9	45.7	41.2
ALM02	22.6	22.8	43.3	44.9
ALM03	22.9	22.1	40.5	41.5
ALM04	37.6	37.6	50.5	----------[c]
ALM05	39.0	40.0	53.0	52.5
ALM06	35.6	34.5	60.9	60.9
ALM07	55.1	53.4	76.6	76.4
ALM08	44.8	41.8	81.5	85.3
ALM09	56.9	60.6	82.5	80.0
TPM2A	34.6	33.8	18.4	----------[b]

[b] - Glass Shattered Upon Impact

[c] - No Scope Data

more accurate results. Immediately after impact, vibrations pass through the test specimen and into the frame. These vibrations affect the oscilloscope. One can see the effect of the waves on the oscilloscope in Figure 4.3a. The area just to the right of the horizontal line in this figure shows the vibrations passing through the oscilloscope. The vibrations damp out by the time the glass support frame reaches its maximum angle after impact.

4.2. Analysis of Results

During the experiment, three distinct outcomes resulted from the impacts. The first outcome consisted of the missile perforating the test specimen while the test specimen remained in the glazing support frame. This outcome occurred for series LAM and LHS. The second outcome resulted in the missile perforating the test specimen while the test specimen fractured and fell out of the glazing support frame. This outcome occurred for series MON and the lower corner shot of series TPM. The final outcome resulted in the missile rebounding off the test specimen after impact. This outcome corresponds to series ALM, HS9, and the center of mass impact of series TPM.

Tables 4.2-4.12 list the angular momentum of the system for each test series. In Tables 4.2-4.12, the first five columns correspond to data measured directly. The seventh column corresponds to the angular velocity of the frame after impact determined using Equation 4.1. Equation 2.6 is used to calculate

Table 4.2. Angular Momentum for Test Series LAM, Center of Mass Impact

Series	Missile Weight (lb.)	Missile Velocity Before Impact (ft/sec.)	Missile Velocity After Impact (ft/sec.)	Vertical Impact Location (in.)	Linear Impulse (lb-sec.)	Angular Velocity of Frame After Impact (rad/sec.)	Angular Momentum of Frame After Impact (ft-lb-sec.)	Missile Angular Momentum After Impact (ft-lb-sec.)	System Angular Momentum Before Impact (ft-lb-sec.)	System Angular Momentum After Impact (ft-lb-sec.)
LAM01[d]	9.00	52.8	45.0	18.75	1.83	0.076	2.86	19.7	23.0	22.5
LAM02[d]	8.90	48.6	41.3	22.25	0.70	0.034	1.29	21.2	24.9	22.4
LAM03[d]	9.00	52.6	51.3	23.50	1.63	0.076	3.20	28.1	28.8	31.3
LAM04[d]	4.50	71.3	60.0	24.00	1.91	0.087	3.81	16.8	19.9	20.6
LAM05[d]	4.50	73.3	60.0	22.25	1.69	0.070	3.14	15.5	19.0	18.7
LAM06[d]	4.50	74.0	63.8	21.50	1.95	0.083	3.50	16.0	18.5	19.5

[d] - Missile Passed Through Test Specimen

Table 4.3. Angular Momentum for Test Series LHS, Center of Mass Impact

Series	Missile Weight (lb.)	Missile Velocity Before Impact (ft/sec.)	Missile Velocity After Impact (ft/sec.)	Vertical Impact Location (in.)	Linear Impulse (lb-sec.)	Angular Velocity of Frame After Impact (rad/sec.)	Angular Momentum of Frame After Impact (ft-lb-sec.)	Missile Angular Momentum After Impact (ft-lb-sec.)	System Angular Momentum Before Impact (ft-lb-sec.)	System Angular Momentum After Impact (ft-lb-sec.)
LHS01[d]	8.90	51.4	45.0	25.50	2.30	0.119	4.88	26.4	30.2	31.3
LHS02[d]	9.00	51.8	48.8	24.25	0.76	0.036	1.53	27.6	29.2	29.1
LHS03[d]	9.00	51.8	43.1	22.75	1.77	0.075	3.35	22.8	27.5	26.2

[d] - Missile Passed Through Test Specimen

Table 4.4. Angular Momentum for Test Series HS9, Center of Mass Impact

Series	Missile Weight (lb.)	Missile Velocity Before Impact (ft/sec.)	Missile Velocity After Impact (ft/sec.)	Vertical Impact Location (in.)	Linear Impulse (lb-sec.)	Angular Velocity of Frame After Impact (rad/sec.)	Angular Momentum of Frame After Impact (ft-lb-sec.)	Missile Angular Momentum After Impact (ft-lb-sec.)	System Angular Momentum Before Impact (ft-lb-sec.)	System Angular Momentum After Impact (ft-lb-sec.)
HS901	9.00	53.0	-5.8	26.25	16.1	0.718	35.2	-3.5	32.4	31.6
HS902	9.00	51.6	-6.3	24.50	16.6	0.704	33.8	-3.6	29.7	30.2
HS907[c]	9.00	51.2	-3.1	24.50	14.6	0.659	29.8	-1.8	29.2	28.0
HS903[c]	18.0	37.3	-3.8	16.50	22.7	0.707	31.2	-2.9	28.6	28.3
HS904	18.0	37.0	-5.2	21.25	22.2	0.845	39.4	-5.1	36.6	34.2
HS909	18.0	34.7	-3.3	27.75	21.2	1.01	49.1	-4.3	44.9	44.8
HS905	4.55	72.9	-4.6	24.00	11.5	0.475	22.9	-1.3	20.6	21.6
HS906	4.50	74.6	-7.5	24.50	11.4	0.496	23.3	-2.1	21.3	21.1
HS908	4.50	71.4	-3.8	25.25	10.6	0.487	22.2	-1.1	21.0	21.1

[c] - No Scope Data

Table 4.5. Angular Momentum for Test Series TPM2, Center of Mass Impact

Series	Missile Weight (lb.)	Missile Velocity Before Impact (ft/sec.)	Missile Velocity After Impact (ft/sec.)	Vertical Impact Location (in.)	Linear Impulse (lb-sec.)	Angular Velocity of Frame After Impact (rad/sec.)	Angular Momentum of Frame After Impact (ft-lb-sec.)	Missile Angular Momentum After Impact (ft-lb-sec.)	System Angular Momentum Before Impact (ft-lb-sec.)	System Angular Momentum After Impact (ft-lb-sec.)
TPM2D	9.00	51.5	-10.0	25.50	16.3	0.698	34.6	-5.9	30.6	28.7

Table 4.6. Angular Momentum for Test Series ALM, Center of Mass Impact

Series	Missile Weight (lb.)	Missile Velocity Before Impact (ft/sec.)	Missile Velocity After Impact (ft/sec.)	Vertical Impact Location (in.)	Linear Impulse (lb-sec.)	Angular Velocity of Frame After Impact (rad/sec.)	Angular Momentum of Frame After Impact (ft-lb-sec.)	Missile Angular Momentum After Impact (ft-lb-sec.)	System Angular Momentum Before Impact (ft-lb-sec.)	System Angular Momentum After Impact (ft-lb-sec.)
ALM01	4.50	73.2	-7.9	23.25	11.3	0.545	21.8	-2.1	19.8	19.7
ALM02	4.50	73.6	-9.4	21.75	12.5	0.573	22.6	-2.4	18.6	20.2
ALM03	4.50	72.6	-10.2	23.75	11.6	0.574	22.9	-2.8	20.1	20.1
ALM04	9.00	49.4	-17.5	25.00	18.0	0.920	37.6	-10.2	28.7	27.4
ALM05	9.00	49.4	-15.0	24.50	19.1	0.921	39.0	-8.6	28.2	30.5
ALM06	8.90	48.2	-12.3	26.00	16.4	0.871	35.6	-7.4	28.9	28.3
ALM07	18.0	34.8	11.9	24.38	27.1	1.36	55.1	13.5	39.5	41.4
ALM08	18.0	37.4	-10.0	22.25	24.2	1.10	44.8	-10.4	38.7	34.4
ALM09	18.1	37.2	-12.9	24.25	28.2	1.44	56.9	-14.6	42.2	42.3

Table 4.7. Angular Momentum for Test Series MON, Center of Mass Impact

Series	Missile Weight (lb.)	Missile Velocity Before Impact (ft/sec.)	Missile Velocity After Impact (ft/sec.)	Vertical Impact Location (in.)	Linear Impulse (lb-sec.)	Angular Velocity of Frame After Impact (rad/sec.)	Angular Momentum of Frame After Impact (ft-lb-sec.)	Missile Angular Momentum After Impact (ft-lb-sec.)	System Angular Momentum Before Impact (ft-lb-sec.)	System Angular Momentum After Impact (ft-lb-sec.)
MON01[b,c,d]	9.00	49.2	45.0	24.00	1.06	0.050	2.12	25.2	27.5	27.3
MON02[b,c,d]	9.00	50.7	52.5[d]	25.00	0.21	0.009	0.43	30.6	29.5	31.0
MON03[b,c,d]	9.00	53.0	60.0[d]	24.25	0.20	0.011	0.41	33.9	29.9	34.3

[b] - Glass Shattered Upon Impact [c] - No Scope Data [d] - Missile Passed Through Test Specimen

Table 4.8. Angular Momentum for Test Series LAM, Lower Corner Impact

Series	Missile Weight (lb.)	Missile Velocity Before Impact (ft/sec.)	Missile Velocity After Impact (ft/sec.)	Vertical Impact Location (in.)	Linear Impulse (lb-sec.)	Angular Velocity of Frame After Impact (rad/sec.)	Angular Momentum of Frame After Impact (ft-lb-sec.)	Missile Angular Momentum After Impact (ft-lb-sec.)	System Angular Momentum Before Impact (ft-lb-sec.)	System Angular Momentum After Impact (ft-lb-sec.)
LAM01[d]	9.00	50.0	37.5	41.00	3.19	0.297	10.9	35.8	47.8	46.7
LAM02[d]	9.00	53.9	52.5	43.50	0.71	0.068	2.59	53.2	54.6	55.8
LAM03[d,c]	9.00	48.7	43.8	44.25	--------	No Data	No Data	45.1	50.2	45.1
LAM04[d]	4.50	71.6	67.5	43.00	1.35	0.110	4.82	33.8	35.9	38.6
LAM05[d]	4.45	73.0	75.0	41.50	0.48	0.082	1.65	35.8	34.9	39.5
LAM06[d,e]	4.50	73.8	71.3	42.50	1.30	0.109	4.62	35.3	36.5	39.9

c - Oscilloscope Failed to Record Data [d] - Missile Passed Through Test Specimen [e] - Missile Stopped in Glass

Table 4.9. Angular Momentum for Test Series LHS, Lower Corner Impact

Series	Missile Weight (lb.)	Missile Velocity Before Impact (ft/sec.)	Missile Velocity After Impact (ft/sec.)	Vertical Impact Location (in.)	Linear Impulse (lb-sec.)	Angular Velocity of Frame After Impact (rad/sec.)	Angular Momentum of Frame After Impact (ft-lb-sec.)	Missile Angular Momentum After Impact (ft-lb-sec.)	System Angular Momentum Before Impact (ft-lb-sec.)	System Angular Momentum After Impact (ft-lb-sec.)
LHS01[d]	9.00	48.0	35.0	44.50	3.29	0.297	12.2	36.3	49.7	48.5
LHS02[d]	9.00	48.4	33.8	42.50	3.47	0.289	12.3	33.5	47.9	45.7
LHS03[d]	9.00	51.1	35.6	41.00	4.16	0.319	14.2	34.0	48.8	48.2

[d] - Missile Passed Through Test Specimen [e] - Missile Stopped in Glass

Table 4.10. Angular Momentum for Test Series HS9, Lower Corner Impact

Series	Missile Weight (lb.)	Missile Velocity Before Impact (ft/sec.)	Missile Velocity After Impact (ft/sec.)	Vertical Impact Location (in.)	Linear Impulse (lb-sec.)	Angular Velocity of Frame After Impact (rad/sec.)	Angular Momentum of Frame After Impact (ft-lb-sec.)	Missile Angular Momentum After Impact (ft-lb-sec.)	System Angular Momentum Before Impact (ft-lb-sec.)	System Angular Momentum After Impact (ft-lb-sec.)
HS901	9.00	52.3	-0.6	40.50	16.0	1.10	54.0	-0.6	49.4	53.4
HS902	9.00	51.8	2.5	41.50	15.7	1.13	54.3	2.4	50.1	51.9
HS907	9.00	51.6	1.7	44.25	14.3	1.17	52.9	1.8	53.1	54.6
HS903	18.0	38.8	3.8	48.00	19.8	1.79	79.2	8.5	86.4	87.5
HS904	18.0	36.3	0.8	39.25	20.2	1.42	66.1	1.5	66.4	67.7
HS909	18.0	33.1	2.3	45.75	18.9	1.49	72.2	4.9	70.6	77.1
HS905	4.50	72.1	-5.2	43.50	11.6	0.876	42.2	-2.6	36.5	39.6
HS906	4.50	72.2	-3.8	42.00	10.9	0.816	38.2	-1.9	35.3	36.4
HS908	4.50	69.6	-3.3	43.75	10.7	0.854	39.0	-1.7	35.4	37.3

Table 4.11. Angular Momentum for Test Series TPM2, Lower Corner Impact

Series	Missile Weight (lb.)	Missile Velocity Before Impact (ft/sec.)	Missile Velocity After Impact (ft/sec.)	Vertical Impact Location (in.)	Linear Impulse (lb-sec.)	Angular Velocity of Frame After Impact (rad/sec.)	Angular Momentum of Frame After Impact (ft-lb-sec.)	Missile Angular Momentum After Impact (ft-lb-sec.)	System Angular Momentum Before Impact (ft-lb-sec.)	System Angular Momentum After Impact (ft-lb-sec.)
TPM2D[b,d]	9.00	54.0	26.3	43.00	5.13	0.569	18.4	26.3	50.5	44.7

[b] - Glass Shattered Upon Impact

[d] - Missile Passed Through Test Specimen

Table 4.12. Angular Momentum for Test Series ALM, Lower Corner Impact

Series	Missile Weight (lb.)	Missile Velocity Before Impact (ft/sec.)	Missile Velocity After Impact (ft/sec.)	Vertical Impact Location (in.)	Linear Impulse (lb-sec.)	Angular Velocity of Frame After Impact (rad/sec.)	Angular Momentum of Frame After Impact (ft-lb-sec.)	Missile Angular Momentum After Impact (ft-lb-sec.)	System Angular Momentum Before Impact (ft-lb-sec.)	System Angular Momentum After Impact (ft-lb-sec.)
ALM01[f]	4.50	72.3	No Data	42.50	12.9	1.14	45.7	No Data	35.8	45.7
ALM02	4.50	71.2	-10.4	44.50	11.7	1.10	43.3	-5.4	36.9	37.9
ALM03	4.50	71.5	-12.5	42.75	11.4	1.02	40.5	-6.2	35.6	34.3
ALM04[c]	9.00	48.0	-8.8	41.00	14.8	1.24	50.5	-8.4	45.9	42.1
ALM05	9.00	46.3	-8.8	42.00	15.1	1.25	53.0	-8.6	45.3	44.5
ALM06	8.90	49.0	-6.7	46.75	15.6	1.49	60.9	-7.2	52.7	53.7
ALM07	18.1	34.2	-2.5	44.50	20.7	1.89	76.6	-5.2	71.2	71.4
ALM08	18.0	37.0	-2.1	42.75	22.9	2.01	81.5	-4.2	73.7	77.4
ALM09	18.1	37.9	-6.7	38.00	26.1	2.08	82.5	-11.9	67.3	70.6

[c] - No Scope Data

[f] - Missile Data After Impact Not Obtained

the angular momentum of the frame after impact in eighth column. The ninth column uses Equation 2.5 to determine the missile's angular momentum after impact about point O. Finally, Equation 4.2 leads to the calculation of the system's angular momentum before and after impact, displayed in the eleventh and twelfth columns respectively. The missile's angular momentum before impact constitutes the total system's angular momentum since the frame is at rest before impact.

The data in Tables 4.2-4.12 shows that conservation of angular momentum occurs for the system in this experiment. The data suggests that missiles exert a larger impulse on the test specimen when the missile does not perforate the test specimen. For a given test series, the data suggest that a relationship between the impulse that acts upon the frame and the missile's initial momentum exists. The data also suggests that higher initial missile momentum results in it exerting a correspondingly larger impulse acting on the glazing support frame. The larger impulse gives the glazing support assembly a larger angular momentum after impact. The data also suggests that a smaller impulse acts on a test specimen if the missile perforates the test specimen.

Tables 4.13-4.23 list the kinetic energy associated with each component of the system before and after impact. In Tables 4.13-4.23, the first four columns correspond to their respective measured quantities. The values in columns five

Table 4.13. Energy of System Components for Test Series LAM, Center of Mass Impact

Series	Missile Weight (lb.)	Missile Velocity Before Impact (ft/sec.)	Missile Velocity After Impact (ft/sec.)	Missile Energy Before Impact (ft-lb.)	Missile Energy After Impact (ft-lb.)	Energy Transferred to Frame, Maximum Angle Method (ft-lb.)	Energy Transferred to Frame, From Scope Data (ft-lb.)	Energy Not Accounted For After Impact (ft-lb.)
LAM01[d]	9.00	52.8	45.0	390	283	2.29	0.11	104
LAM02[d]	8.90	48.6	41.3	326	236	4.06	0.02	86.6
LAM03[d]	9.00	52.6	51.3	387	368	2.41	0.12	16.5
LAM04[d]	4.50	71.3	60.0	355	252	1.08	0.17	103
LAM05[d]	4.50	73.3	60.0	375	252	0.50	0.11	123
LAM06[d]	4.50	74.0	63.8	383	284	0.85	0.14	97.4

[d] - Missile Passed Through Test Specimen

Table 4.14. Energy of System Components for Test Series LHS, Center of Mass Impact

Series	Missile Weight (lb.)	Missile Velocity Before Impact (ft/sec.)	Missile Velocity After Impact (ft/sec.)	Missile Energy Before Impact (ft-lb.)	Missile Energy After Impact (ft-lb.)	Energy Transferred to Frame, Maximum Angle Method (ft-lb.)	Energy Transferred to Frame, From Scope Data (ft-lb.)	Energy Not Accounted For After Impact (ft-lb.)
LHS01[d]	8.90	51.4	45.0	365	280	3.25	0.29	82.0
LHS02[d]	9.00	51.8	48.8	375	333	1.79	0.03	40.4
LHS03[d]	9.00	51.8	43.1	375	260	2.60	0.13	113

[d] - Missile Passed Through Test Specimen

Table 4.15. Energy of System Components for Test Series TPM2, Center of Mass Impact

Series	Missile Weight (lb.)	Missile Velocity Before Impact (ft/sec.)	Missile Velocity After Impact (ft/sec.)	Missile Energy Before Impact (ft-lb.)	Missile Energy After Impact (ft-lb.)	Energy Transferred to Frame, Maximum Angle Method (ft-lb.)	Energy Transferred to Frame, From Scope Data (ft-lb.)	Energy Not Accounted For After Impact (ft-lb.)
TPM2D	9.00	51.5	-10.0	371	14.0	12.1	12.1	345

Table 4.16. Energy of System Components for Test Series HS9, Center of Mass Impact

Series	Missile Weight (lb.)	Missile Velocity Before Impact (ft/sec.)	Missile Velocity After Impact (ft/sec.)	Missile Energy Before Impact (ft-lb.)	Missile Energy After Impact (ft-lb.)	Energy Transferred to Frame, Maximum Angle Method (ft-lb.)	Energy Transferred to Frame, From Scope Data (ft-lb.)	Energy Not Accounted For After Impact (ft-lb.)
HS901	9.00	53.0	-5.8	393	4.70	12.6	12.6	375
HS902	9.00	51.6	-6.3	372	5.55	11.9	11.9	355
HS907[c]	9.00	51.2	-3.1	366	1.34	9.80	9.80	355
HS903[c]	18.0	37.3	-3.8	388	4.02	11.0	11.0	373
HS904	18.0	37.0	-5.2	383	7.56	16.6	16.6	358
HS909	18.0	34.7	-3.3	337	3.04	24.9	24.9	309
HS905	4.55	72.9	-4.6	375	1.50	5.44	4.80	369
HS906	4.50	74.6	-7.5	389	3.93	5.77	5.63	379
HS908	4.50	71.4	-3.8	356	1.01	5.41	5.94	350

[c] - No Scope Data

Table 4.17. Energy of System Components for Test Series ALM, Center of Mass Impact

Series	Missile Weight (lb.)	Missile Velocity Before Impact (ft/sec.)	Missile Velocity After Impact (ft/sec.)	Missile Energy Before Impact (ft-lb.)	Missile Energy After Impact (ft-lb.)	Energy Transferred to Frame, Maximum Angle Method (ft-lb.)	Energy Transferred to Frame, From Scope Data (ft-lb.)	Energy Not Accounted For After Impact (ft-lb.)
ALM01	4.50	73.2	-7.9	374	4.36	5.95	5.44	364
ALM02	4.50	73.6	-9.4	379	6.17	6.47	6.58	366
ALM03	4.50	72.6	-10.2	368	7.27	6.57	6.14	354
ALM04	9.00	49.4	-17.5	341	42.8	17.3	17.3	281
ALM05	9.00	49.4	-15.0	341	31.4	18.0	18.0	292
ALM06	8.90	48.2	-12.3	321	20.9	15.5	15.5	285
ALM07	18.0	34.8	-11.9	338	39.6	37.5	37.5	261
ALM08	18.0	37.4	-10.0	391	28.0	24.7	24.7	338
ALM09	18.1	37.2	-12.9	388	46.6	40.9	40.9	300

Table 4.18. Energy of System Components for Test Series MON, Center of Mass Impact

Series	Missile Weight (lb.)	Missile Velocity Before Impact (ft/sec.)	Missile Velocity After Impact (ft/sec.)	Missile Energy Before Impact (ft-lb.)	Missile Energy After Impact (ft-lb.)	Energy Transferred to Frame, Maximum Angle Method (ft-lb.)	Energy Transferred to Frame, From Scope Data (ft-lb.)	Energy Not Accounted For After Impact (ft-lb.)
MON1[c,d]	9.00	49.2	45.0	338	283	0.05	0.05	55
MON2[c,d]	9.00	50.7	52.5	359	385	0	0	------
MON3[c,d]	9.00	53.0	60.0	393	503	0	0	------

[b] - Glass Shattered Upon Impact
[c] - No Scope Data
[d] - Missile Passed Through Test Specimen

Table 4.19. Energy of System Components for Test Series LAM, Lower Corner Impact

Series	Missile Weight (lb.)	Missile Velocity Before Impact (ft/sec.)	Missile Velocity After Impact (ft/sec.)	Missile Energy Before Impact (ft-lb.)	Missile Energy After Impact (ft-lb.)	Energy Transferred to Frame, Maximum Angle Method (ft-lb.)	Energy Transferred to Frame, From Scope Data (ft-lb.)	Energy Not Accounted For After Impact (ft-lb.)
LAM01[d,e]	9.00	50.0	37.5	349	197	24.8	1.62	128
LAM02[d]	9.00	53.9	52.5	406	385	6.10	0.09	14.7
LAM03[d]	9.00	48.7	43.8	331	268	10.0	0.00	53.3
LAM04[d]	4.50	71.6	67.5	358	318	2.65	0.24	37.2
LAM05[d]	4.45	73.0	75.0	368	389	1.39	0.15	------
LAM06[d]	4.50	73.8	71.3	381	355	1.73	0.25	23.6

[d] - Missile Passed Through Test Specimen
[e] - Missile Stopped in Glass

Table 4.20. Energy of System Components for Test Series LHS, Lower Corner Impact

Series	Missile Weight (lb.)	Missile Velocity Before Impact (ft/sec.)	Missile Velocity After Impact (ft/sec.)	Missile Energy Before Impact (ft-lb.)	Missile Energy After Impact (ft-lb.)	Energy Transferred to Frame, Maximum Angle Method (ft-lb.)	Energy Transferred to Frame, From Scope Data (ft-lb.)	Energy Not Accounted For After Impact (ft-lb.)
LHS01[d]	9.00	48.0	35.0	322	171	12.0	1.81	139
LHS02[d]	9.00	48.4	33.8	327	160	13.1	1.78	155
LHS03[d,e]	9.00	51.1	35.6	365	177	19.1	2.26	169

[a] - Oscilloscope Data Not Saved

[d] - Missile Passed Through Test Specimen

[e] - Missile Stopped in Glass

Table 4.21. Energy of System Components for Test Series HS9, Lower Corner Impact

Series	Missile Weight (lb.)	Missile Velocity Before Impact (ft/sec.)	Missile Velocity After Impact (ft/sec.)	Missile Energy Before Impact (ft-lb.)	Missile Energy After Impact (ft-lb.)	Energy Transferred to Frame, Maximum Angle Method (ft-lb.)	Energy Transferred to Frame, From Scope Data (ft-lb.)	Energy Not Accounted For After Impact (ft-lb.)
HS901	9.00	52.3	-0.6	382	0.05	29.7	29.7	353
HS902	9.00	51.8	-2.5	375	0.87	30.7	30.7	343
HS907	9.00	51.6	1.7	372	0.40	30.9	30.9	341
HS903	18.0	38.8	3.8	420	4.02	71.0	71.0	345
HS904	18.0	36.3	0.8	368	0.18	46.9	46.9	321
HS909	18.0	33.1	2.3	306	1.48	53.8	53.8	251
HS905	4.50	72.1	-5.2	363	1.89	18.5	18.5	343
HS906	4.50	72.2	-3.8	364	1.01	15.6	15.6	348
HS908	4.50	69.6	-3.3	338	0.76	16.6	16.6	321

Table 4.22. Energy of System Components for Test Series TPM2, Lower Corner Impact

Series	Missile Weight (lb.)	Missile Velocity Before Impact (ft/sec.)	Missile Velocity After Impact (ft/sec.)	Missile Energy Before Impact (ft-lb.)	Missile Energy After Impact (ft-lb.)	Energy Transferred to Frame, Maximum Angle Method (ft-lb.)	Energy Transferred to Frame, From Scope Data (ft-lb.)	Energy Not Accounted For After Impact (ft-lb.)
TPM2D[b]	9.00	54.0	26.3	408	96.7	5.22	1.11	306

[d] - Missile Passed Through Test Specimen

[b] - Glass Shattered Upon Impact

Table 4.23. Energy of System Components for Test Series ALM, Lower Corner Impact

Series	Missile Weight (lb.)	Missile Velocity Before Impact (ft/sec.)	Missile Velocity After Impact (ft/sec.)	Missile Energy Before Impact (ft-lb.)	Missile Energy After Impact (ft-lb.)	Energy Transferred to Frame, Maximum Angle Method (ft-lb.)	Energy Transferred to Frame, From Scope Data (ft-lb.)	Energy Not Accounted For After Impact (ft-lb.)
ALM01[f]	4.50	72.3	No Data	365	---------	26.1	26.1	339
ALM02	4.50	71.2	10.4	354	7.56	23.8	23.8	323
ALM03	4.50	71.5	12.5	357	10.9	20.6	20.6	326
ALM04[c]	9.00	48.0	8.8	322	10.8	31.2	31.2	280
ALM05	9.00	46.3	8.8	300	10.8	33.2	33.2	256
ALM06	8.90	49.0	6.7	332	6.20	45.3	45.3	280
ALM07	18.1	34.2	2.5	329	1.76	72.5	72.5	254
ALM08	18.0	37.0	2.1	383	1.23	81.9	81.9	300
ALM09	18.1	37.9	6.7	403	12.6	85.9	85.9	304

[c] - No Scope Data

[f] - Missile Data After Impact Not Obtained

and six correspond to the values resulting from Equation 2.1. The values in columns seven and eight are found using Equation 2.2.

The last column in Tables 4.13-4.23 lists the kinetic energy unaccounted for after the impact. This is the energy lost during the impact and is found by subtracting the values of column six and seven from the value in column five. The lost energy damages the test specimen and the missile. The absorption of energy by the test specimens results in damage to them. The missiles often deform or crack upon impact which also absorbs energy. Deformation and/or cracking occurred frequently to heavier missiles. More deformation of the test specimens occurred with the heavier missiles. The author believes that the loss of a greater amount of energy occurs when a test specimen resists a missile impact rather than when the missile perforates the test specimen since the damaged glass absorbs energy while it breaks. Appendix B contains pictures of the test specimens after impact.

Figures 4.4 and 4.5 show the kinetic energy transferred to the glazing support frame after impact versus the angular momentum of the missile before impact. Figure 4.4 displays the center of mass impact data while Figure 4.5 displays the lower corner impact data. Both figures show that a negligible amount of energy transfers to the framing system when a missile perforates a test specimen. A test specimen from which a missile rebounded after impact

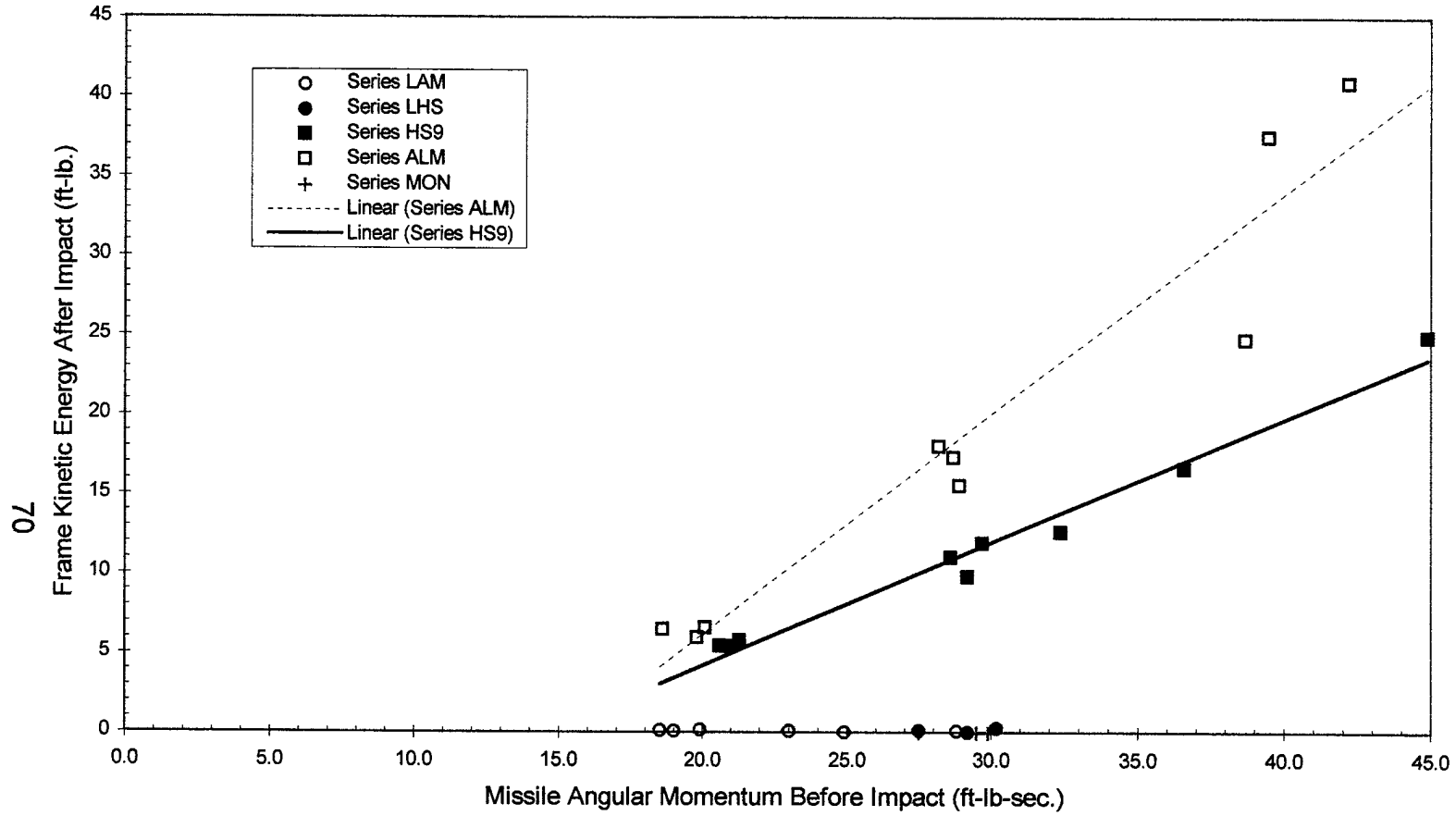

Figure 4.4. Frame Energy After Impact Versus Missile Angular Momentum Before Impact, Center of Mass Impacts

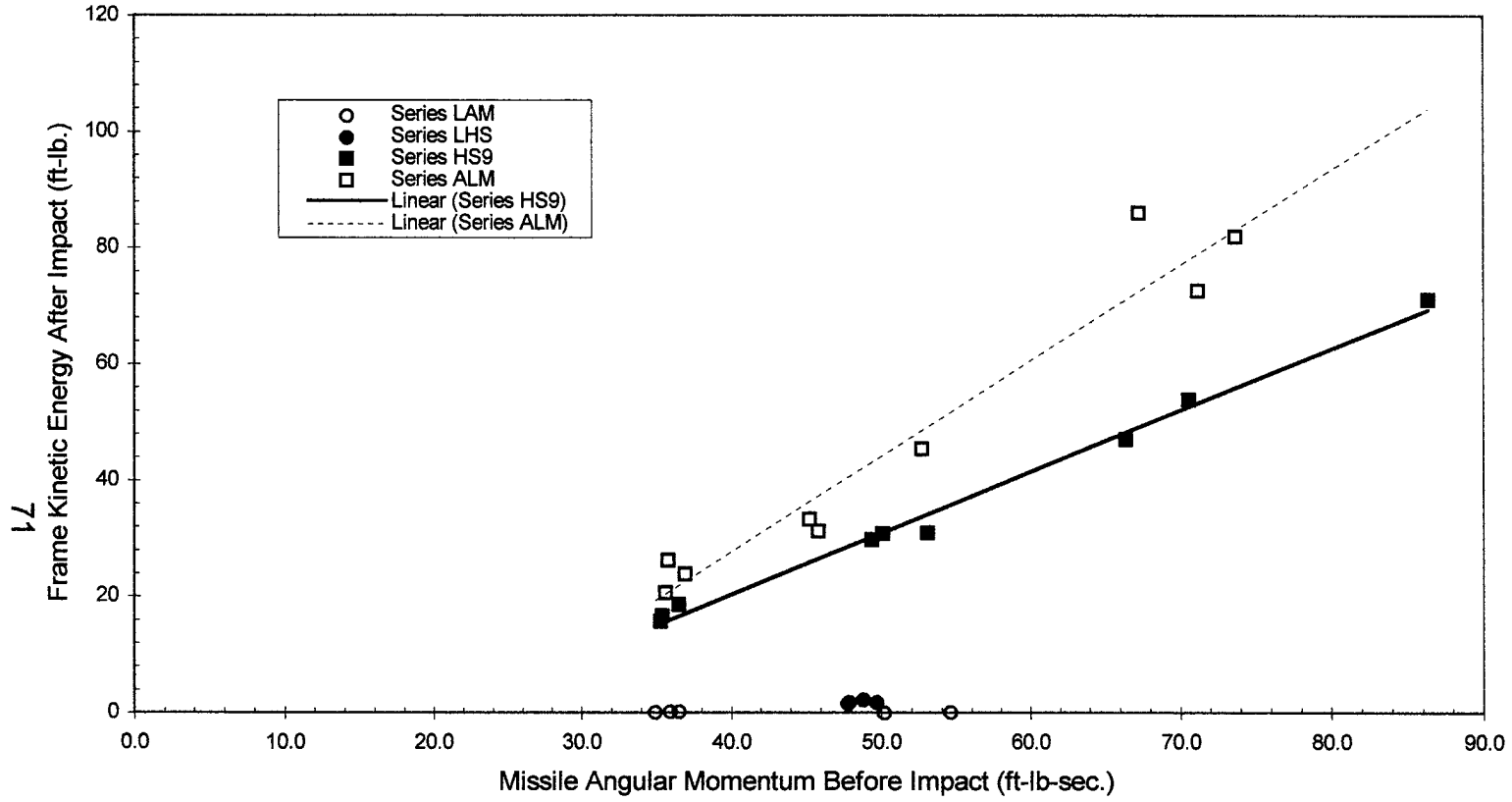

Figure 4.5. Frame Energy After Impact Versus Missile Angular Momentum Before Impact, Lower Corner Impacts

displays a linear relationship between the frame's kinetic energy after impact and the initial angular momentum of the missile. The trendlines one all figures results from linear regression.

Figures 4.6 and 4.7 display the kinetic energy transferred to the frame versus the linear momentum of the missile before impact for the center of mass and lower corner impacts, respectively. These figures also show negligible energy transfer occurring during a perforation of the test specimen. The figures indicate a linear relationship between the energy transferred to the frame and linear momentum of the missile before impact. In Figures 4.6 and 4.7, the data appears closer together since the linear momentum of the missile ignores the effect of impact location.

Figures 4.8 and 4.9 illustrate the angular momentum of the frame after impact versus the angular momentum of the missile before impact. A distinct difference appears between the behavior of the frame when a missile perforates the test specimen and a missile rebounds off the test specimen. The angular momentum transferred to the frame displays a linear relationship with the angular momentum of the missile before impact.

Figures 4.10 and 4.11 display the angular momentum of the frame after impact versus the linear momentum of the missile before impact. The linear momentum of the missile before impact ignores the effect of the missile impact

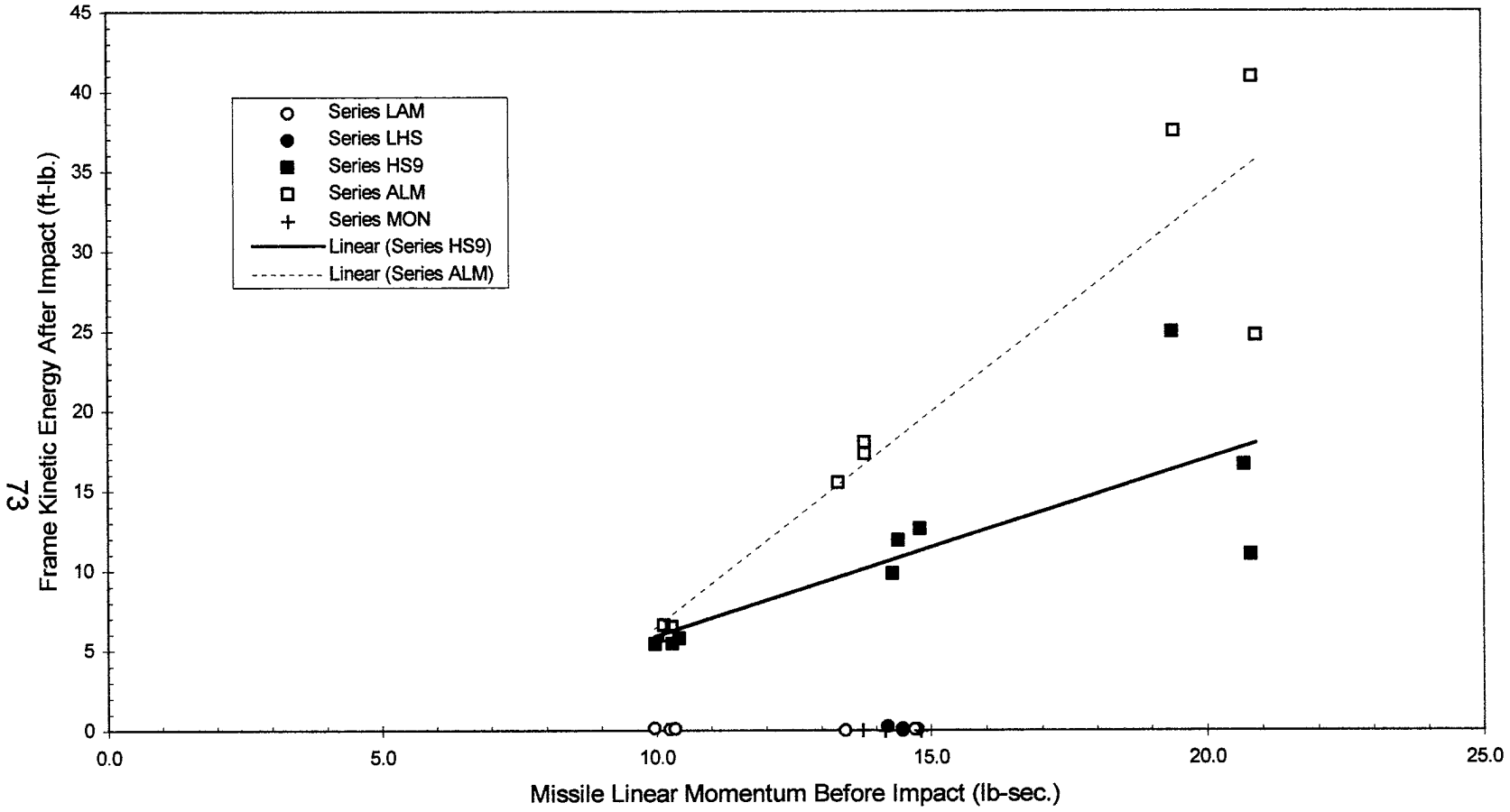

Figure 4.6. Frame Energy After Impact Versus Missile Linear Momentum Before Impact, Center of Mass Impacts

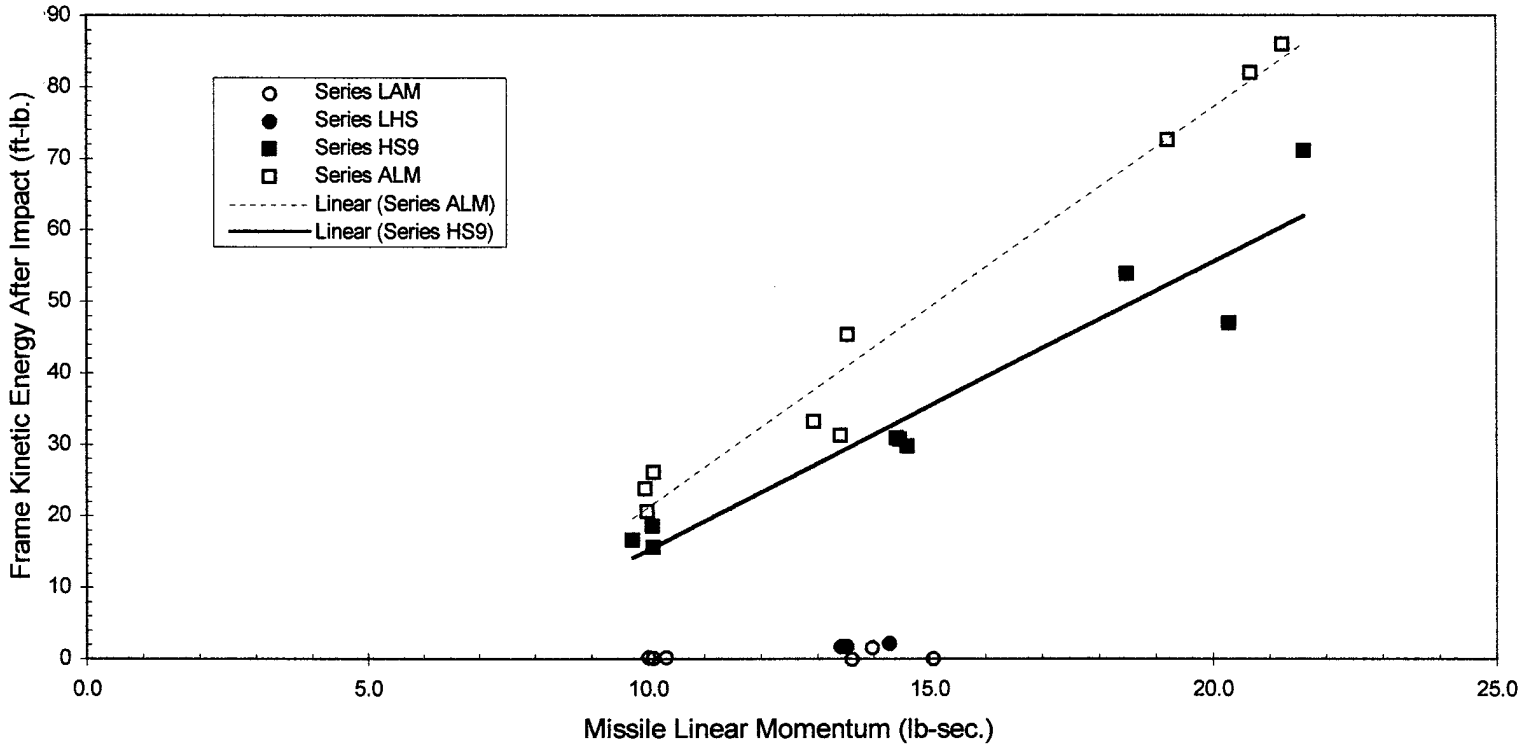

Figure 4.7. Frame Energy After Impact Versus Missile Linear Momentum Before Impact, Lower Corner Impacts

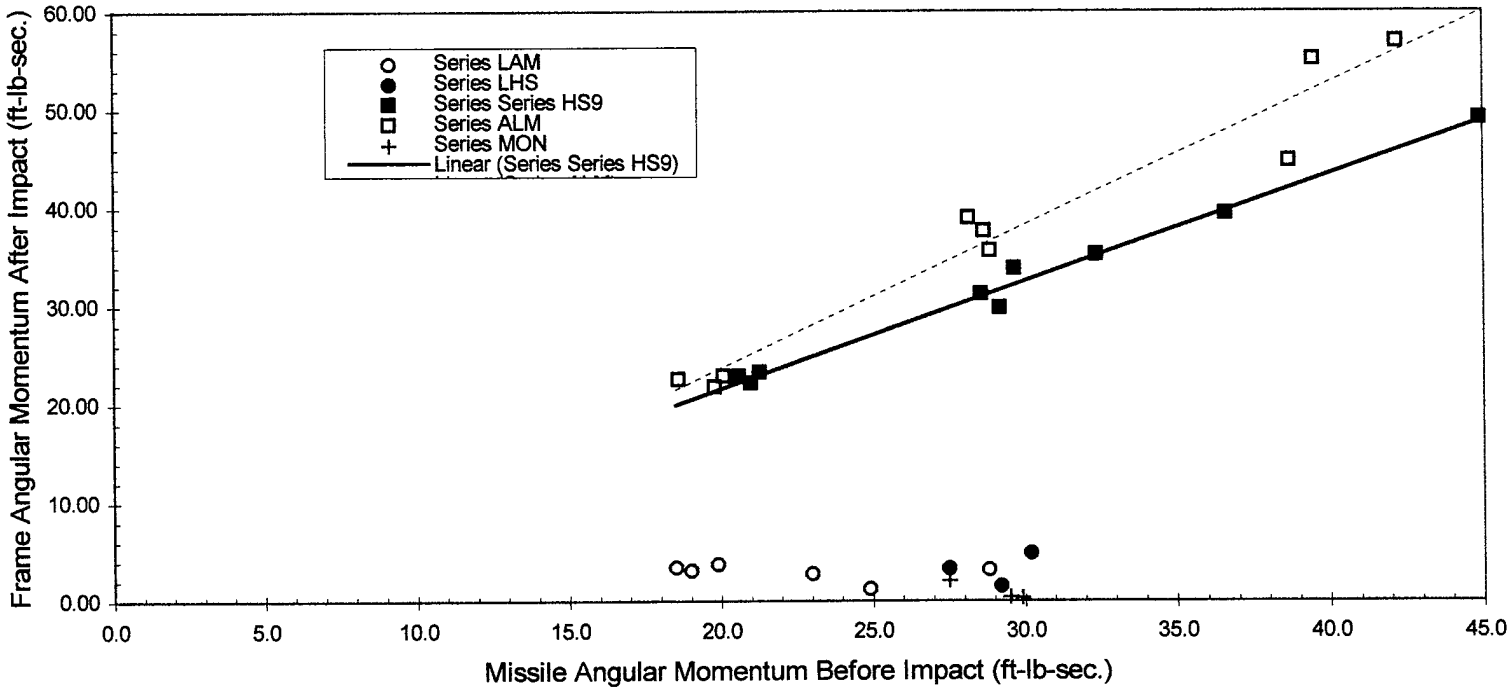

Figure 4.8. Frame Angular Momentum After Impact Versus Missile Angular Momentum Before Impact, Center of Mass Impacts

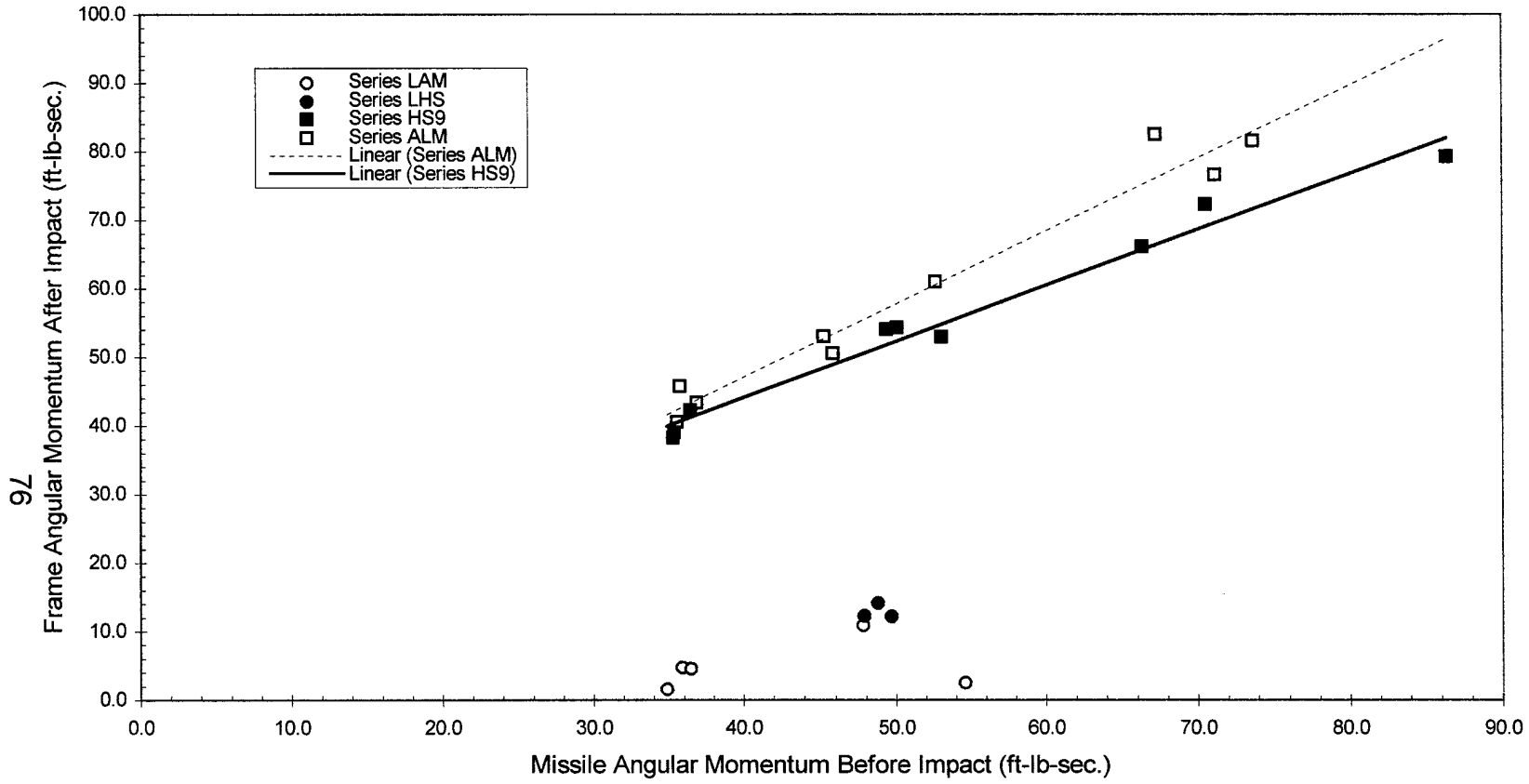

Figure 4.9. Frame Angular Momentum After Impact Versus Missile Angular Momentum Before Impact, Lower Corner Impacts

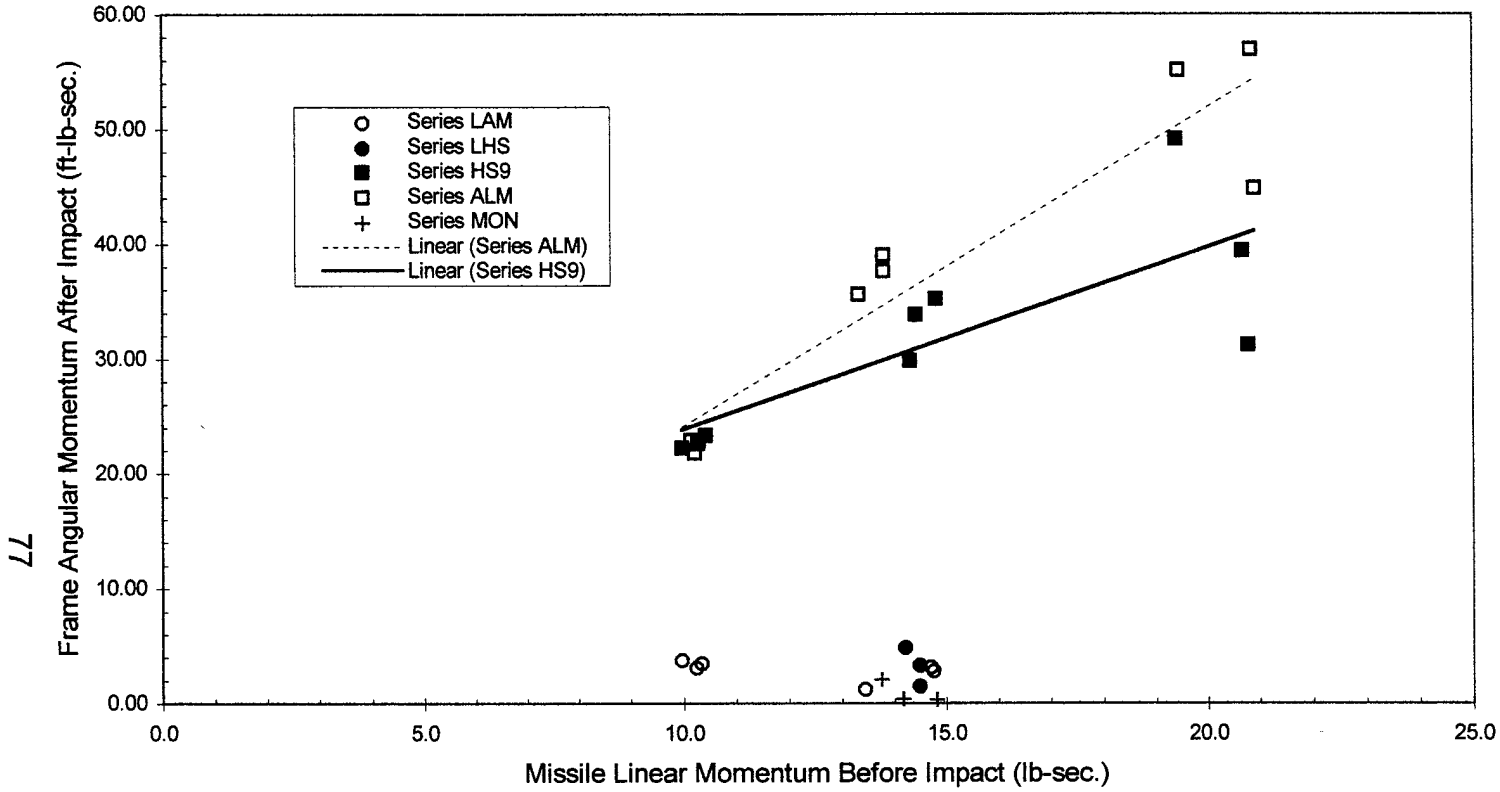

Figure 4.10. Frame Angular Momentum After Impact Versus Missile Linear Momentum Before Impact, Center of Mass Impacts

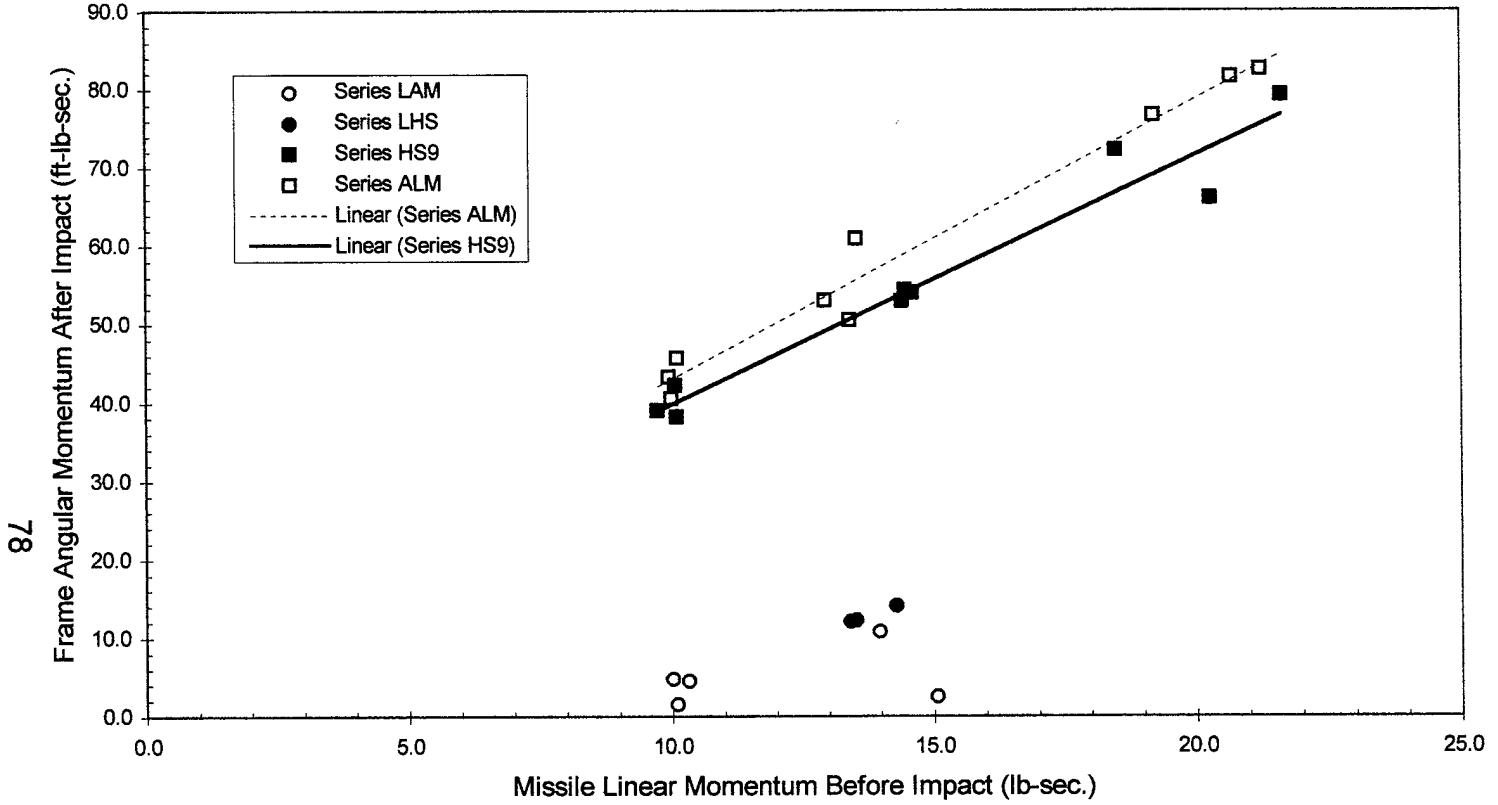

Figure 4.11. Frame Angular Momentum After Impact Versus Missile Linear Momentum Before Impact, Lower Corner Impacts

location. Again, a distinct difference in the behavior of the frame after impact appears between a missile perforation and a missile rebound. The data appears to have a linear relationship between the angular momentum of the frame after impact and the linear momentum of the missile before impact.

Figures 4.12 and 4.13 show the velocity of the missile after impact versus the velocity of the missile before impact. A significant difference in the velocity after impact occurs when a missile perforates the test specimen versus when a missile rebounds off the test specimen. The velocity of the missile after impact when a missile does not perforate the test specimen appears to relate the velocity before impact. For the lower corner impacts of series HS9, all of the 18.0-lb. missiles continue to move in the same direction after impact, but do not perforate the test specimen. This also occurs for one of the 9.00-lb. missiles.

Figures 4.14 and 4.15 display the energy lost during the center of mass and lower corner impacts, respectively. In Figures 4.14 and 4.15, the solid bars represent missile perforations while the outlined bars represent missile rebounds. The figures illustrate that a distinct difference in energy loss exists when a missile perforates the test specimen or rebounds off the test specimen. The loss of more energy occurs when a missile rebounds off the test specimen.

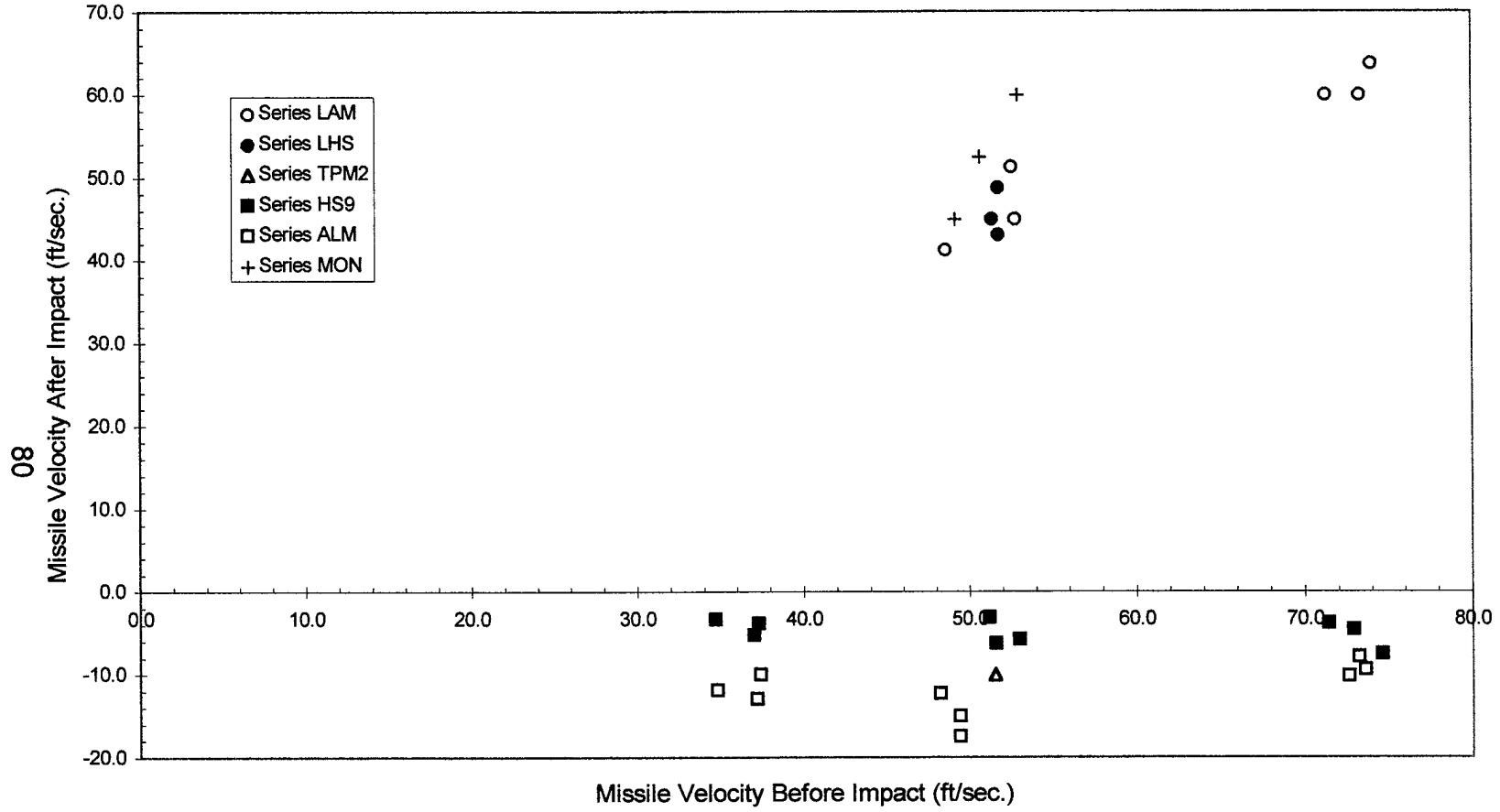

Figure 4.12. Missile Velocity After Impact Versus Missile Velocity Before Impact, Center of Mass Impacts

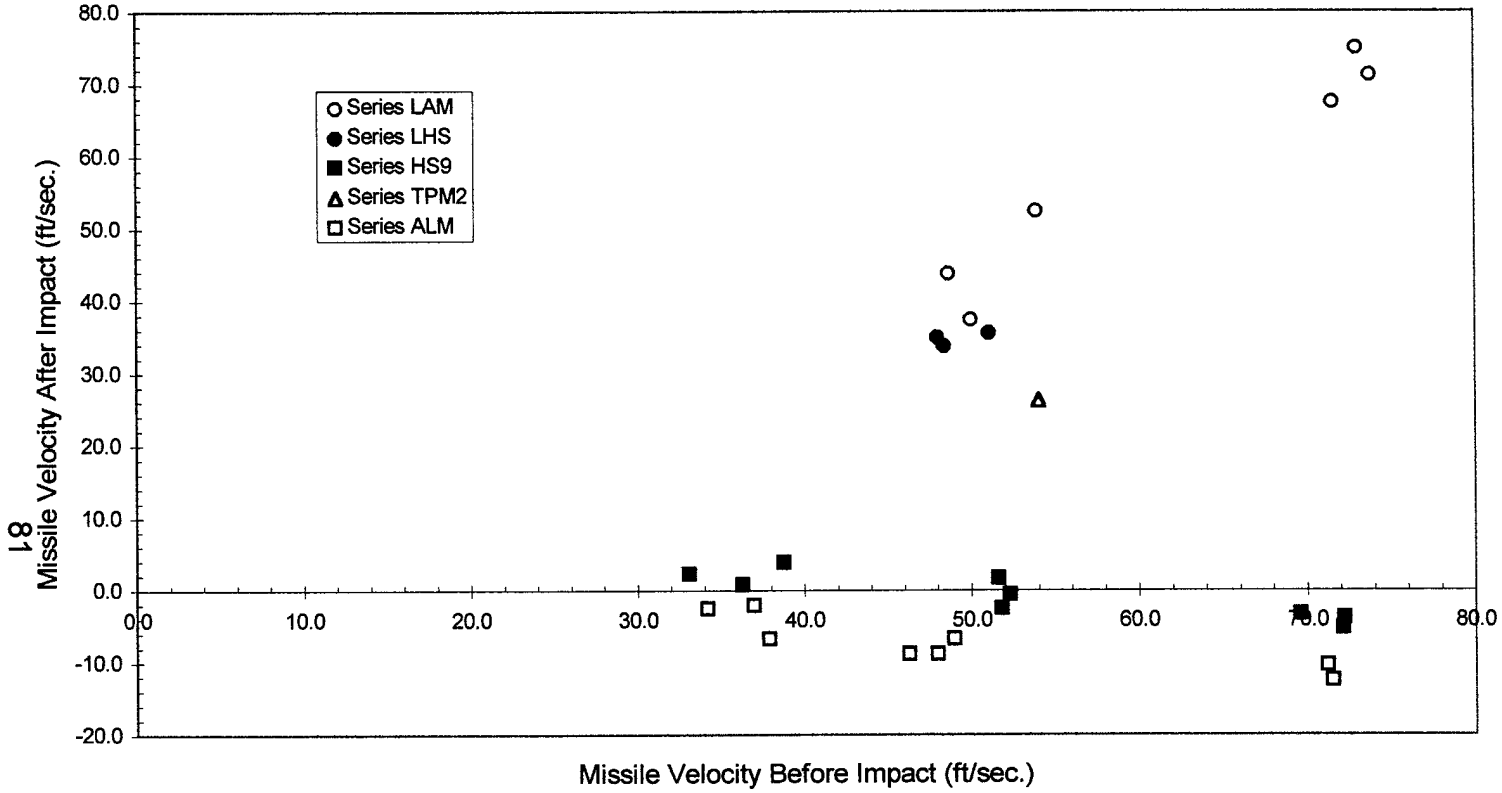

Figure 4.13. Missile Velocity After Impact Versus Missile Velocity Before Impact, Lower Corner Impacts

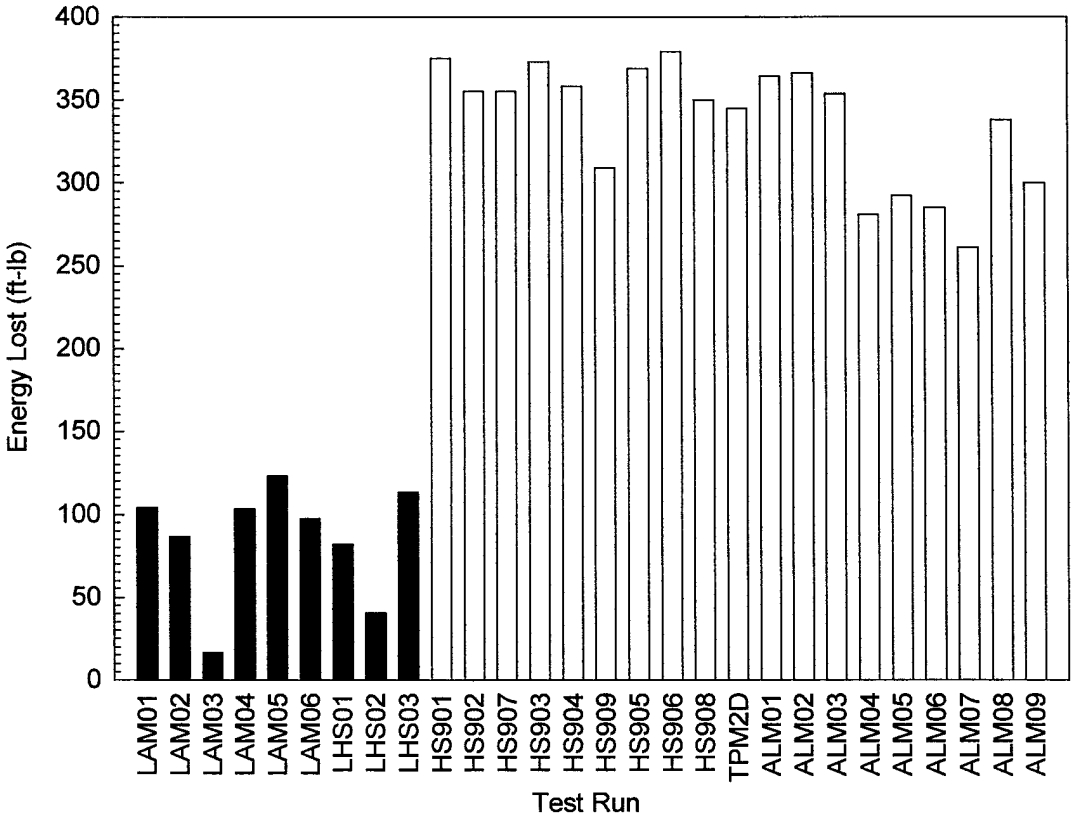

Figure 4.14. Energy Lost During Center of Mass Impacts

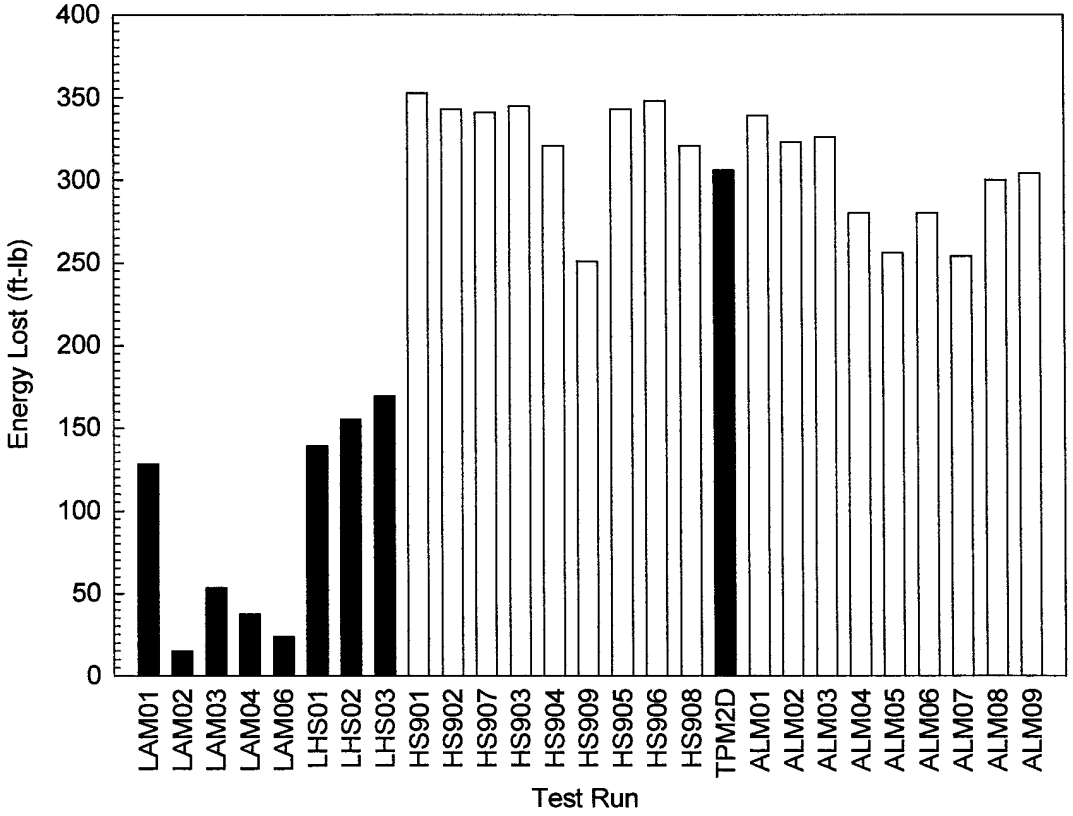

Figure 4.15. Energy Lost During Lower Corner Impacts

4.3. Sources of Error

Researchers attempted to minimize the possible number of sources of error whenever possible. The largest source of error results from estimating the velocity of the missile immediately after impact. If the test specimen resists the missile impact, the missile's reference lines are visible during a frame by frame analysis of the video taped impact. The distance between these lines is 3 in. Accuracy of the distance measurements from the video tapes is within 0.5 in. However, if a missile perforates the test specimen, the missile moves too fast for the camera to detect the reference lines on the missile. For these test runs, the missile speed results from determining the number of reference lines on the backdrop that the rear of missile passes in a set number of frames. The reference lines on the backdrop are 6 in. apart. For this case, accuracy of the distance measurements from the video tapes is within 1 in. After impact missile velocities reported are to the nearest 0.1 ft/sec.

CHAPTER 5

CONCLUSIONS AND RECOMMENDATIONS

The primary objective of this research consists of determining whether a simple statement of missile energy is sufficient to define the outcome of a missile impact test. Secondary objectives include the determination of whether or not the energy or momentum associated with the objects involved in an impact defines the outcome of an impact. All test specimens had 48x48-in. dimensions. The type and thickness of the test specimens varied. All missiles launched at the test specimens had kinetic energies near 350 ft-lb. A cannon that uses compressed air as its launching mechanism provided the means for the simulation of a windborne missile impact. Researchers recorded data pertaining to the motion of the objects involved in the impact before and after the impact. Following the collection of the impact data, researchers analyzed the data in an attempt to determine the governing factors in a windborne missile impact.

5.1. Conclusions

The data from the experimental research conducted produced the following conclusions:

1. Three different missiles having different mass and momenta but the same kinetic energy upon impact produced vastly different results.

Therefore, kinetic energy of an impacting missile by itself cannot serve to predict the response of the impacted system components.

2. Conservation of angular momentum occurs during missile impacts on window glass.
3. Energy loss occurs during a windborne missile impact. More energy loss occurs when the missile rebounds after impact than when the missile perforates the test specimen. Deformation of the missile or the aluminum plate and the breaking of the glass specimens provide a means for the absorption of the missile's initial kinetic energy. The deformation of the PVB interlayer of a laminated glass lite also provides an energy absorption mechanism.

5.2. Recommendations for Future Research

The glazing support frame used in this research rotated about a fixed axis after impact. Window frames rigidly attach to the structure they are a part of and therefore cannot rotate after impact. While this experiment does not exactly model the real situation, it allows researchers to make measurements of controlled factors as well as observations of the damage resulting from the missile impacts. The author recommends that future research investigates the following:

1. The effect of glass thickness and PVB interlayer thickness on the behavior of laminated glass lites during a missile impact;
2. The effect of the mass distribution of the missile on a missile impact.

REFERENCES

Abraham, Vinu J., (1995). "Missile Impact Resistance of Window Glass Constructions," Master's Thesis, Department of Civil Engineering, Texas Tech University, Lubbock, TX.

Abrate, Serge, (1998). Impact on Composite Structures, Cambridge University Press, Cambridge, United Kingdom.

ASTM, (1997). Standard Practice for Determining the Load Resistance of Glass In Buidlings, ASTM E 1300-97, 1997 Annual Book of ASTM Standards, V. 4.11, ASTM, West Conshohocken, PA.

ASTM, (1997). Standard Test Method for Performance of Exterior Windows, Curtain Walls, Doors, and Storm Shutters Impacted Windborne Debris in Hurricanes, ASTM E 1996-99, 1999 Annual Book of ASTM Standards, V. 4.11, ASTM, West Conshohocken, PA.

ASTM, (1999). Standard Test Method for Performance of Exterior Windows, Curtain Walls, Doors, and Storm Shutters Impacted by Missile(s) and Exposed to Cyclic Pressure Differentials, ASTM E 1886-97, 1997 Annual Book of ASTM Standards, V. 4.11, ASTM, West Conshohocken, PA.

Batts, Martin E., Cordes, Martin R., Russell, Larry R., Shaver, James R., and Simiu, Emil, (1980). "Hurricane Wind Speeds in the United States," U.S. Department of Commerce, Washington.

Beason, William L., (1974). "Breakage Characteristics of Window Glass Subjected to Small Missile Impact," Master's Thesis, Department of Civil Engineering, Texas Tech University, Lubbock, TX.

Brach, Raymond M., (1991). Mechanical Impact Dynamics: Rigid Body Collisions, John Wiley & Sons, New York.

Carter, Russell R., (1998). "Wind-Generated Missile Impact on Composite Wall Systems," Master's Thesis, Department of Civil Engineering, Texas Tech University, Lubbock, TX.

Curtain Wall Manual 12, (1984). American Architectural Manufacturing Association (AAMA), Schaumburg, IL.

Gomes, L., and Vickery, B. J., (1976). "The Prediction of Tropical Cyclone Gust Speeds Along the Northern Australia Coast," The Institution of Engineers, Australia, Civil Engineering Transactions, pp 40-49.

Gwaltney, R.C., (1968). "Missile Generation and Protection in Light-Water-Cooled Reactor Plants," ORNL-NSIC-22, Oak Ridge National Laboratory, Oak Ridge, TN.

Harris, Phillip L., Beason, W. Lynn, and Minor, Joseph E., (1978). "The Effects of Thickness and Temper on the Resistance of Glass to Small Missile Impact," Institute for Disaster Research, Texas Tech University, Lubbock, TX.

Hibbeler, R.C., (1995). Engineering Mechanics: Dynamics, Seventh Ed., Prentice Hall, Englewood Cliffs, NJ.

McDonald, James R., (1970). "Tornado Generated Missiles and Their Effects," Presented at Symposium on Tornadoes, Lubbock, TX.

McDonald, James R., (1994). "Wind Effects on Buildings," Proceedings, International Wind Engineering Forum, Tokyo, Japan.

McDonald, James R., Minor, Joseph E., and Mehta, Kishor C., (1973). "Tornado Generated Missiles," Proceedings, Specialty Conference on Structural Design of Nuclear Power Plant Facilities, Structural Division, ASCE, Chicago, IL, 17-18 Dec.

Minor, Joseph E. (1984). "How to Prepare Glass Buildings for Hurricanes," Glass Digest, 15 Nov, pp 60-64.

Minor, Joseph E., (1997). "New Philosophy Guides Design of the Building Envelope," Proceedings, Texas Section of ASCE, 7 Apr, pp 346-355.

Minor, Joseph E., (1985). "Structural Design With Glass," Glass Magazine, V. 35, No. 11, pp 97-100.

Minor, Joseph E., Beason, W. Lynn, and Harris, Phillip L., (1978). "Designing for Windborne Missiles in Urban Areas," Journal of Structural Engineering, ASCE Vol. 104, No. 11, pp 1749-1759.

Simiu, Emil, and Scanlan, Robert H., (1996). Wind Effects on Structures, John Wiley & Sons, Inc. New York.

Southern Building Code Congress International (SBCCI), (1999). SBCCI Test Standard For Determining Impact Resistance From Windborne Debris, SSTD 12-99, SBCCI, Inc., Birmingham, Alabama.

Twisdale, Lawrence A., (1977). "Probabilistic Considerations in Missile Impact Assessments," Presented at International Seminar on Probabilistic and Extreme Load Design of Nuclear Plant Facilities, August 22-23, pp 1-29.

Twisdale, L.A., Dunn, W.L., and Davis, T.L., (1979). "Tornado Missile Transport Analysis," Nuclear Engineering and Design, Vol. 51, pp 295-308.

Twisdale, L. A., Vickery, P.J., and Steckley, A.C., (1996). "Analysis of Hurricane WIndborne Debris Impact Risk for Residential Structures," Applied Research Associates, Inc., Raleigh, NC.

Willis, John, Wyatt, Tom, and Lee, Bryan, (1998). "Warnings of High Winds in Densely Populated Areas," Thomas Telford Publishing, London.

Willis, Robert J., (1994). "The Impact of Hurricane Andrew on Wind Engineering," Modern Steel Construction, V. 34, No. 5, pp 58-63.

APPENDIX A

TEST DATA RECORDED

Test Run: LAM01

Glass Type: 1/4-in. AN - 0.030-in. - 1/4-in. AN

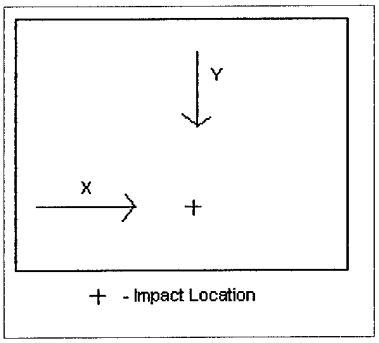

General Information:

Specimen Thickness (in.):	0.2817
Specimen Length (in.):	48.0
Weight of Frame (lb.):	119.5
Weight of Shims (lb.):	2.60
Weight of Glass (lb.):	55.60
Total Weight (lb.):	177.7

Center of Mass Impact Information

Support Frame Mass Moment of Inertia (ft-lb-sec^2.):	37.6
Support Frame Center of Mass (in.):	24.1

Missile Length (in.):	107.125	Missile Velocity After Impact (ft/sec.):	45.0
Missile Weight (lb.):	9.00	Angle Observed (deg.):	6.5
Impact Velocity (ft/sec.):	52.8	Horizontal Impact Location (in.):	25.75
Vertical Impact Location (in.):	18.75		

After Impact Angular Velocity of Frame, From Oscilloscope (rad/sec.):	0.0760
After Impact Angular Velocity of Frame, From Angle (rad/sec.):	N/A

Notes: Missile Perforated Test Specimen

Lower Corner Impact Information

Support Frame Mass Moment of Inertia (ft-lb-sec^2.):	36.7
Support Frame Center of Mass (in.):	23.6

Missile Information

Missile Length (in.):	97.75	Missile Velocity After Impact (ft/sec.):	37.5
Missile Weight (lb.):	9.00	Angle Observed (deg.):	21.8
Impact Velocity (ft/sec.):	50.0	Horizontal Impact Location (in.):	43.25
Vertical Impact Location (in.):	41.00		

After Impact Angular Velocity of Frame, From Oscilloscope (rad/sec.):	0.297
After Impact Angular Velocity of Frame, From Angle (rad/sec.):	N/A

Notes: Missile Perforated Test Specimen
Missile Stuck in Test Specimen

Test Run: LAM02

Glass Type: 1/4-in. AN - 0.030-in. - 1/4-in. AN

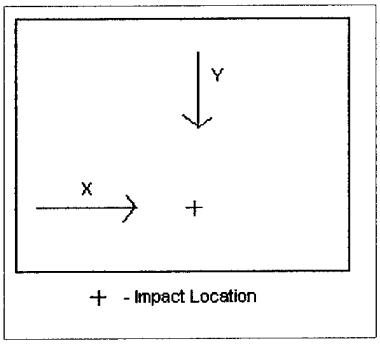

General Information:

Specimen Thickness (in.):	0.2831
Specimen Length (in.):	48.0
Weight of Frame (lb.):	119.5
Weight of Shims (lb.):	2.80
Weight of Glass (lb.):	55.30
Total Weight (lb.):	177.6

Center of Mass Impact Information

Support Frame Mass Moment of Inertia (ft-lb-sec^2.):	38.0
Support Frame Center of Mass (in.):	24.1

Missile Length (in.):	97.75	Missile Velocity After Impact (ft/sec.):	41.3
Missile Weight (lb.):	8.90	Angle Observed (deg.):	8.7
Impact Velocity (ft/sec.):	48.6	Horizontal Impact Location (in.):	27.00
Vertical Impact Location (in.):	22.25		

After Impact Angular Velocity of Frame, From Oscilloscope (rad/sec.):	0.0340
After Impact Angular Velocity of Frame, From Angle (rad/sec.):	N/A

Notes: Missile Perforated Test Specimen

Lower Corner Impact Information

Support Frame Mass Moment of Inertia (ft-lb-sec^2.):	38.0
Support Frame Center of Mass (in.):	24.1

Missile Information

Missile Length (in.):	90.50	Missile Velocity After Impact (ft/sec.):	52.5
Missile Weight (lb.):	9.00	Angle Observed (deg.):	10.6
Impact Velocity (ft/sec.):	53.9	Horizontal Impact Location (in.):	43.00
Vertical Impact Location (in.):	43.50		

After Impact Angular Velocity of Frame, From Oscilloscope (rad/sec.):	0.068
After Impact Angular Velocity of Frame, From Angle (rad/sec.):	N/A

Notes: Missile Perforated Test Specimen

Test Run: LAM03

Glass Type: 1/4-in. AN - 0.030-in. - 1/4-in. AN

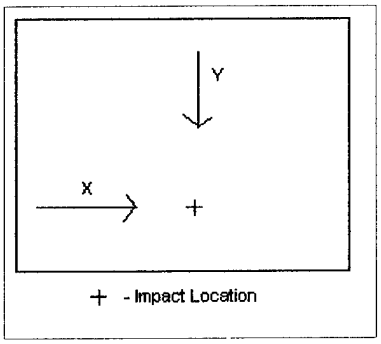

General Information:

Specimen Thickness (in.):	0.2824
Specimen Length (in.):	48.1
Weight of Frame (lb.):	119.5
Weight of Shims (lb.):	2.80
Weight of Glass (lb.):	56.00
Total Weight (lb.):	178.3

Center of Mass Impact Information

Support Frame Mass Moment of Inertia (ft-lb-sec^2.):	42.4
Support Frame Center of Mass (in.):	24.8

Missile Length (in.):	96.00	Missile Velocity After Impact (ft/sec.):	51.3
Missile Weight (lb.):	9.00		
Impact Velocity (ft/sec.):	52.6	Angle Observed (deg.):	6.6
Vertical Impact Location (in.):	23.50	Horizontal Impact Location (in.):	28.75

After Impact Angular Velocity of Frame, From Oscilloscope (rad/sec.):	0.0760
After Impact Angular Velocity of Frame, From Angle (rad/sec.):	N/A

Notes: Missile Perforated Test Specimen

Lower Corner Impact Information

Support Frame Mass Moment of Inertia (ft-lb-sec^2.):	42.4
Support Frame Center of Mass (in.):	24.8

Missile Information

Missile Length (in.):	96.00	Missile Velocity After Impact (ft/sec.):	37.5
Missile Weight (lb.):	9.00		
Impact Velocity (ft/sec.):	48.7	Angle Observed (deg.):	13.4
Vertical Impact Location (in.):	44.25	Horizontal Impact Location (in.):	44.25

After Impact Angular Velocity of Frame, From Oscilloscope (rad/sec.):	No Data
After Impact Angular Velocity of Frame, From Angle (rad/sec.):	N/A

Notes: Missile Perforated Test Specimen
No Scope Data, Pen and Paper Backup Used

Test Run: LAM04

Glass Type: 1/4-in. AN - 0.030-in. - 1/4-in. AN

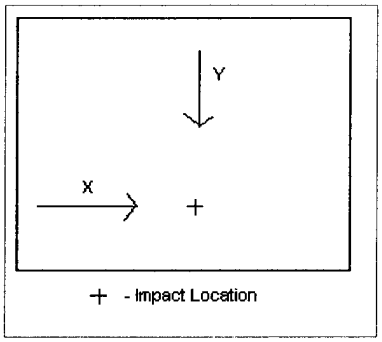

General Information:

Specimen Thickness (in.):	0.2835
Specimen Length (in.):	48.0
Weight of Frame (lb.):	119.5
Weight of Shims (lb.):	2.80
Weight of Glass (lb.):	55.70
Total Weight (lb.):	178.0

Center of Mass Impact Information

Support Frame Mass Moment of Inertia (ft-lb-sec^2.):	43.9
Support Frame Center of Mass (in.):	25.0

Missile Length (in.):	49.375	Missile Velocity After Impact (ft/sec.):	60.0
Missile Weight (lb.):	4.50		
Impact Velocity (ft/sec.):	71.3	Angle Observed (deg.):	4.4
Vertical Impact Location (in.):	24.00	Horizontal Impact Location (in.):	26.75

After Impact Angular Velocity of Frame, From Oscilloscope (rad/sec.):	0.0870
After Impact Angular Velocity of Frame, From Angle (rad/sec.):	N/A

Notes: Missile Perforated Test Specimen

Lower Corner Impact Information

Support Frame Mass Moment of Inertia (ft-lb-sec^2.):	43.9
Support Frame Center of Mass (in.):	25.0

Missile Information

Missile Length (in.):	49.125	Missile Velocity After Impact (ft/sec.):	67.5
Missile Weight (lb.):	4.50		
Impact Velocity (ft/sec.):	71.6	Angle Observed (deg.):	6.8
Vertical Impact Location (in.):	43.00	Horizontal Impact Location (in.):	10.00

After Impact Angular Velocity of Frame, From Oscilloscope (rad/sec.):	0.110
After Impact Angular Velocity of Frame, From Angle (rad/sec.):	N/A

Notes: Missile Perforated Test Specimen

Test Run: LAM05

Glass Type: 1/4-in. AN - 0.030-in. - 1/4-in. AN

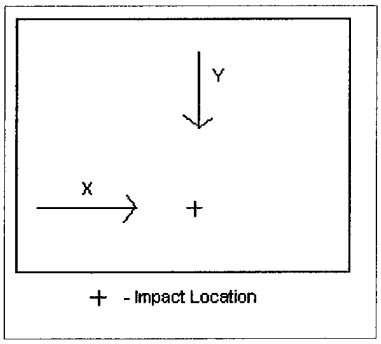

General Information:

Specimen Thickness (in.):	0.2827
Specimen Length (in.):	48.0
Weight of Frame (lb.):	119.5
Weight of Shims (lb.):	2.65
Weight of Glass (lb.):	55.20
Total Weight (lb.):	177.4

Center of Mass Impact Information

Support Frame Mass Moment of Inertia (ft-lb-sec^2.):	44.6
Support Frame Center of Mass (in.):	25.4

Missile Length (in.):	42.125	Missile Velocity After Impact (ft/sec.):	60.0
Missile Weight (lb.):	4.50		
Impact Velocity (ft/sec.):	73.3	Angle Observed (deg.):	3.0
Vertical Impact Location (in.):	22.25	Horizontal Impact Location (in.):	27.50

After Impact Angular Velocity of Frame, From Oscilloscope (rad/sec.):	0.0700
After Impact Angular Velocity of Frame, From Angle (rad/sec.):	N/A

Notes: Missile Perforated Test Specimen

Lower Corner Impact Information

Support Frame Mass Moment of Inertia (ft-lb-sec^2.):	44.6
Support Frame Center of Mass (in.):	25.4

Missile Information

Missile Length (in.):	42.125	Missile Velocity After Impact (ft/sec.):	75.0
Missile Weight (lb.):	4.45		
Impact Velocity (ft/sec.):	73.0	Angle Observed (deg.):	4.9
Vertical Impact Location (in.):	41.50	Horizontal Impact Location (in.):	9.375

After Impact Angular Velocity of Frame, From Oscilloscope (rad/sec.):	0.0820
After Impact Angular Velocity of Frame, From Angle (rad/sec.):	N/A

Notes: Missile Perforated Test Specimen
VHS Tape Data Suspicious, Missile Velocity Increased After Impact

Test Run: LAM06

Glass Type: 1/4-in. AN - 0.030-in. - 1/4-in. AN

General Information:

Specimen Thickness (in.):	0.2827
Specimen Length (in.):	48.0
Weight of Frame (lb.):	119.5
Weight of Shims (lb.):	2.70
Weight of Glass (lb.):	55.30
Total Weight (lb.):	177.5

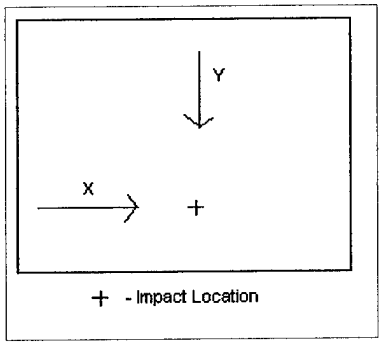

Center of Mass Impact Information

Support Frame Mass Moment of Inertia (ft-lb-sec^2.):	42.4
Support Frame Center of Mass (in.):	25.6

Missile Length (in.):	46.50	Missile Velocity After Impact (ft/sec.):	63.8
Missile Weight (lb.):	4.50	Angle Observed (deg.):	3.8
Impact Velocity (ft/sec.):	74.0	Horizontal Impact Location (in.):	21.75
Vertical Impact Location (in.):	21.50		

After Impact Angular Velocity of Frame, From Oscilloscope (rad/sec.):	0.0830
After Impact Angular Velocity of Frame, From Angle (rad/sec.):	N/A

Notes: Missile Perforated Test Specimen

Lower Corner Impact Information

Support Frame Mass Moment of Inertia (ft-lb-sec^2.):	42.4
Support Frame Center of Mass (in.):	25.6

Missile Information

Missile Length (in.):	52.00	Missile Velocity After Impact (ft/sec.):	71.3
Missile Weight (lb.):	4.50	Angle Observed (deg.):	5.5
Impact Velocity (ft/sec.):	73.8	Horizontal Impact Location (in.):	10.00
Vertical Impact Location (in.):	42.50		

After Impact Angular Velocity of Frame, From Oscilloscope (rad/sec.):	0.109
After Impact Angular Velocity of Frame, From Angle (rad/sec.):	N/A

Notes: Missile Perforated Test Specimen

Test Run: LHS01

Glass Type: 1/4-in. AN - 0.030-in. - 1/4-in. HS

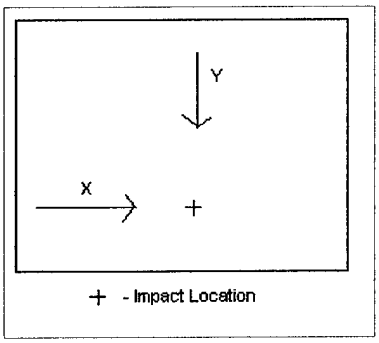

General Information:

Specimen Thickness (in.):	0.2843
Specimen Length (in.):	48.0
Weight of Frame (lb.):	119.5
Weight of Shims (lb.):	2.70
Weight of Glass (lb.):	55.50
Total Weight (lb.):	177.7

Center of Mass Impact Information

Support Frame Mass Moment of Inertia (ft-lb-sec^2.):	41.0
Support Frame Center of Mass (in.):	24.5

Missile Length (in.):	95.75	Missile Velocity After Impact (ft/sec.):	45.0
Missile Weight (lb.):	8.90		
Impact Velocity (ft/sec.):	51.4	Angle Observed (deg.):	7.7
Vertical Impact Location (in.):	25.50	Horizontal Impact Location (in.):	29.50

After Impact Angular Velocity of Frame, From Oscilloscope (rad/sec.):	0.119
After Impact Angular Velocity of Frame, From Angle (rad/sec.):	N/A

Notes: Missile Perforated Test Specimen
Heat Strengthened Ply Placed on Non-impact Side

Lower Corner Impact Information

Support Frame Mass Moment of Inertia (ft-lb-sec^2.):	41.0
Support Frame Center of Mass (in.):	24.5

Missile Information

Missile Length (in.):	118.00	Missile Velocity After Impact (ft/sec.):	35.0
Missile Weight (lb.):	9.00		
Impact Velocity (ft/sec.):	48.0	Angle Observed (deg.):	14.8
Vertical Impact Location (in.):	44.50	Horizontal Impact Location (in.):	9.50

After Impact Angular Velocity of Frame, From Oscilloscope (rad/sec.):	0.297
After Impact Angular Velocity of Frame, From Angle (rad/sec.):	N/A

Notes: Missile Perforated Test Specimen
Heat Strengthened Ply Placed on Non-impact Side

Test Run: LHS02

Glass Type: 1/4-in. AN - 0.030-in. - 1/4-in. HS

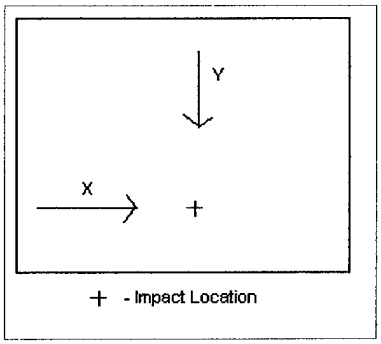

General Information:

Specimen Thickness (in.):	0.2845
Specimen Length (in.):	48.0
Weight of Frame (lb.):	119.5
Weight of Shims (lb.):	2.70
Weight of Glass (lb.):	55.90
Total Weight (lb.):	178.1

Center of Mass Impact Information

Support Frame Mass Moment of Inertia (ft-lb-sec^2.):	42.6
Support Frame Center of Mass (in.):	24.0

Missile Length (in.):	112.25	Missile Velocity After Impact (ft/sec.):	48.8
Missile Weight (lb.):	9.00		
Impact Velocity (ft/sec.):	51.8	Angle Observed (deg.):	5.7
Vertical Impact Location (in.):	24.25	Horizontal Impact Location (in.):	22.00

After Impact Angular Velocity of Frame, From Oscilloscope (rad/sec.):	0.0360
After Impact Angular Velocity of Frame, From Angle (rad/sec.):	N/A

Notes: Missile Perforated Test Specimen
Heat Strengthened Ply Placed on Non-impact Side

Lower Corner Impact Information

Support Frame Mass Moment of Inertia (ft-lb-sec^2.):	42.6
Support Frame Center of Mass (in.):	24.0

Missile Information

Missile Length (in.):	118.50	Missile Velocity After Impact (ft/sec.):	33.8
Missile Weight (lb.):	9.00		
Impact Velocity (ft/sec.):	48.4	Angle Observed (deg.):	15.6
Vertical Impact Location (in.):	42.50	Horizontal Impact Location (in.):	10.50

After Impact Angular Velocity of Frame, From Oscilloscope (rad/sec.):	0.289
After Impact Angular Velocity of Frame, From Angle (rad/sec.):	N/A

Notes: Missile Perforated Test Specimen
Heat Strengthened Ply Placed on Non-impact Side

Test Run: LHS03

Glass Type: 1/4-in. AN - 0.030-in. - 1/4-in. HS

General Information:

Specimen Thickness (in.):	0.2831
Specimen Length (in.):	48.0
Weight of Frame (lb.):	119.5
Weight of Shims (lb.):	2.70
Weight of Glass (lb.):	56.10
Total Weight (lb.):	178.3

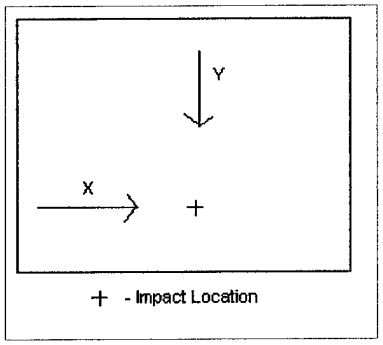

Center of Mass Impact Information

Support Frame Mass Moment of Inertia (ft-lb-sec^2.):	44.5
Support Frame Center of Mass (in.):	24.5

Missile Length (in.):	118.125	Missile Velocity After Impact (ft/sec.):	43.1
Missile Weight (lb.):	9.00		
Impact Velocity (ft/sec.):	51.8	Angle Observed (deg.):	6.8
Vertical Impact Location (in.):	22.75	Horizontal Impact Location (in.):	26.00

After Impact Angular Velocity of Frame, From Oscilloscope (rad/sec.):	0.0750
After Impact Angular Velocity of Frame, From Angle (rad/sec.):	N/A

Notes: Missile Perforated Test Specimen
Heat Strengthened Ply Placed on Non-impact Side

Lower Corner Impact Information

Support Frame Mass Moment of Inertia (ft-lb-sec^2.):	44.5
Support Frame Center of Mass (in.):	24.5

Missile Information

Missile Length (in.):	118.25	Missile Velocity After Impact (ft/sec.):	35.6
Missile Weight (lb.):	9.00		
Impact Velocity (ft/sec.):	51.1	Angle Observed (deg.):	18.6
Vertical Impact Location (in.):	41.00	Horizontal Impact Location (in.):	39.50

After Impact Angular Velocity of Frame, From Oscilloscope (rad/sec.):	0.319
After Impact Angular Velocity of Frame, From Angle (rad/sec.):	N/A

Notes: Missile Perforated Test Specimen
Missile Stuck In Test Specimen
Heat Strengthened Ply Placed on Non-impact Side

Test Run: HS9_01

Glass Type: 3/16-in. HS - 0.090 in. - 3/16-in. HS

General Information:

Specimen Thickness (in.):	0.4590
Specimen Length (in.):	48.0
Weight of Frame (lb.):	119.5
Weight of Shims (lb.):	3.65
Weight of Glass (lb.):	84.30
Total Weight (lb.):	207.5

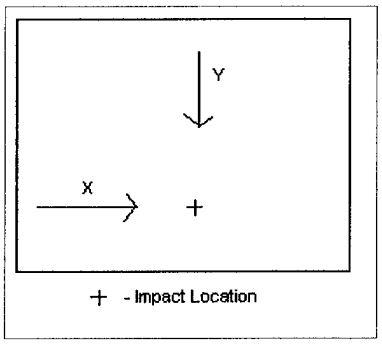

Center of Mass Impact Information

Support Frame Mass Moment of Inertia (ft-lb-sec^2.):	49.0
Support Frame Center of Mass (in.):	25.7

Missile Length (in.):	105.50	Missile Velocity After Impact (ft/sec.):	-5.8
Missile Weight (lb.):	9.00		
Impact Velocity (ft/sec.):	53.0	Angle Observed (deg.):	4.7
Vertical Impact Location (in.):	26.25	Horizontal Impact Location (in.):	26.00

After Impact Angular Velocity of Frame, From Oscilloscope (rad/sec.):	0.700
After Impact Angular Velocity of Frame, From Angle (rad/sec.):	0.718

Notes:

Lower Corner Impact Information

Support Frame Mass Moment of Inertia (ft-lb-sec^2.):	49.0
Support Frame Center of Mass (in.):	25.7

Missile Information

Missile Length (in.):	105.50	Missile Velocity After Impact (ft/sec.):	-0.6
Missile Weight (lb.):	9.00		
Impact Velocity (ft/sec.):	52.3	Angle Observed (deg.):	21.1
Vertical Impact Location (in.):	40.50	Horizontal Impact Location (in.):	9.00

After Impact Angular Velocity of Frame, From Oscilloscope (rad/sec.):	1.05
After Impact Angular Velocity of Frame, From Angle (rad/sec.):	1.10

Notes:

Test Run: HS9_02

Glass Type: 3/16-in. HS - 0.090 in. - 3/16-in. HS

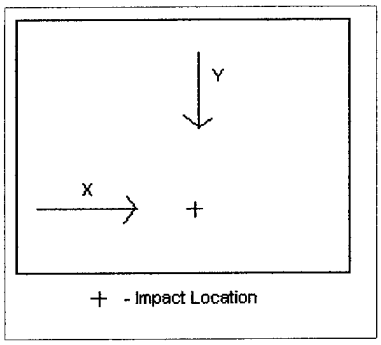

General Information:

Specimen Thickness (in.):	0.4584
Specimen Length (in.):	48.0
Weight of Frame (lb.):	119.5
Weight of Shims (lb.):	3.65
Weight of Glass (lb.):	84.10
Total Weight (lb.):	207.3

Center of Mass Impact Information

Support Frame Mass Moment of Inertia (ft-lb-sec^2.):	48.0
Support Frame Center of Mass (in.):	25.2

Missile Length (in.):	97.00	Missile Velocity After Impact (ft/sec.):	-6.3
Missile Weight (lb.):	9.00		
Impact Velocity (ft/sec.):	51.6	Angle Observed (deg.):	13.4
Vertical Impact Location (in.):	24.50	Horizontal Impact Location (in.):	25.50

After Impact Angular Velocity of Frame, From Oscilloscope (rad/sec.):	0.692
After Impact Angular Velocity of Frame, From Angle (rad/sec.):	0.704

Notes:

Lower Corner Impact Information

Support Frame Mass Moment of Inertia (ft-lb-sec^2.):	48.0
Support Frame Center of Mass (in.):	25.2

Missile Information

Missile Length (in.):	97.00	Missile Velocity After Impact (ft/sec.):	-2.5
Missile Weight (lb.):	9.00		
Impact Velocity (ft/sec.):	51.8	Angle Observed (deg.):	21.6
Vertical Impact Location (in.):	41.50	Horizontal Impact Location (in.):	40.00

After Impact Angular Velocity of Frame, From Oscilloscope (rad/sec.):	1.07
After Impact Angular Velocity of Frame, From Angle (rad/sec.):	1.13

Notes:

Test Run: HS9_03

Glass Type: 3/16-in. HS - 0.090 in. - 3/16-in. HS

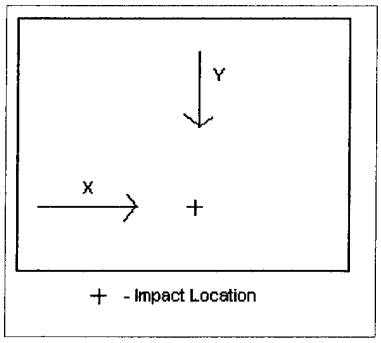

General Information:

Specimen Thickness (in.):	0.4598
Specimen Length (in.):	48.0
Weight of Frame (lb.):	119.5
Weight of Shims (lb.):	3.65
Weight of Glass (lb.):	84.70
Total Weight (lb.):	207.9

Center of Mass Impact Information

Support Frame Mass Moment of Inertia (ft-lb-sec^2.):	44.1
Support Frame Center of Mass (in.):	24.8

Missile Length (in.):	103.50	Missile Velocity After	
Missile Weight (lb.):	17.95	Impact (ft/sec.):	-3.8
Impact Velocity (ft/sec.):	37.3	Angle Observed (deg.):	13
Vertical Impact Location (in.):	16.50	Horizontal Impact Location (in.):	28.00

After Impact Angular Velocity of Frame, From Oscilloscope (rad/sec.):	No Data
After Impact Angular Velocity of Frame, From Angle (rad/sec.):	0.707

Notes: Oscilloscope Failed to Record Data, Angle From Pen and Paper Backup

Lower Corner Impact Information

Support Frame Mass Moment of Inertia (ft-lb-sec^2.):	44.1
Support Frame Center of Mass (in.):	24.8

Missile Information

Missile Length (in.):	98.00	Missile Velocity After	
Missile Weight (lb.):	17.95	Impact (ft/sec.):	3.8
Impact Velocity (ft/sec.):	38.8	Angle Observed (deg.):	33.4
Vertical Impact Location (in.):	48.00	Horizontal Impact Location (in.):	11.75

After Impact Angular Velocity of Frame, From Oscilloscope (rad/sec.):	1.79
After Impact Angular Velocity of Frame, From Angle (rad/sec.):	1.79

Notes: Missile Impact Location Near Outer Glass Stops, Edge of Support Frame

Test Run: HS9_04

Glass Type: 3/16-in. HS - 0.090 in. - 3/16-in. HS

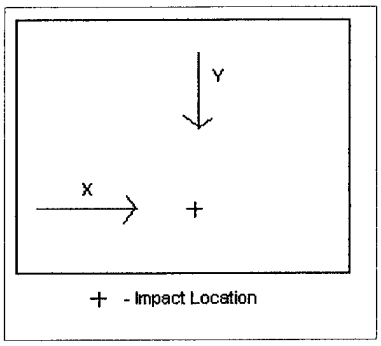

General Information:

Specimen Thickness (in.):	0.4582
Specimen Length (in.):	48.0
Weight of Frame (lb.):	119.5
Weight of Shims (lb.):	3.65
Weight of Glass (lb.):	84.80
Total Weight (lb.):	208.0

Center of Mass Impact Information

Support Frame Mass Moment of Inertia (ft-lb-sec^2.):	46.6
Support Frame Center of Mass (in.):	25.2

Missile Length (in.):	96.75	Missile Velocity After Impact (ft/sec.):	-5.2
Missile Weight (lb.):	18.00		
Impact Velocity (ft/sec.):	37.0	Angle Observed (deg.):	15.9
Vertical Impact Location (in.):	21.25	Horizontal Impact Location (in.):	28.00

After Impact Angular Velocity of Frame, From Oscilloscope (rad/sec.):	0.834
After Impact Angular Velocity of Frame, From Angle (rad/sec.):	0.845

Notes:

Lower Corner Impact Information

Support Frame Mass Moment of Inertia (ft-lb-sec^2.):	46.6
Support Frame Center of Mass (in.):	25.2

Missile Information

Missile Length (in.):	96.75	Missile Velocity After Impact (ft/sec.):	0.8
Missile Weight (lb.):	18.00		
Impact Velocity (ft/sec.):	36.3	Angle Observed (deg.):	26.8
Vertical Impact Location (in.):	39.25	Horizontal Impact Location (in.):	9.50

After Impact Angular Velocity of Frame, From Oscilloscope (rad/sec.):	1.36
After Impact Angular Velocity of Frame, From Angle (rad/sec.):	1.42

Notes:

Test Run: HS9_05

Glass Type: 3/16-in. HS - 0.090 in. - 3/16-in. HS

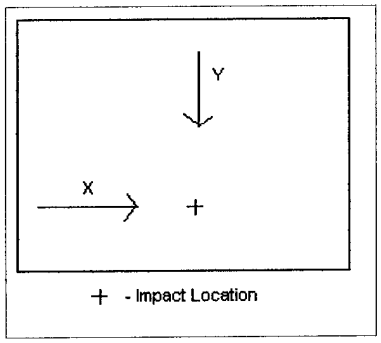

General Information:

Specimen Thickness (in.):	0.4546
Specimen Length (in.):	48.0
Weight of Frame (lb.):	119.5
Weight of Shims (lb.):	3.65
Weight of Glass (lb.):	83.90
Total Weight (lb.):	207.1

Center of Mass Impact Information

Support Frame Mass Moment of Inertia (ft-lb-sec^2.):	48.2
Support Frame Center of Mass (in.):	25.4

Missile Length (in.):	48.00	Missile Velocity After Impact (ft/sec.):	-4.6
Missile Weight (lb.):	4.55	Angle Observed (deg.):	9.0
Impact Velocity (ft/sec.):	72.9	Horizontal Impact Location (in.):	21.50
Vertical Impact Location (in.):	24.00		

After Impact Angular Velocity of Frame, From Oscilloscope (rad/sec.):	0.446
After Impact Angular Velocity of Frame, From Angle (rad/sec.):	0.475

Notes:

Lower Corner Impact Information

Support Frame Mass Moment of Inertia (ft-lb-sec^2.):	48.2
Support Frame Center of Mass (in.):	25.4

Missile Information

Missile Length (in.):	48.00	Missile Velocity After Impact (ft/sec.):	-5.2
Missile Weight (lb.):	4.50	Angle Observed (deg.):	16.7
Impact Velocity (ft/sec.):	72.1	Horizontal Impact Location (in.):	43.00
Vertical Impact Location (in.):	43.50		

After Impact Angular Velocity of Frame, From Oscilloscope (rad/sec.):	0.861
After Impact Angular Velocity of Frame, From Angle (rad/sec.):	0.876

Notes:

Test Run: HS9_06

Glass Type: 3/16-in. HS - 0.090 in. - 3/16-in. HS

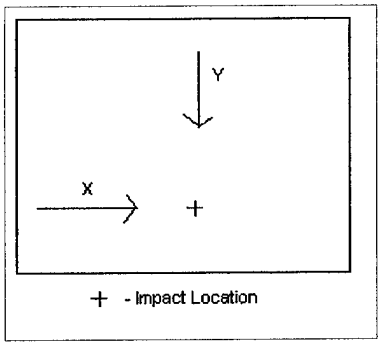

General Information:

Specimen Thickness (in.):	0.4543
Specimen Length (in.):	48.0
Weight of Frame (lb.):	119.5
Weight of Shims (lb.):	3.65
Weight of Glass (lb.):	83.80
Total Weight (lb.):	207.0

Center of Mass Impact Information

Support Frame Mass Moment of Inertia (ft-lb-sec^2.):	46.9
Support Frame Center of Mass (in.):	25.4

Missile Length (in.):	51.50	Missile Velocity After Impact (ft/sec.):	-7.5
Missile Weight (lb.):	4.50	Angle Observed (deg.):	9.3
Impact Velocity (ft/sec.):	74.6	Horizontal Impact Location (in.):	25.50
Vertical Impact Location (in.):	24.50		

After Impact Angular Velocity of Frame, From Oscilloscope (rad/sec.):	0.490
After Impact Angular Velocity of Frame, From Angle (rad/sec.):	0.496

Notes:

Lower Corner Impact Information

Support Frame Mass Moment of Inertia (ft-lb-sec^2.):	46.9
Support Frame Center of Mass (in.):	25.4

Missile Information

Missile Length (in.):	51.50	Missile Velocity After Impact (ft/sec.):	-3.8
Missile Weight (lb.):	4.50	Angle Observed (deg.):	15.3
Impact Velocity (ft/sec.):	72.2	Horizontal Impact Location (in.):	6.50
Vertical Impact Location (in.):	42.00		

After Impact Angular Velocity of Frame, From Oscilloscope (rad/sec.):	0.828
After Impact Angular Velocity of Frame, From Angle (rad/sec.):	0.816

Notes:

Test Run: HS9_07

Glass Type: 3/16-in. HS - 0.090 in. - 3/16-in. HS

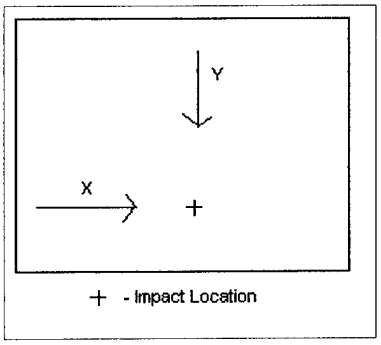

General Information:

Specimen Thickness (in.):	0.4603
Specimen Length (in.):	48.0
Weight of Frame (lb.):	119.5
Weight of Shims (lb.):	3.65
Weight of Glass (lb.):	85.10
Total Weight (lb.):	208.3

Center of Mass Impact Information

Support Frame Mass Moment of Inertia (ft-lb-sec^2.):	45.3
Support Frame Center of Mass (in.):	25.9

Missile Length (in.):	97.00	Missile Velocity After Impact (ft/sec.):	-3.1
Missile Weight (lb.):	9.00	Angle Observed (deg.):	12
Impact Velocity (ft/sec.):	51.2	Horizontal Impact Location (in.):	26.25
Vertical Impact Location (in.):	24.50		

After Impact Angular Velocity of Frame, From Oscilloscope (rad/sec.):	No Data
After Impact Angular Velocity of Frame, From Angle (rad/sec.):	0.659

Notes: Oscilloscope Failed to Record Data, Angle From Pen and Paper Backup

Lower Corner Impact Information

Support Frame Mass Moment of Inertia (ft-lb-sec^2.):	45.3
Support Frame Center of Mass (in.):	25.9

Missile Information

Missile Length (in.):	97.00	Missile Velocity After Impact (ft/sec.):	1.7
Missile Weight (lb.):	9.00	Angle Observed (deg.):	21.4
Impact Velocity (ft/sec.):	51.6	Horizontal Impact Location (in.):	7.25
Vertical Impact Location (in.):	44.25		

After Impact Angular Velocity of Frame, From Oscilloscope (rad/sec.):	1.17
After Impact Angular Velocity of Frame, From Angle (rad/sec.):	1.17

Notes:

Test Run: HS9_08

Glass Type: 3/16-in. HS - 0.090 in. - 3/16-in. HS

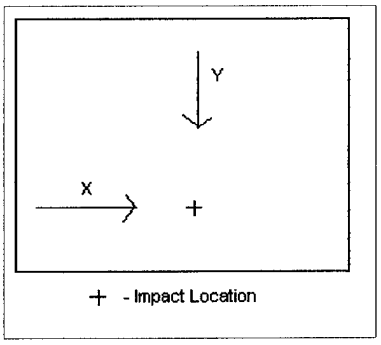

General Information:

Specimen Thickness (in.):	0.4583
Specimen Length (in.):	48.0
Weight of Frame (lb.):	119.5
Weight of Shims (lb.):	3.65
Weight of Glass (lb.):	84.50
Total Weight (lb.):	207.7

Center of Mass Impact Information

Support Frame Mass Moment of Inertia (ft-lb-sec^2.):	45.6
Support Frame Center of Mass (in.):	25.2

Missile Length (in.):	46.50	Missile Velocity After Impact (ft/sec.):	-3.8
Missile Weight (lb.):	4.50		
Impact Velocity (ft/sec.):	71.4	Angle Observed (deg.):	9.0
Vertical Impact Location (in.):	25.25	Horizontal Impact Location (in.):	26.50

After Impact Angular Velocity of Frame, From Oscilloscope (rad/sec.):	0.510
After Impact Angular Velocity of Frame, From Angle (rad/sec.):	0.487

Notes:

Lower Corner Impact Information

Support Frame Mass Moment of Inertia (ft-lb-sec^2.):	45.6
Support Frame Center of Mass (in.):	25.2

Missile Information

Missile Length (in.):	47.00	Missile Velocity After Impact (ft/sec.):	-3.3
Missile Weight (lb.):	4.50		
Impact Velocity (ft/sec.):	69.6	Angle Observed (deg.):	15.9
Vertical Impact Location (in.):	43.75	Horizontal Impact Location (in.):	45.25

After Impact Angular Velocity of Frame, From Oscilloscope (rad/sec.):	0.778
After Impact Angular Velocity of Frame, From Angle (rad/sec.):	0.854

Notes:

Test Run: HS9_09

Glass Type: 3/16-in. HS - 0.090 in. - 3/16-in. HS

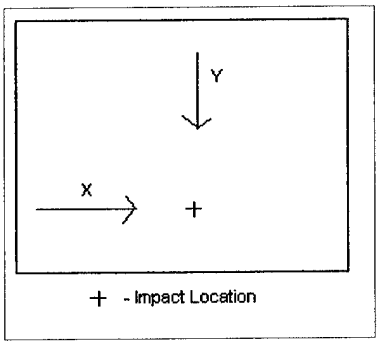

General Information:

Specimen Thickness (in.):	0.4592
Specimen Length (in.):	48.0
Weight of Frame (lb.):	119.5
Weight of Shims (lb.):	3.65
Weight of Glass (lb.):	85.00
Total Weight (lb.):	208.2

Center of Mass Impact Information

Support Frame Mass Moment of Inertia (ft-lb-sec^2.):	48.5
Support Frame Center of Mass (in.):	26.6

Missile Length (in.):	96.75	Missile Velocity After Impact (ft/sec.):	-3.3
Missile Weight (lb.):	18.00	Angle Observed (deg.):	18.9
Impact Velocity (ft/sec.):	34.7	Horizontal Impact Location (in.):	27.75
Vertical Impact Location (in.):	27.75		

After Impact Angular Velocity of Frame, From Oscilloscope (rad/sec.):	1.05
After Impact Angular Velocity of Frame, From Angle (rad/sec.):	1.01

Notes:

Lower Corner Impact Information

Support Frame Mass Moment of Inertia (ft-lb-sec^2.):	48.5
Support Frame Center of Mass (in.):	26.6

Missile Information

Missile Length (in.):	96.75	Missile Velocity After Impact (ft/sec.):	2.3
Missile Weight (lb.):	18.00	Angle Observed (deg.):	27.9
Impact Velocity (ft/sec.):	33.1	Horizontal Impact Location (in.):	7.50
Vertical Impact Location (in.):	45.75		

After Impact Angular Velocity of Frame, From Oscilloscope (rad/sec.):	1.43
After Impact Angular Velocity of Frame, From Angle (rad/sec.):	1.49

Notes:

Test Run: ALM01

Type: 1/4-in. Aluminum Plate

General Information:

Specimen Thickness (in.):	0.2406
Specimen Length (in.):	48.0
Weight of Frame (lb.):	119.5
Weight of Shims (lb.):	2.70
Weight of Glass (lb.):	54.20
Total Weight (lb.):	176.4

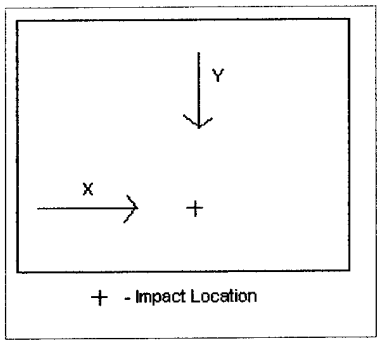

Center of Mass Impact Information

Support Frame Mass Moment of Inertia (ft-lb-sec^2.):	40.1
Support Frame Center of Mass (in.):	24.6

Missile Length (in.):	60.75	Missile Velocity After Impact (ft/sec.):	-7.9
Missile Weight (lb.):	4.50		
Impact Velocity (ft/sec.):	73.2	Angle Observed (deg.):	10.4
Vertical Impact Location (in.):	23.25	Horizontal Impact Location (in.):	24.50

After Impact Angular Velocity of Frame, From Oscilloscope (rad/sec.):	0.521
After Impact Angular Velocity of Frame, From Angle (rad/sec.):	0.545

Notes:

Lower Corner Impact Information

Support Frame Mass Moment of Inertia (ft-lb-sec^2.):	40.1
Support Frame Center of Mass (in.):	24.6

Missile Information

Missile Length (in.):	60.75	Missile Velocity After Impact (ft/sec.):	No Data
Missile Weight (lb.):	4.50		
Impact Velocity (ft/sec.):	72.3	Angle Observed (deg.):	21.9
Vertical Impact Location (in.):	42.50	Horizontal Impact Location (in.):	40.00

After Impact Angular Velocity of Frame, From Oscilloscope (rad/sec.):	0.578
After Impact Angular Velocity of Frame, From Angle (rad/sec.):	0.573

Notes: VHS Camera Did Not Record Missile Data After Impact

Test Run: ALM02

Type: 1/4-in. Aluminum Plate

General Information:

Specimen Thickness (in.):	0.2402
Specimen Length (in.):	48.0
Weight of Frame (lb.):	119.5
Weight of Shims (lb.):	2.70
Weight of Glass (lb.):	54.10
Total Weight (lb.):	176.3

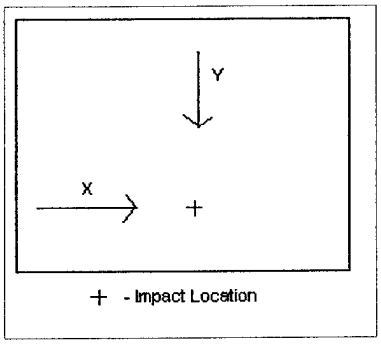

Center of Mass Impact Information

Support Frame Mass Moment of Inertia (ft-lb-sec^2.):	39.4
Support Frame Center of Mass (in.):	24.2

Missile Length (in.):	49.50	Missile Velocity After Impact (ft/sec.):	-9.4
Missile Weight (lb.):	4.50		
Impact Velocity (ft/sec.):	73.6	Angle Observed (deg.):	11.0
Vertical Impact Location (in.):	21.75	Horizontal Impact Location (in.):	25.75

After Impact Angular Velocity of Frame, From Oscilloscope (rad/sec.):	0.578
After Impact Angular Velocity of Frame, From Angle (rad/sec.):	0.573

Notes:

Lower Corner Impact Information

Support Frame Mass Moment of Inertia (ft-lb-sec^2.):	39.4
Support Frame Center of Mass (in.):	24.2

Missile Information

Missile Length (in.):	49.50	Missile Velocity After Impact (ft/sec.):	-10.4
Missile Weight (lb.):	4.50		
Impact Velocity (ft/sec.):	71.2	Angle Observed (deg.):	21.1
Vertical Impact Location (in.):	44.50	Horizontal Impact Location (in.):	11.50

After Impact Angular Velocity of Frame, From Oscilloscope (rad/sec.):	1.14
After Impact Angular Velocity of Frame, From Angle (rad/sec.):	1.10

Notes:

Test Run: ALM03

Type: 1/4-in. Aluminum Plate

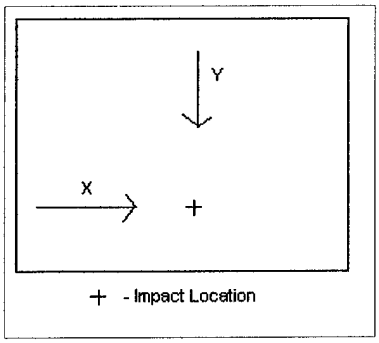

General Information:

Specimen Thickness (in.):	0.2411
Specimen Length (in.):	48.0
Weight of Frame (lb.):	119.5
Weight of Shims (lb.):	2.60
Weight of Glass (lb.):	54.10
Total Weight (lb.):	176.2

Center of Mass Impact Information

Support Frame Mass Moment of Inertia (ft-lb-sec^2.):	39.9
Support Frame Center of Mass (in.):	24.6

Missile Length (in.):	49.50	Missile Velocity After Impact (ft/sec.):	-10.2
Missile Weight (lb.):	4.50		
Impact Velocity (ft/sec.):	72.6	Angle Observed (deg.):	11.0
Vertical Impact Location (in.):	23.75	Horizontal Impact Location (in.):	25.75

After Impact Angular Velocity of Frame, From Oscilloscope (rad/sec.):	0.555
After Impact Angular Velocity of Frame, From Angle (rad/sec.):	0.574

Notes:

Lower Corner Impact Information

Support Frame Mass Moment of Inertia (ft-lb-sec^2.):	39.9
Support Frame Center of Mass (in.):	24.6

Missile Information

Missile Length (in.):	49.50	Missile Velocity After Impact (ft/sec.):	-12.5
Missile Weight (lb.):	4.50		
Impact Velocity (ft/sec.):	71.5	Angle Observed (deg.):	19.4
Vertical Impact Location (in.):	42.75	Horizontal Impact Location (in.):	42.75

After Impact Angular Velocity of Frame, From Oscilloscope (rad/sec.):	1.04
After Impact Angular Velocity of Frame, From Angle (rad/sec.):	1.02

Notes:

Test Run: ALM04

Type: 1/4-in. Aluminum Plate

General Information:

Specimen Thickness (in.):	0.2404
Specimen Length (in.):	48.0
Weight of Frame (lb.):	119.5
Weight of Shims (lb.):	2.60
Weight of Glass (lb.):	54.00
Total Weight (lb.):	176.1

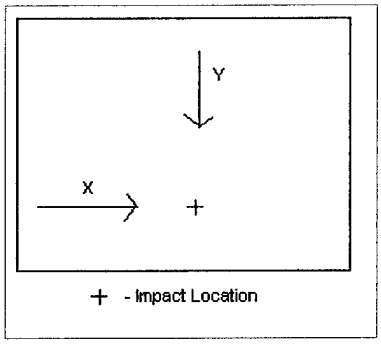

Center of Mass Impact Information

Support Frame Mass Moment of Inertia (ft-lb-sec^2.):	40.8
Support Frame Center of Mass (in.):	24.6

Missile Length (in.):	88.75	Missile Velocity After Impact (ft/sec.):	-17.5
Missile Weight (lb.):	9.00		
Impact Velocity (ft/sec.):	49.4	Angle Observed (deg.):	17.8
Vertical Impact Location (in.):	25.00	Horizontal Impact Location (in.):	26.25

After Impact Angular Velocity of Frame, From Oscilloscope (rad/sec.):	0.922
After Impact Angular Velocity of Frame, From Angle (rad/sec.):	0.920

Notes:

Lower Corner Impact Information

Support Frame Mass Moment of Inertia (ft-lb-sec^2.):	40.8
Support Frame Center of Mass (in.):	24.6

Missile Information

Missile Length (in.):	88.75	Missile Velocity After Impact (ft/sec.):	-8.8
Missile Weight (lb.):	9.00		
Impact Velocity (ft/sec.):	48.0	Angle Observed (deg.):	24.0
Vertical Impact Location (in.):	41.00	Horizontal Impact Location (in.):	11.00

After Impact Angular Velocity of Frame, From Oscilloscope (rad/sec.):	No Data
After Impact Angular Velocity of Frame, From Angle (rad/sec.):	1.24

Notes: Oscilloscope Failed To Record Data, Pen and Paper Backup Used

Test Run: ALM05

Type: 1/4-in. Aluminum Plate

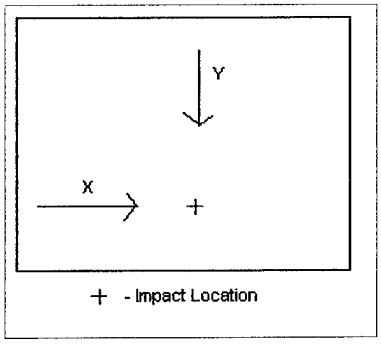

General Information:

Specimen Thickness (in.):	0.2407
Specimen Length (in.):	48.0
Weight of Frame (lb.):	119.5
Weight of Shims (lb.):	2.60
Weight of Glass (lb.):	54.00
Total Weight (lb.):	176.1

Center of Mass Impact Information

Support Frame Mass Moment of Inertia (ft-lb-sec^2.):	42.4
Support Frame Center of Mass (in.):	24.8

Missile Length (in.):	87.125	Missile Velocity After Impact (ft/sec.):	-15.0
Missile Weight (lb.):	9.00		
Impact Velocity (ft/sec.):	49.4	Angle Observed (deg.):	18.1
Vertical Impact Location (in.):	24.50	Horizontal Impact Location (in.):	22.50

After Impact Angular Velocity of Frame, From Oscilloscope (rad/sec.):	0.945
After Impact Angular Velocity of Frame, From Angle (rad/sec.):	0.921

Notes:

Lower Corner Impact Information

Support Frame Mass Moment of Inertia (ft-lb-sec^2.):	42.4
Support Frame Center of Mass (in.):	24.8

Missile Information

Missile Length (in.):	87.125	Missile Velocity After Impact (ft/sec.):	-8.8
Missile Weight (lb.):	9.00		
Impact Velocity (ft/sec.):	46.3	Angle Observed (deg.):	24.6
Vertical Impact Location (in.):	42.00	Horizontal Impact Location (in.):	42.50

After Impact Angular Velocity of Frame, From Oscilloscope (rad/sec.):	1.24
After Impact Angular Velocity of Frame, From Angle (rad/sec.):	1.25

Notes:

Test Run: ALM06

Type: 1/4-in. Aluminum Plate

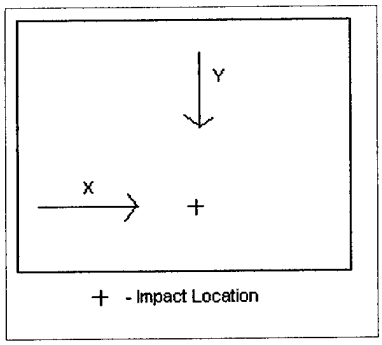

General Information:

Specimen Thickness (in.):	0.2402
Specimen Length (in.):	48.0
Weight of Frame (lb.):	119.5
Weight of Shims (lb.):	2.60
Weight of Glass (lb.):	54.10
Total Weight (lb.):	176.2

Center of Mass Impact Information

Support Frame Mass Moment of Inertia (ft-lb-sec^2.):	40.9
Support Frame Center of Mass (in.):	25.0

Missile Length (in.):	87.125	Missile Velocity After Impact (ft/sec.):	-12.3
Missile Weight (lb.):	8.90	Angle Observed (deg.):	16.7
Impact Velocity (ft/sec.):	48.2	Horizontal Impact Location (in.):	24.50
Vertical Impact Location (in.):	26.00		

After Impact Angular Velocity of Frame, From Oscilloscope (rad/sec.):	0.845
After Impact Angular Velocity of Frame, From Angle (rad/sec.):	0.871

Notes:

Lower Corner Impact Information

Support Frame Mass Moment of Inertia (ft-lb-sec^2.):	40.9
Support Frame Center of Mass (in.):	25.0

Missile Information

Missile Length (in.):	87.125	Missile Velocity After Impact (ft/sec.):	-6.7
Missile Weight (lb.):	9.00	Angle Observed (deg.):	28.7
Impact Velocity (ft/sec.):	49.0	Horizontal Impact Location (in.):	10.50
Vertical Impact Location (in.):	46.75		

After Impact Angular Velocity of Frame, From Oscilloscope (rad/sec.):	1.49
After Impact Angular Velocity of Frame, From Angle (rad/sec.):	1.49

Notes:

Test Run: ALM07

Type: 1/4-in. Aluminum Plate

General Information:

Specimen Thickness (in.):	0.2404
Specimen Length (in.):	48.0
Weight of Frame (lb.):	119.5
Weight of Shims (lb.):	2.60
Weight of Glass (lb.):	54.10
Total Weight (lb.):	176.2

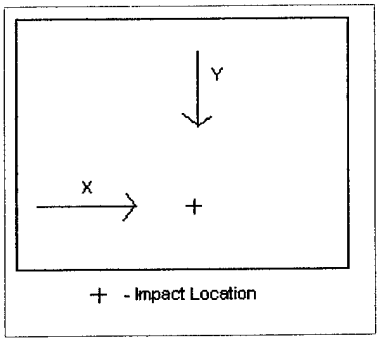

Center of Mass Impact Information

Support Frame Mass Moment of Inertia (ft-lb-sec^2.):	40.4
Support Frame Center of Mass (in.):	24.2

Missile Length (in.):	96.625	Missile Velocity After Impact (ft/sec.):	-11.9
Missile Weight (lb.):	18.00	Angle Observed (deg.):	26.6
Impact Velocity (ft/sec.):	34.8	Horizontal Impact Location (in.):	23.25
Vertical Impact Location (in.):	24.375		

After Impact Angular Velocity of Frame, From Oscilloscope (rad/sec.):	1.32
After Impact Angular Velocity of Frame, From Angle (rad/sec.):	1.36

Notes:

Lower Corner Impact Information

Support Frame Mass Moment of Inertia (ft-lb-sec^2.):	40.4
Support Frame Center of Mass (in.):	24.2

Missile Information

Missile Length (in.):	96.625	Missile Velocity After Impact (ft/sec.):	-2.5
Missile Weight (lb.):	18.00	Angle Observed (deg.):	37.2
Impact Velocity (ft/sec.):	34.2	Horizontal Impact Location (in.):	43.50
Vertical Impact Location (in.):	44.50		

After Impact Angular Velocity of Frame, From Oscilloscope (rad/sec.):	1.89
After Impact Angular Velocity of Frame, From Angle (rad/sec.):	1.89

Notes:

Test Run: ALM08

Type: 1/4-in. Aluminum Plate

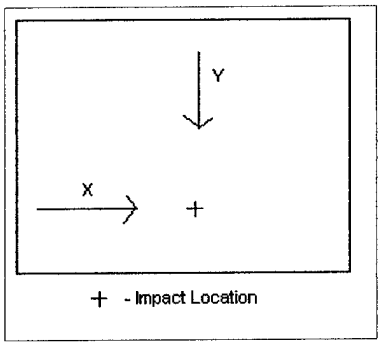

General Information:

Specimen Thickness (in.):	0.2403
Specimen Length (in.):	48.0
Weight of Frame (lb.):	119.5
Weight of Shims (lb.):	2.70
Weight of Glass (lb.):	54.10
Total Weight (lb.):	176.3

Center of Mass Impact Information

Support Frame Mass Moment of Inertia (ft-lb-sec^2.):	40.6
Support Frame Center of Mass (in.):	23.8

Missile Length (in.):	102.25	Missile Velocity After Impact (ft/sec.):	-10.0
Missile Weight (lb.):	18.00		
Impact Velocity (ft/sec.):	37.4	Angle Observed (deg.):	21.6
Vertical Impact Location (in.):	22.50	Horizontal Impact Location (in.):	22.50

After Impact Angular Velocity of Frame, From Oscilloscope (rad/sec.):	1.03
After Impact Angular Velocity of Frame, From Angle (rad/sec.):	1.10

Notes:

Lower Corner Impact Information

Support Frame Mass Moment of Inertia (ft-lb-sec^2.):	40.6
Support Frame Center of Mass (in.):	23.8

Missile Information

Missile Length (in.):	102.25	Missile Velocity After Impact (ft/sec.):	-2.1
Missile Weight (lb.):	18.00		
Impact Velocity (ft/sec.):	37.0	Angle Observed (deg.):	40.0
Vertical Impact Location (in.):	42.75	Horizontal Impact Location (in.):	7.00

After Impact Angular Velocity of Frame, From Oscilloscope (rad/sec.):	2.10
After Impact Angular Velocity of Frame, From Angle (rad/sec.):	2.01

Notes:

Test Run: ALM09

Type: 1/4-in. Aluminum Plate

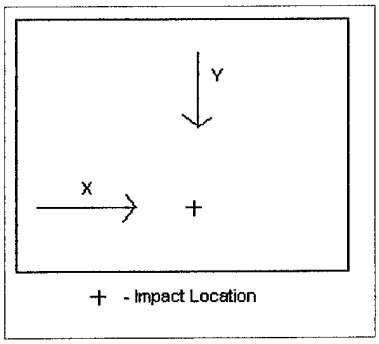

General Information:

Specimen Thickness (in.):	0.2399
Specimen Length (in.):	48.0
Weight of Frame (lb.):	119.5
Weight of Shims (lb.):	2.70
Weight of Glass (lb.):	54.10
Total Weight (lb.):	176.3

Center of Mass Impact Information

Support Frame Mass Moment of Inertia (ft-lb-sec^2.):	39.6
Support Frame Center of Mass (in.):	24.4

Missile Length (in.):	102.125	Missile Velocity After Impact (ft/sec.):	-12.9
Missile Weight (lb.):	18.05		
Impact Velocity (ft/sec.):	37.2	Angle Observed (deg.):	17.8
Vertical Impact Location (in.):	24.25	Horizontal Impact Location (in.):	26.50

After Impact Angular Velocity of Frame, From Oscilloscope (rad/sec.):	1.53
After Impact Angular Velocity of Frame, From Angle (rad/sec.):	1.44

Notes:

Lower Corner Impact Information

Support Frame Mass Moment of Inertia (ft-lb-sec^2.):	39.6
Support Frame Center of Mass (in.):	24.4

Missile Information

Missile Length (in.):	102.125	Missile Velocity After Impact (ft/sec.):	-6.7
Missile Weight (lb.):	18.05		
Impact Velocity (ft/sec.):	37.9	Angle Observed (deg.):	24.0
Vertical Impact Location (in.):	38.00	Horizontal Impact Location (in.):	44.00

After Impact Angular Velocity of Frame, From Oscilloscope (rad/sec.):	2.02
After Impact Angular Velocity of Frame, From Angle (rad/sec.):	2.08

Notes:

Test Run: MON01

Glass Type: 1/4-in. Annealed Monolithic

General Information:

Specimen Thickness (in.):	0.2236
Specimen Length (in.):	48.0
Weight of Frame (lb.):	119.5
Weight of Shims (lb.):	2.80
Weight of Glass (lb.):	47.40
Total Weight (lb.):	169.7

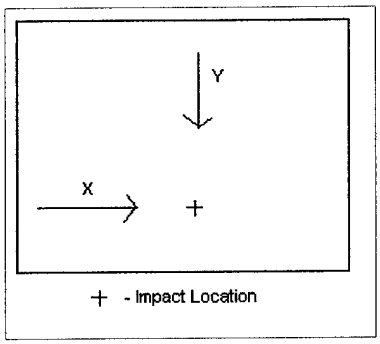

Center of Mass Impact Information

Support Frame Mass Moment of Inertia (ft-lb-sec^2.):	42.7
Support Frame Center of Mass (in.):	26.7

Missile Length (in.):	89.75	Missile Velocity After Impact (ft/sec.):	45.0
Missile Weight (lb.):	9.00	Angle Observed (deg.):	1
Impact Velocity (ft/sec.):	49.2	Horizontal Impact Location (in.):	26
Vertical Impact Location (in.):	24		

After Impact Angular Velocity of Frame, From Oscilloscope (rad/sec.):	No Data
After Impact Angular Velocity of Frame, From Angle (rad/sec.):	0.050

Notes: Oscilloscope Failed To Record Data, Pen and Paper Backup Used
Glass Did Not Survive First Impact

Test Run: MON02

Glass Type: 1/4-in. Annealed Monolithic

General Information:

Specimen Thickness (in.):	0.2248
Specimen Length (in.):	48.0
Weight of Frame (lb.):	119.5
Weight of Shims (lb.):	2.80
Weight of Glass (lb.):	47.40
Total Weight (lb.):	169.7

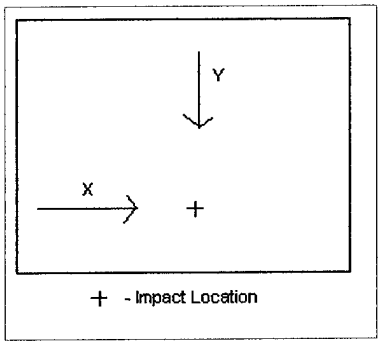

Center of Mass Impact Information

Support Frame Mass Moment of Inertia (ft-lb-sec^2.):	45.7
Support Frame Center of Mass (in.):	25.9

Missile Length (in.):	89.75	Missile Velocity After Impact (ft/sec.):	52.5
Missile Weight (lb.):	9.00	Angle Observed (deg.):	0.2
Impact Velocity (ft/sec.):	50.7	Horizontal Impact Location (in.):	26
Vertical Impact Location (in.):	25		

After Impact Angular Velocity of Frame, From Oscilloscope (rad/sec.):	No Data
After Impact Angular Velocity of Frame, From Angle (rad/sec.):	0.009

Notes: Oscilloscope Was Not Triggered. Missile Rebounded into frame causing bad backup Data. Angle Estimated From Trigger Level
Missile Speed After Impact Seems Questionable
Specimen Did Not Survive First Impact

Test Run: MON03

Glass Type: 1/4-in. Annealed Monolithic

General Information:

Specimen Thickness (in.):	0.2240
Specimen Length (in.):	48.0
Weight of Frame (lb.):	119.5
Weight of Shims (lb.):	2.70
Weight of Glass (lb.):	47.10
Total Weight (lb.):	169.3

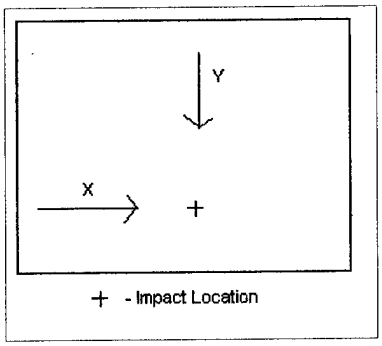

Center of Mass Impact Information

Support Frame Mass Moment of Inertia (ft-lb-sec^2.):	37.0
Support Frame Center of Mass (in.):	26.0

Missile Length (in.):	96.00	Missile Velocity After Impact (ft/sec.):	60.0
Missile Weight (lb.):	9.00	Angle Observed (deg.):	0.2
Impact Velocity (ft/sec.):	53.0	Horizontal Impact Location (in.):	25
Vertical Impact Location (in.):	24.25		

After Impact Angular Velocity of Frame, From Oscilloscope (rad/sec.):	No Data
After Impact Angular Velocity of Frame, From Angle (rad/sec.):	0.011

Notes: Oscilloscope Was Not Triggered. Missile Rebounded into frame causing bad backup Data. Angle Estimated From Trigger Level
Missile Speed After Impact Seems Questionable
Specimen Did Not Survive First Impact

Test Run: TPM2A

Glass Type: 1/2-in. Tempered Monolithic

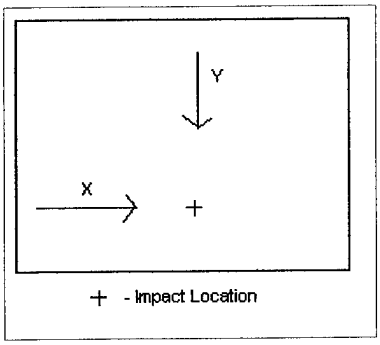

General Information:

Specimen Thickness (in.):	0.4832
Specimen Length (in.):	48.0
Weight of Frame (lb.):	119.5
Weight of Shims (lb.):	3.96
Weight of Glass (lb.):	100.60
Total Weight (lb.):	224.1

Center of Mass Impact Information

Support Frame Mass Moment of Inertia (ft-lb-sec^2.):	49.6
Support Frame Center of Mass (in.):	25.8

Missile Length (in.):	97.00	Missile Velocity After Impact (ft/sec.):	-10.0
Missile Weight (lb.):	9.00	Angle Observed (deg.):	12.9
Impact Velocity (ft/sec.):	51.5	Horizontal Impact Location (in.):	24.25
Vertical Impact Location (in.):	25.50		

After Impact Angular Velocity of Frame, From Oscilloscope (rad/sec.):	0.681
After Impact Angular Velocity of Frame, From Angle (rad/sec.):	0.689

Notes:

Lower Corner Impact Information

Support Frame Mass Moment of Inertia (ft-lb-sec^2.):	49.6
Support Frame Center of Mass (in.):	25.8

Missile Information

Missile Length (in.):	97.00	Missile Velocity After Impact (ft/sec.):	26.3
Missile Weight (lb.):	9.00	Angle Observed (deg.):	11.0
Impact Velocity (ft/sec.):	50.4	Horizontal Impact Location (in.):	43.00
Vertical Impact Location (in.):	43.00		

After Impact Angular Velocity of Frame, From Oscilloscope (rad/sec.):	0.262
After Impact Angular Velocity of Frame, From Angle (rad/sec.):	0.569

Notes: Test Specimen Destroyed By Impact
Scope Data is jumpy immediately after impact

APPENDIX B

PICTURES OF TEST SPECIMENS AFTER IMPACT

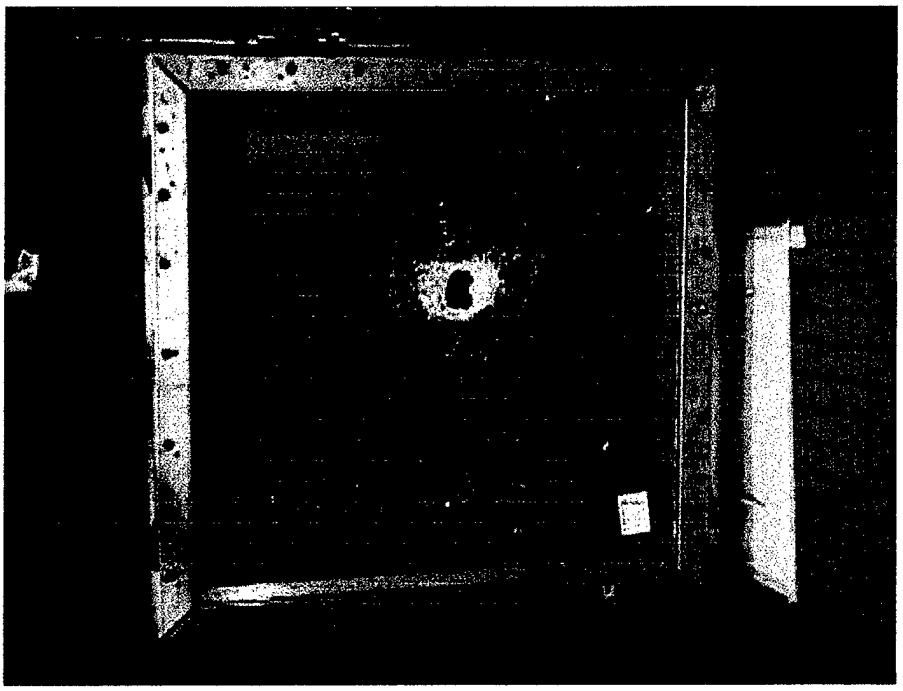

Figure B.1. LAM05 After Center of Mass Impact

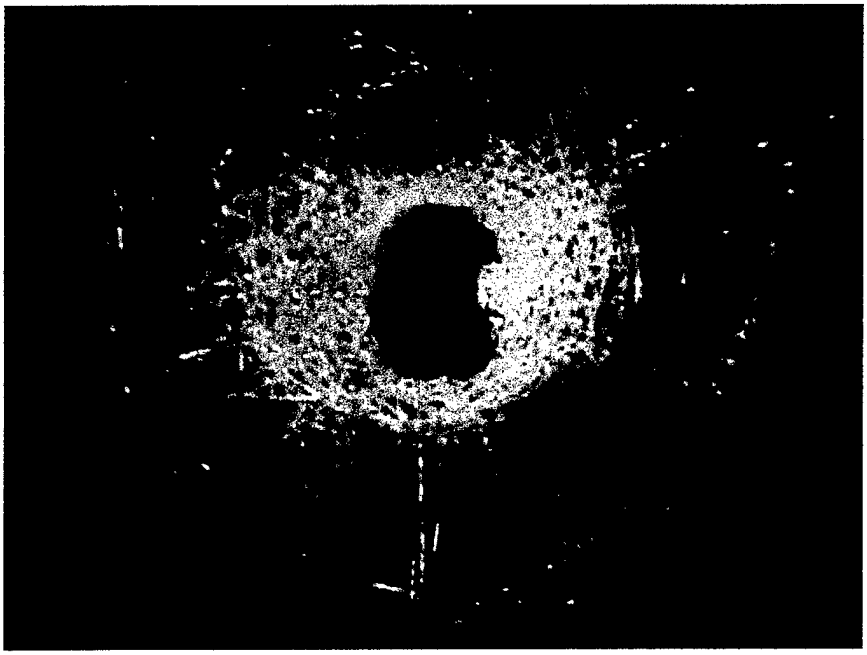

Figure B.2. Missile Perforation, Center of Mass Shot (LAM05)

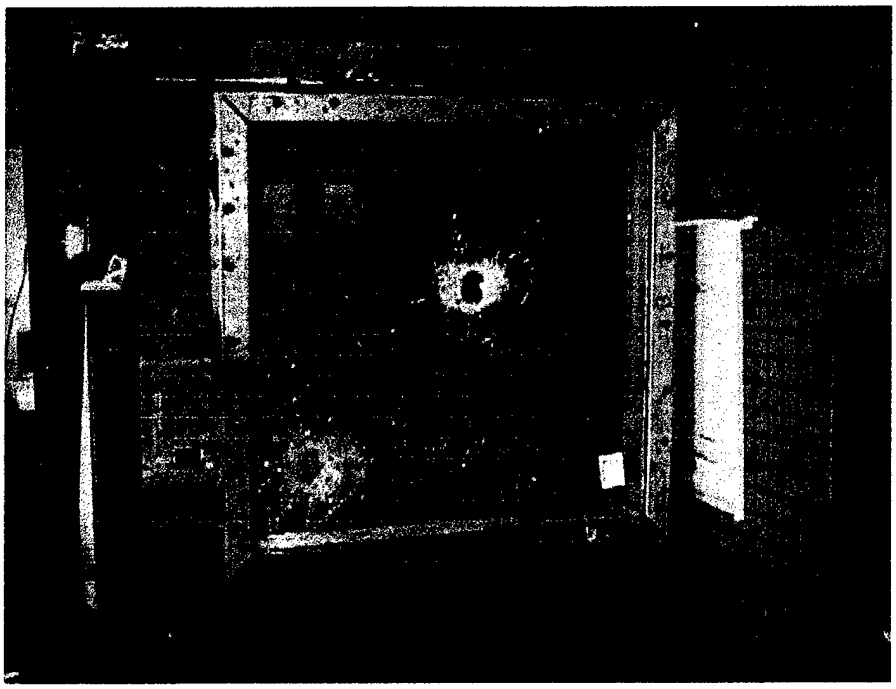

Figure B.3. Example of Laminated Glass Lite After Two Impacts (LAM05)

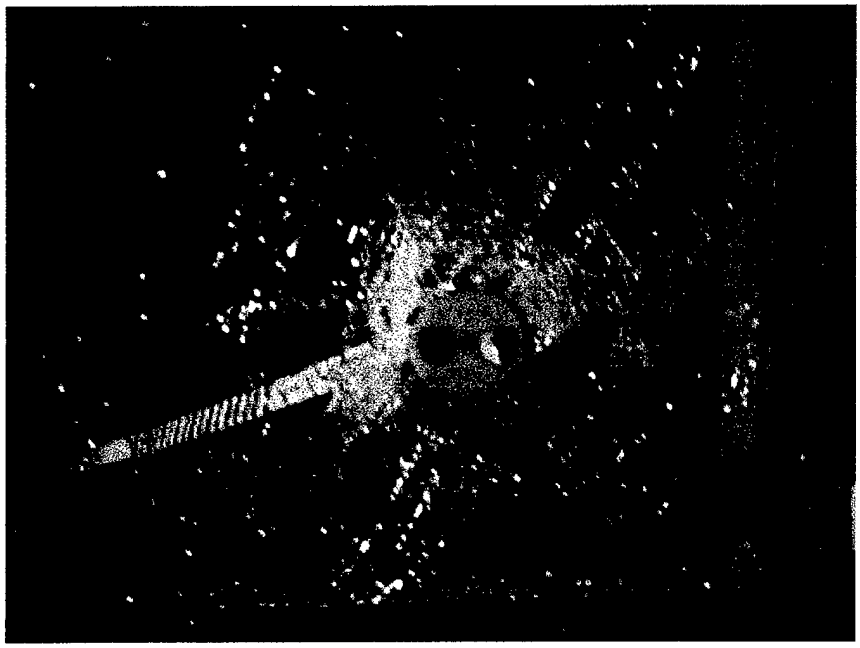

Figure B.4. Missile Stopped By Glass Lite, Lower Corner Impact (LHS03)

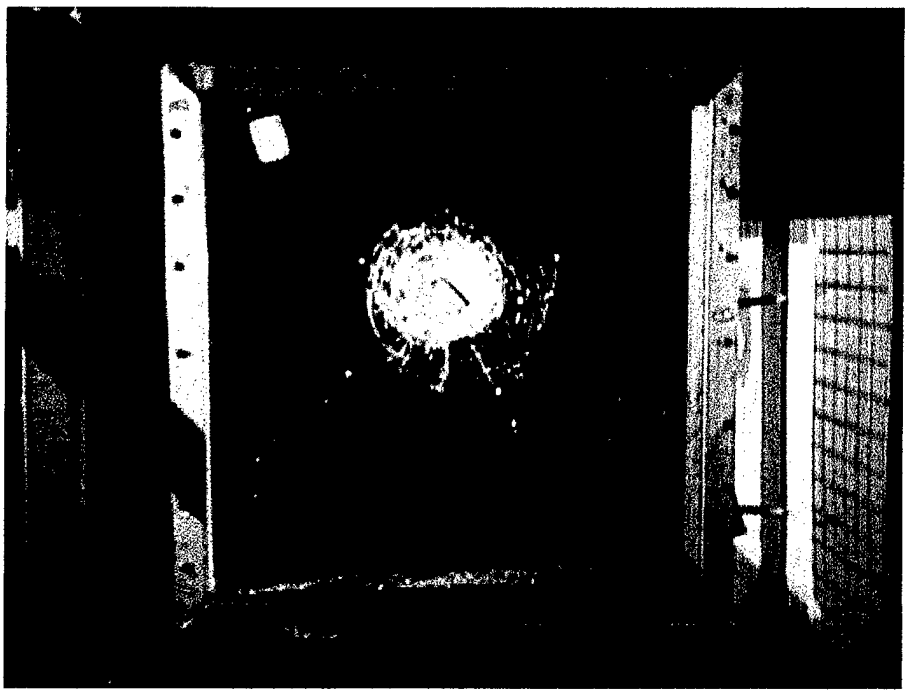

Figure B.5. Missile Perforation, Center of Mass Impact (LHS03)

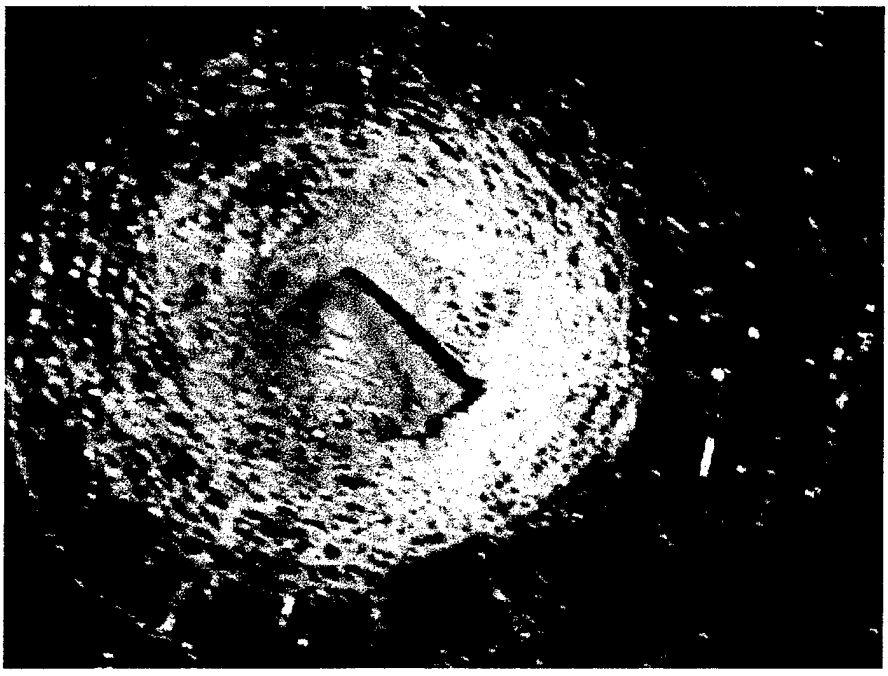

Figure B.6. Center of Mass Impact (LHS03)

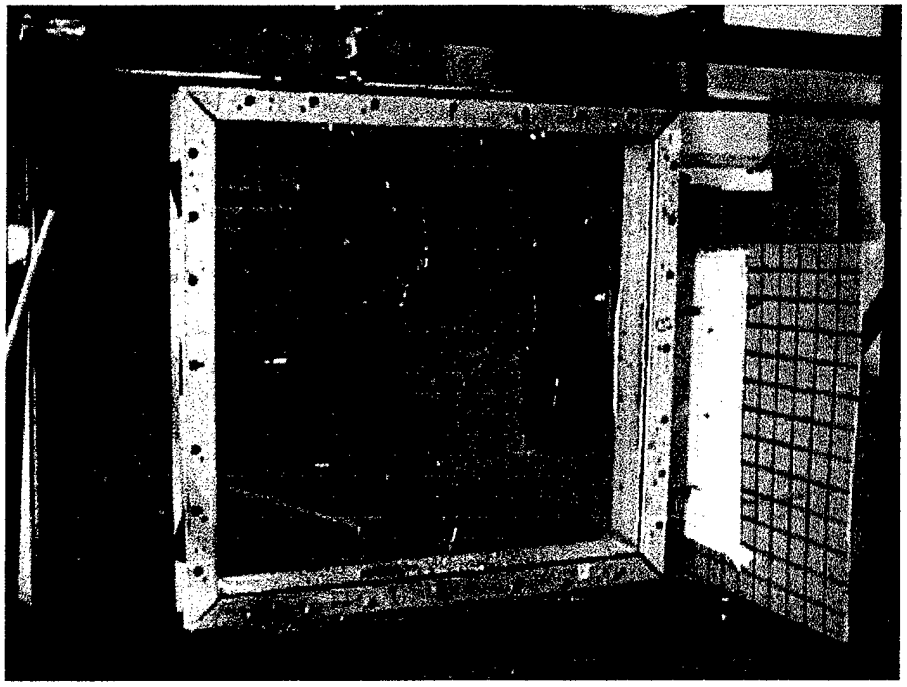

Figure B.7. Center of Mass Impact (MON01)

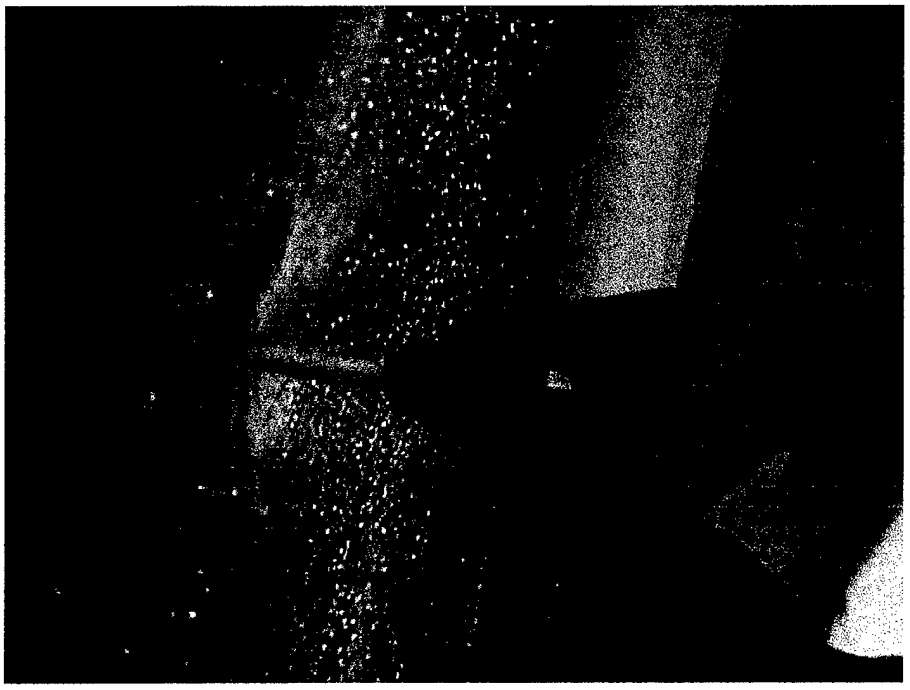

Figure B.8. Deformation Resulting From Center of Mass Impact, HS9_09 (Front View)

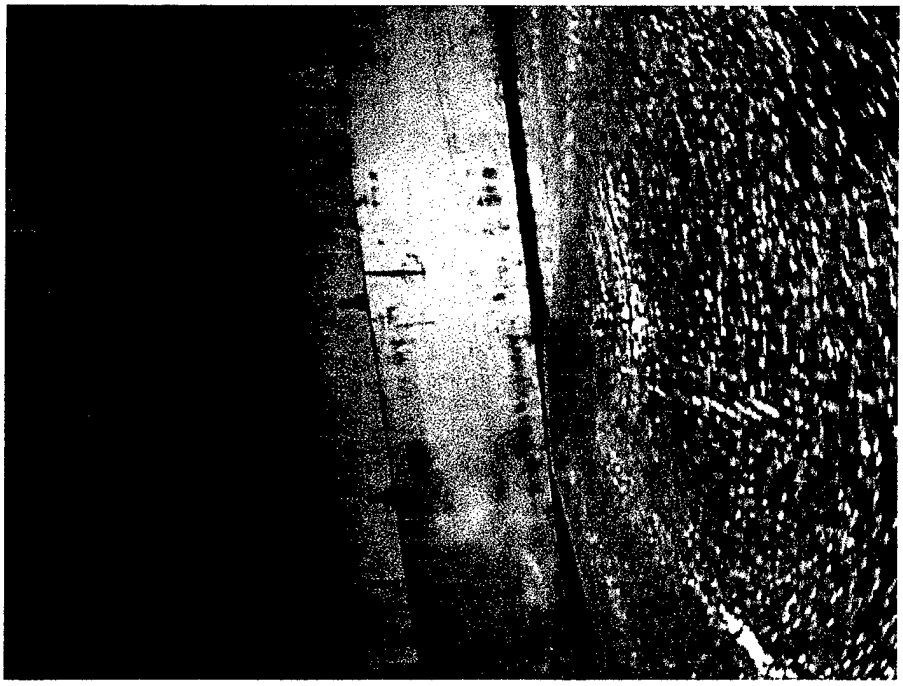

Figure B.9. Deformation Resulting From Center of Mass Impact, HS9_09 (Rear View)

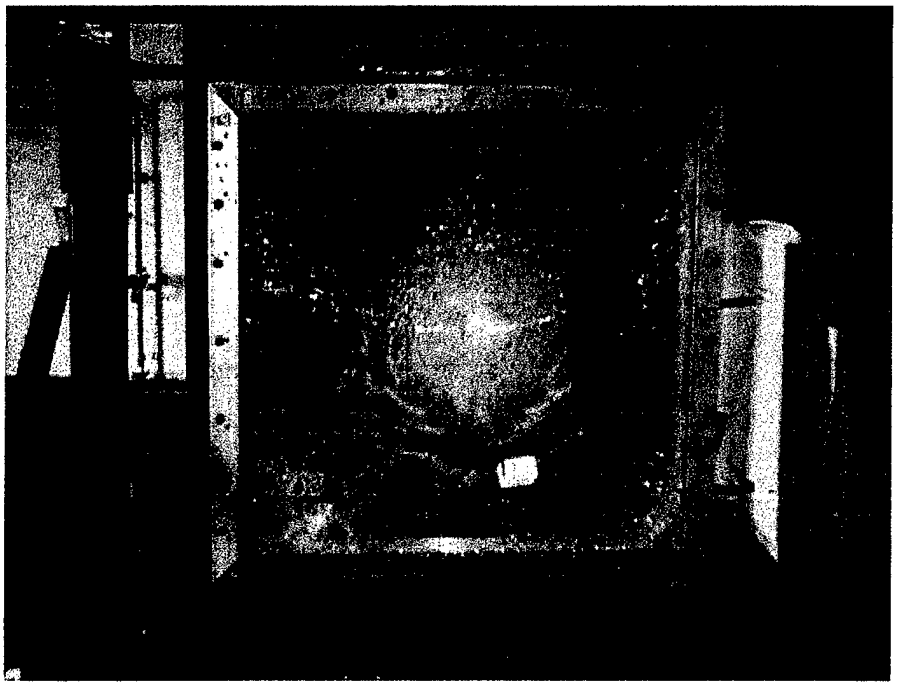

Figure B.10. Example of Resistance of Both Impacts (HS9_09)

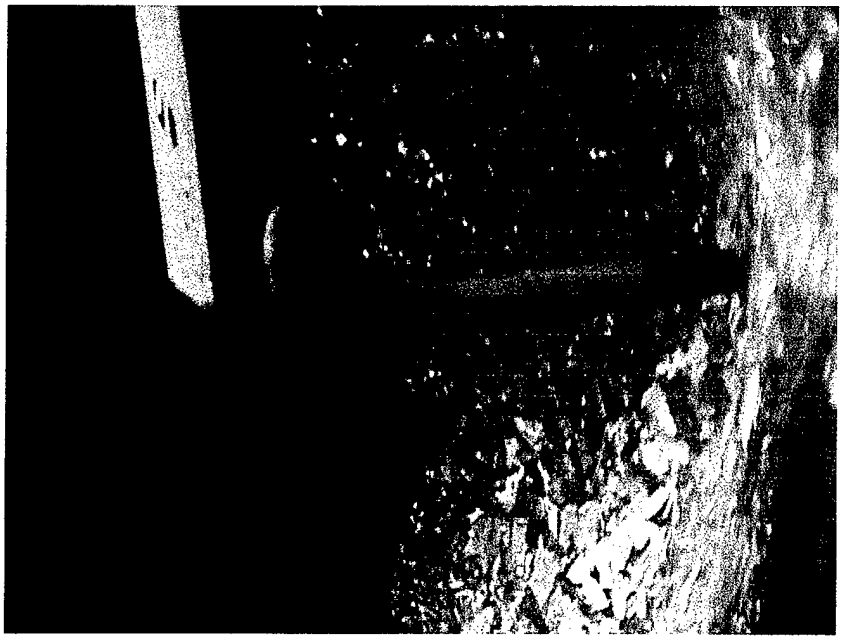

Figure B.11. Deformation Resulting From Lower Corner Impact, HS9_07, 9.00-lb. Missile (Front View)

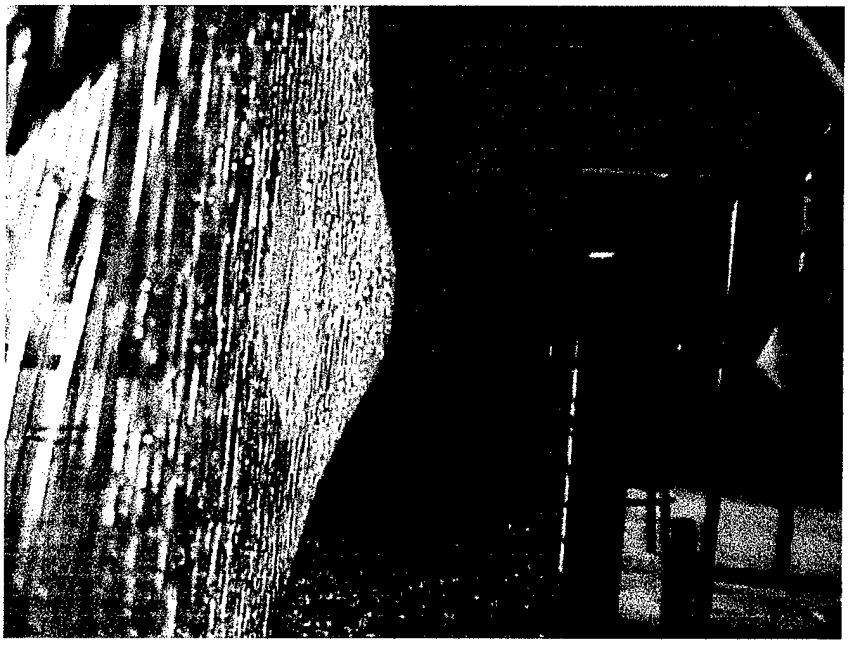

Figure B.12. Deformation Resulting From Lower Corner Impact, HS9_07, 9.00-lb. Missile (Rear View)

Figure B.13. Deformation Resulting From Lower Corner Impact, HS9_09, 18.0-lb. Missile (Front View)

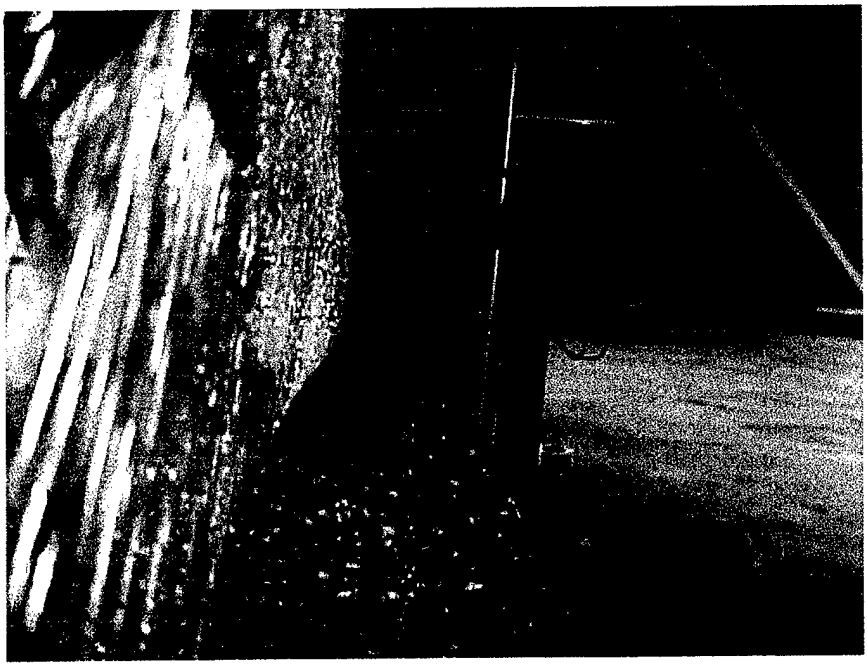

Figure B.14. Deformation Resulting From Lower Corner Impact, HS9_09, 18.0-lb. Missile (Rear View)

Figure B.15. Deformation Resulting From Lower Corner Impact, HS9_08, 4.50-lb. Missile (Front View)

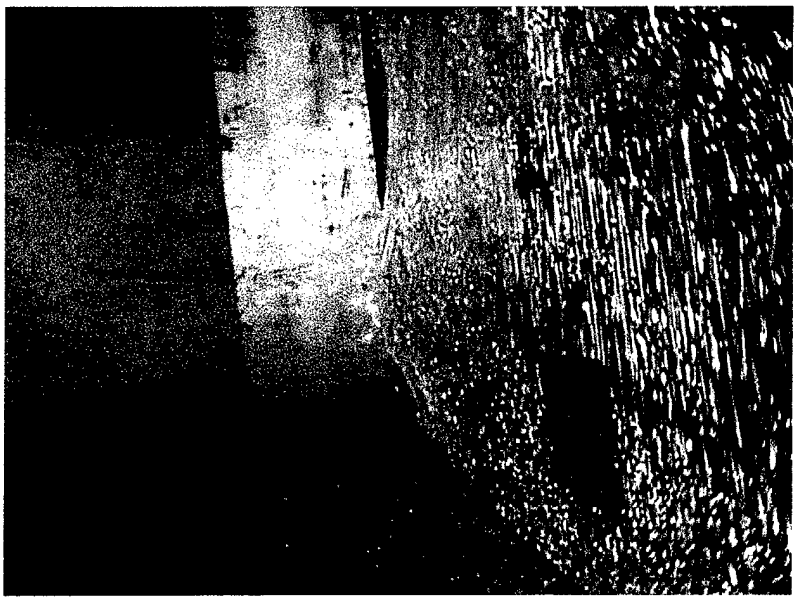

Figure B.16. Deformation Resulting From Lower Corner Impact, HS9_08, 4.50-lb. Missile (Rear View)

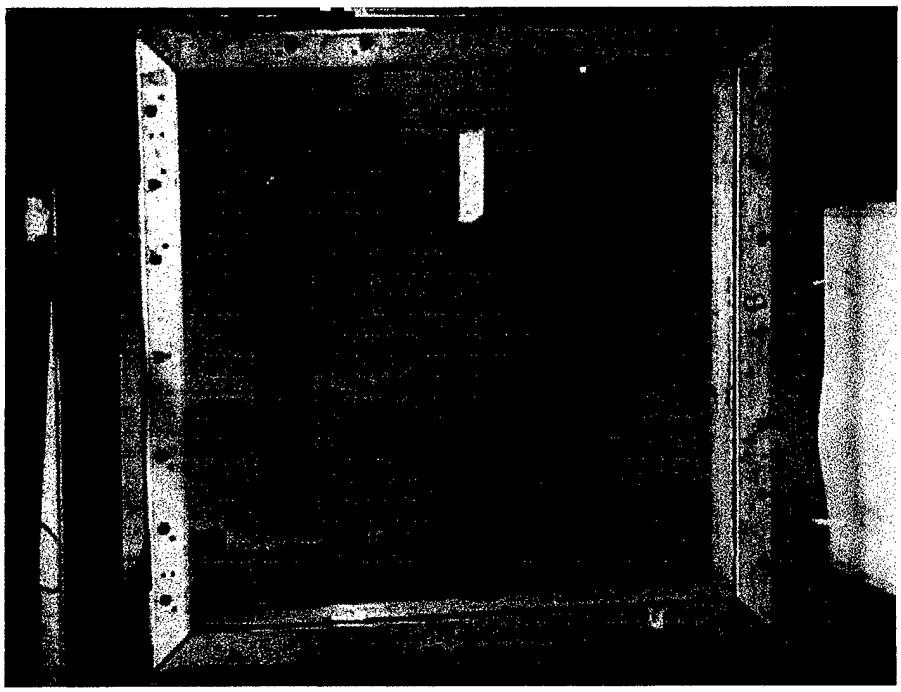

Figure B.17. Tempered Monolithic Lite Installed in Glazing Support Frame

Figure B.18. Center of Mass Impact on Tempered Monolithic Lite (TPM2A)

Figure B.19. Destroyed Tempered Monolithic Lite, Lower Right Corner (TPM2A)

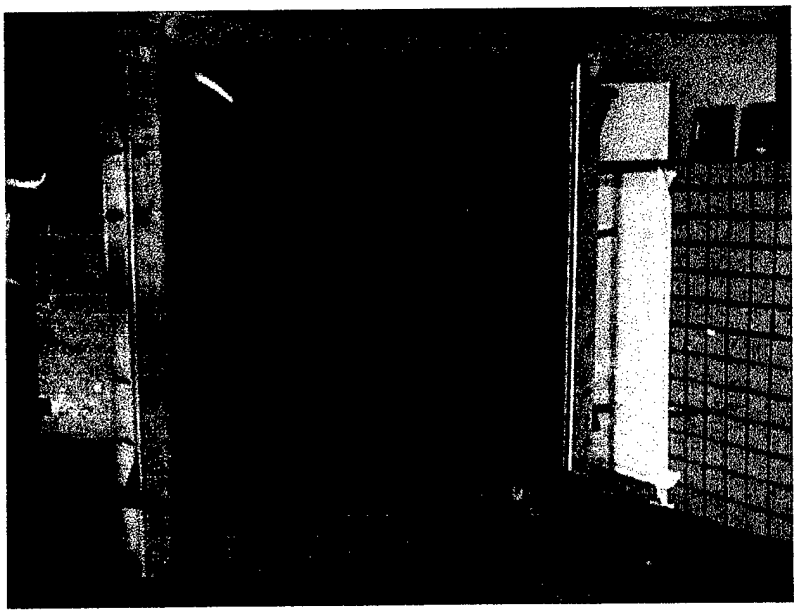

Figure B.20. Aluminum Plate Installed in Glazing Support Frame

PERMISSION TO COPY

In presenting this thesis in partial fulfillment of the requirements for a master's degree at Texas Tech University or Texas Tech University Health Sciences Center, I agree that the Library and my major department shall make it freely available for research purposes. Permission to copy this thesis for scholarly purposes may be granted by the Director of the Library or my major professor. It is understood that any copying or publication of this thesis for financial gain shall not be allowed without my further written permission and that any user may be liable for copyright infringement.

Agree (Permission is granted.)

Scott A. Bak — Student's Signature

10 Nov 99 — Date

Disagree (Permission is not granted.)

Student's Signature

Date